NORTHWESTERN UNIVERSITY

# The Role of the Host Response and Viral Genetic Variation in the Pathogenesis of Herpes Simplex Encephalitis

A DISSERTATION

SUBMITTED TO THE GRADUATE SCHOOL

IN PARTIAL FULFILLMENT OF THE REQUIREMENTS

for the degree

DOCTOR OF PHILOSOPHY

Field of Life Sciences

By

Cooper Kincaid Hayes

EVANSTON, ILLINOIS

June 2022

# ABSTRACT

Herpes simplex virus (HSV) encephalitis (HSE) is the most common cause of sporadic fatal encephalitis, and despite targeted antiviral therapy, outcomes remain poor. While rare in adults, neonates are significantly more susceptible to severe HSV disease. Understanding both the host and viral factors that contribute to pathogenesis is critical to improving outcomes in this devastating illness. Although the innate immune system is critical for restricting HSV-1 replication in the brain, a careful balance must be struck between effective antiviral control and excessive neuroinflammation. In Chapter III, I investigated the contribution of inflammasomes to pathogenesis in a murine model of HSE. Inflammasomes are signaling platforms that initiate a proinflammatory response by activating the cytokines IL-1β and IL-18. I found that mice deficient in the inflammasome adaptor protein, ASC, had significantly improved survival and lower levels of IL-1β and IL-18 in the brain during infection. Importantly, this difference in survival was independent of viral replication in the central nervous system. I identified microglia, the resident macrophages of the CNS, as the essential mediators of this response. These results suggest a promising new target in combating harmful inflammation in HSE.

In Chapter IV, I used single-nucleus RNA sequencing of brain tissue from adult and neonatal mice infected with HSV-1 to identify host factors that contribute to age-dependent susceptibility to infection. The neonatal brain was overwhelmingly more susceptible to infection without an age-dependent tropism towards a particular cell type. Surprisingly, I found that transcriptional levels of antiviral genes were similar between neonates and adults at baseline. Instead, I found that the long noncoding RNA Meg3 is expressed at higher levels in the neonatal brain and inhibits host cell apoptosis during HSV-1 infection. Our study highlights a potential

role for the developmental state of a cell to influence viral susceptibility outside of traditional antiviral gene expression.

Finally, in Chapter V I investigated the contribution of viral variation to HSE pathogenesis. As a DNA virus, HSV is traditionally thought of as relatively invariant and previous studies have focused on host genetic factors to explain varied clinical courses in neonates. I evaluated clinical HSV-2 isolates from neonates with different neurologic outcomes in several models of HSV infection. I found that isolates taken from neonates with encephalitis are more neurovirulent in human neuronal culture and mouse models of HSV encephalitis, as compared to isolates collected from neonates with mild peripheral disease. These findings suggest that inherent characteristics of the infecting HSV strain contribute to disease outcome following neonatal infection.

# TABLE OF CONTENTS

# LIST OF FIGURES

# CHAPTER I: INTRODUCTION

## HERPES SIMPLEX VIRUS

Herpes simplex viruses (HSV) are remarkably successful human pathogens. Over half of the United States and European population is seropositive for HSV type 1 (HSV-1), while roughly 15% are seropositive for HSV type 2 (HSV-2) [1,2]. Central to this success is the characteristic HSV life cycle, whereby the virus can remain latent in ganglia for the life of the host and evade immune recognition. Primary infection occurs at mucosal sites where HSV undergoes lytic replication before infecting sensory neurons and traveling retrograde to sensory ganglia. The virus establishes a latent infection from which it can later reactivate, traveling to the original site of infection [3]. Although HSV typically causes mild mucosal lesions, severe forms of infection can also occur, including encephalitis and ocular disease [3]. While rare, neonatal disease is significantly more severe, with over 50% of cases progressing to disseminated disease or encephalitis [4].

### Structure

Herpes simplex viruses are large double-stranded DNA virus with a structure consisting of a core containing the genome, an icosahedral capsid surrounding the core, a lipid envelope with embedded glycoproteins, and a proteinaceous layer called the tegument located between the capsid and envelope [5]. While encapsulated, the DNA genome is linear and double-stranded [6], but circularizes shortly after infection [7]. The genome is composed of two segments, the long (L) and short (S) segments, that are flanked by inverted repeat sections [8]. Both HSV-1 and HSV-2 have large, complex genomes, encoding at least 74 protein-coding genes [9]. HSV is also

known to produce several noncoding RNAs, including the latency associated transcripts (LATs) [3].

**Lytic Replication**

The HSV replication cycle begins when viral particles enter the host cell, either through fusion with the cell membrane or receptor-mediated endocytosis, depending on the target cell type. HSV tends to enter epithelial cells through endocytosis, while entering neurons through membrane fusion [10–15]. In order to make use of either mode of entry, HSV relies on the interaction of several glycoproteins present in its lipid envelope with host cell receptors. After entry, the capsid is released from the envelope and travels to the nucleus using the microtubule system and the molecular motor dynein [16,17]. There, the capsid docks to a nuclear pore and the viral genome is ejected into the nucleus where viral gene expression can begin [18]. HSV genes are expressed in a coordinated cascade of five groups based on their timing: α (immediate-early), $\beta_1$ (early-early), $\beta_2$ (late-early), $\gamma_1$ (leaky-late), and $\gamma_2$ (true late) [19,20]. Structural proteins and glycoproteins, produced during late gene expression, accumulate in the nucleus to begin capsid formation and encapsidation of viral genomes [21]. The mature nucleocapsid buds into the inner nuclear envelope, de-envelopes through the outer nuclear envelope, and buds again into vesicles where they are then transported to the plasma membrane. This model is termed the dual envelopment pathway [22–24].

## Latency

A defining characteristic of human herpes simplex virus infection is the establishment of lifelong latent infection in neural ganglia. After productive replication in epithelial mucosal tissue, HSV can infect innervating sensory or autonomic nerves and travel to the cell body nucleus using the molecular motor protein dynein [25]. Upon entering the nucleus, the viral genome circularizes and is chromatinized through the binding of nucleosomes, silencing the expression of almost all HSV genes [26–28]. During latency, a large viral transcript called the latency-associated transcript (LAT) is expressed that functions as a micro-RNA precursor and regulates viral gene expression to promote latency [29]. The diminished expression of viral proteins during latency allows HSV to evade host immune responses and persist in a quiescent state until reactivation. Although the host and viral factors that regulate latency and reactivation are not well understood, activation of neuronal stress pathways is important for kickstarting lytic gene expression from latent HSV genomes [30]. With reactivation, new viral particles are produced that can then travel anterograde back to the original site of infection [31].

## Genetic Determinants of Neurovirulence

Critical to the HSV life cycle is the counteraction of host antiviral responses by viral accessory proteins. Remarkably, approximately half of the genes encoded in the HSV-1 genome are dispensable for replication in vitro, suggesting that a considerable number of genes exist to aid with in vivo pathogenesis [32,33]. Several of these genes encode proteins that directly or indirectly interfere with the host antiviral response. Infected cell protein 0 (ICP0) performs several different functions that promote viral replication at low multiplicities of infection (MOI)

or in vivo. One of the most important functions of ICP0 is the targeting of host proteins for degradation through its E3 ubiquitin ligase activity [34]. Once the viral genome reaches the nucleus, the host cell attempts to silence viral gene expression by trapping the genome in repressive promyelocytic leukemia nuclear bodies (PML-NBs) [35]. ICP0 counters PML-NB entrapment by targeting components of PML-NBs for degradation [36]. While this function is not essential during in vitro replication at a high MOI, deletion of ICP0 severely impairs in vivo pathogenesis and reactivation [37,38].

The tegument protein VP22 is important for in vivo replication and neurovirulence [39]. Two dileucine motifs in VP22 are essential for the proper cellular localization of VP22 and full expression of other viral proteins. A mutant virus with these two motifs altered had greatly reduced replication in the central nervous system (CNS) of mice compared to wild-type virus and a corresponding decrease in mortality [40]. More recently, VP22 has been shown to inhibit the absent in melanoma 2 (AIM2) inflammasome, a cytoplasmic DNA sensor that initiates a proinflammatory response upon recognizing the HSV genome. HSV-1 with deleted VP22 is unable to replicate to high levels in mouse brains, but full replication capability is restored in $AIM2^{-/-}$ mice, indicating that VP22 is important for neurovirulence [41].

Perhaps the most important HSV neurovirulence factor is infected cell protein 34.5 (ICP34.5). ICP34.5 has long been known to be critical for replication in neurons and ICP34.5-deleted viruses have greatly reduced neuroinvasion, neurovirulence, establishment of latency, and reactivation [42–45]. Both HSV-1 and HSV-2 express ICP34.5, although several strain-specific differences have been identified. The C-terminus of ICP34.5 is well-conserved between HSV-1 and HSV-2 and contains a GADD34 domain that is responsible for preventing host

translational shutoff [46,47]. This domain counteracts the protein kinase R (PKR)-mediated phosphorylation of eIF2, a translation initiator, therefore inhibiting the host shutoff response during infection [46,47]. By contrast, the N-terminus of ICP34.5 is not conserved between HSV-1 and HSV-2. In HSV-1, the ICP34.5 N-terminus contains a Beclin-binding domain that inhibits autophagy [48]. We previously showed that this domain is important for neurovirulence in adult mice but not neonates, suggesting an age-dependent difference in protective autophagy during HSV encephalitis [49]. HSV-1 ICP34.5 also has a TANK-binding kinase 1 (TBK1)-binding domain in its N-terminus that inhibits interferon-regulatory factor 3 (IRF3) activity and interferon beta (IFNβ) expression [50,51]. Only HSV-1 ICP34.5 contains proline-alanine-threonine repeats in the central region that are critical for neuroinvasion [52,53]. The HSV-2 ICP34.5 C-terminus is comparatively less well-characterized, with no Beclin-binding or TBK1-binding domains being reported. HSV-2 ICP34.5, unlike its HSV-1 counterpart, contains an intron and is alternatively spliced into several isoforms [54–56]. The function of these isoforms and the advantages that they confer to HSV-2 are not well characterized.

**Disease Manifestations**

While HSV-1 has traditionally been associated with oral infection and HSV-2 with genital infection, either serotype can infect each site and the rate of HSV-1-associated genital cases is increasing [57–61]. Transmission of HSV begins when an uninfected individual comes into contact with mucosal secretions or skin from an infected individual actively shedding virus [62]. In immunocompetent individuals, primary HSV infection is often asymptomatic, with retrospective studies demonstrating only 20 to 25 percent of seropositive individuals having a

history of herpetic lesions [63,64]. When symptomatic, primary HSV-1 oral infection commonly presents as gingivostomatitis in children and severe pharyngitis in adults [65,66]. During reactivation, painful ulcerative lesions can develop at mucosal sites that are often preceded by a prodrome of burning or "tingling" at the site of recurrence [67,68].

Rarely, patients can present with more severe manifestations of HSV infection. Herpes simplex encephalitis (HSE) is the most common cause of sporadic fatal encephalitis and occurs when the virus gains access to the CNS during primary infection or reactivation [69]. In the absence of prompt antiviral treatment, over 70 percent of HSE cases will lead to mortality, and approximately 2 percent of survivors will regain normal neurological function [70,71]. Even with acyclovir treatment, morbidity and mortality remain high in HSE [70,72]. Understanding how and why some patients develop encephalitis while others remain asymptomatic is an active area of research.

## IMMUNE RESPONSES TO HSV

### The Innate Immune Response

At the center of the innate immune response to HSV-1 is the type I interferon (IFN) response. The type I IFN response is initiated when host pattern recognition receptors (PRRs) recognize pathogen-associated molecular patterns (PAMPs). PRRs that initiate this response include the Toll-like receptors (TLRs) and the cytosolic nucleic acid sensors, such as RIG-I and cGAS. Signaling after PRR activation requires the recruitment of an adaptor protein; most TLRs use MyD88 while cytosolic nucleic acid sensors use MAVS and STING. The exception is TLR3, which signals through TRIF [73,74]. Downstream of adaptor activation is the activation of

transcription factors that subsequently translocate to the nucleus. The transcription factors IRF3 and IRF7 induce transcription of IFNα and IFNβ [75,76]. These cytokines act in an autocrine and paracrine manner to induce an antiviral state in neighboring cells. The transcription factor NF-κB induces production of pro-inflammatory cytokines and chemokines, which are involved in the recruitment of immune cells and induction of the inflammatory response [77]. Upon interaction of type I IFNs with IFN receptors, JAK/STAT pathways are activated resulting in the phosphorylation of the transcription factor STAT1. Phosphorylated STAT1 dimerizes and translocates to the nucleus to upregulate several interferon-stimulated genes (ISGs) [78].

Interferon-stimulated genes are critical for effectively halting HSV replication. HSV nucleic acids are recognized by TLR3 and TLR9, which sense cytosolic viral double-stranded RNA and unmethylated CpG-rich double-stranded DNA, respectively [79,80]. The viral glycoproteins gH/gL and gB are also recognized by TLR2 [81]. In addition to recognition by TLRs, HSV is also recognized by cytosolic nucleic acid sensors. cGAS is a cytosolic DNA sensor that has been shown to initiate the type I IFN cascade during HSV-1 infection [82]. One ISG critical for controlling HSV replication is IFI16, which accumulates on the viral genome to suppress viral gene expression [83]. The importance of the type I IFN response in HSV infection is highlighted by studies using mice with components of the response knocked out [84,85].

**The Inflammasome Response**

A critical aspect of the innate immune response to infection is the release of proinflammatory cytokines and recruitment of leukocytes. Inflammasomes are large signaling platforms that initiate this response when they recognize pathogens and other host cell danger signals.

Inflammasome activation is initiated by engagement of pattern-recognition receptors (PRRs) and results in the downstream activation of caspase-1, leading to the processing and release of the pro-inflammatory cytokines interleukin-1β (IL-1β) and IL-18, and a lytic form of cell death called pyroptosis [86]. Once activated, canonical inflammasomes recruit the adaptor protein apoptosis-associated speck-like protein containing a caspase activation and recruitment domain (ASC) [86]. ASC serves to recruit procaspase-1, which is subsequently cleaved to its active form. Active caspase-1 can then cleave and activate pro-IL-1β, pro-IL-18, and gasdermin-D. Activated gasdermin-D acts as a pore-forming complex, leading to lysis of the host cell and release of the now-activated proinflammatory cytokines [86]. Several inflammasome PRRs have been described from the NOD-like receptor (NLR) family, including NLRP1, NLRC4, and NLRP3. These receptors are activated by a diverse range of PAMPs and DAMPs. Another well-characterized inflammasome PRR, absent-in-melanoma-2 (AIM2), responds to cytosolic double-stranded DNA [87].

HSV-1 is known to trigger several inflammasome PRRs, including NLRP3 and AIM2 [41,88,89]. The significance of this response depends largely on the context of infection. Components of the inflammasome response have been found to be protective. IL-1β knockout mice had increased susceptibility to HSE, suggesting that some minimal level of proinflammatory response is necessary to control infection [90]. IL-18 has also been shown to be protective in mouse models of HSV-1 pneumonitis and HSV-2 genital infection [91–93]. Likewise, NLRP3 knockout mice have been shown to have more severe ocular disease in models of herpes stromal keratitis [94]. By contrast, there is some evidence that inflammasome activation may be detrimental in the brain. IL-1β has been shown to trigger reactivation of HSV

from neurons [95]. Additionally, a high IL-1β to IL-1 receptor antagonist ratio in cerebrospinal fluid (CSF) has been associated with poorer outcomes in HSE [96]. Elucidating the role of inflammasomes in HSE is important for proper targeting of a potentially detrimental host response.

**Age-dependent Susceptibility**

Despite the high prevalence of HSV-1 seropositivity in adults, infection is often asymptomatic and rarely results in encephalitis [97]. Neonatal HSV infection is estimated to occur in approximately 1 in 3,200 live births [98]. In contrast to adult infection, approximately 50% will survive with severe morbidity and one third will develop CNS disease [4,99]. Although several genetic studies have identified mutations in innate immune pathways that confer increased susceptibility of neonates to HSE, these mutations alone do not account for the significantly higher incidence and poor outcome of HSV infection in this age group [100–105]. This suggests that developmental factors, in addition to differences in the innate immune response, likely contribute to this difference.

Recent studies have focused on differences in the immune responses between neonates and adults. Neonates are known to have a predominant $T_H2$ T cell response which is critical for protection against placental and fetal damage [106]. Neonatal monocytes also show decreased production of the pro-inflammatory cytokines TNF, IFNα, IFNγ, and IL-1β when stimulated [106]. Although this may suggest a quantitatively dampened response in the neonate, monocytes isolated from neonates surprisingly show higher levels of IL-6, IL-8 and IL-10 elaboration [107]. These studies suggest that the neonatal and adult immune system may be qualitatively different.

Several studies have identified age-dependent differences in the host response to HSV-1 infection. Early studies identified a correlation between relatively resistant strains of mice with the production of high titers of type I IFNs [108]. Peripheral inoculation of newborn mice with HSV-1 was found to result in reduced natural killer cell activation and type I IFN production compared to adults [109] Previous work in our lab has expanded upon the role that the type I IFN response plays in age-dependent susceptibility to HSV-1. Protein levels of several components of the type I IFN response were found to be lower in neonatal mouse brains compared to adults, including the IFNAR and PKR [110]. Interestingly, protein levels of other components were found at lower levels in adults (STAT1, TBK1, cGAS, and TLR3) while STING was found at comparable levels [110], supporting the idea of a qualitatively different immune environment rather than global type I IFN downregulation. More recently, we demonstrated that treatment with exogenous IFNβ improved mortality in neonatal mice during infection and decreased blood brain barrier permeability, indicating that the type I IFN response is an important, although likely not the only, driver of increased susceptibility [111]. Further study is needed to identify other key pathways that contribute to the susceptibility of this vulnerable population.

# CHAPTER II: MATERIALS AND METHODS

## VIRUSES

HSV-1 KOS and F were propagated in Vero cells and stored in -80℃ until use. Plaque assays were used to determine viral titers as described previously [112]. Clinical HSV-2 isolates were collected from neonates enrolled in clinical studies [72,113,114] by the Collaborative Antiviral Study Group (CASG) at the University of Alabama at Birmingham (UAB) and have been previously described, sequenced, and published [115]. Samples were collected from either the cerebrospinal fluid (CSF) or skin at the time of diagnosis. The clinical morbidity score was determined at 12 months of life as previously defined [70,114]. HSV-2 stocks were prepared by passaging three times on MRC-5 cells, and titering on U2OS cells, as previously described [115].

## CELLS

Vero cells (ATCC, CCL-81), human epithelial bone osteosarcoma U2OS cells (ATCC, HTB-96), and Lund human mesencephalic cells (LUHMES; ATCC, CRL-2927) were cultured under standard conditions. Cells were tested for mycoplasma using the MycoAlert Mycoplasma Detection Kit (Lonza, LT07-118). Primary astrocytes and microglia were isolated from both male and female 6–8-week-old WT or $ASC^{-/-}$ C57BL/6J mice by first generating single-cell suspensions using the Neural Tissue Dissociation Kit (P) (Miltenyi Biotec, San Diego, CA) following the manufacturer's manual dissociation protocol. Astrocytes and microglia were then

sequentially isolated using the anti-ACSA-2 and anti-CD11b microbead kits (Miltenyi Biotec) according to the manufacturer's protocol. Primary cells were maintained in complete Dulbecco's modified Eagle medium (DMEM + 10% FBS + 1% L-glutamate + penicillin/streptomycin) for one week prior to infection.

LUHMES were differentiated as previously described [116,117]. Briefly, cells were changed to DMEM-F12 media (Gibco #12634010) containing N-2 supplement (Invitrogen #17502-048) GlutaMAX (Gibco #35050061), doxycycline at a final concentration of 1ug/ml, dibutyryl cyclic AMP at a final concentration of 1mM (db-cAMP; Sigma #D0627), and GDNF at a final concentration of 2 ng/ml (R&D Systems #212-GD-010). All experiments were conducted with LUHMES following five days of differentiation, at which point they appeared morphologically neuronal with extensive interconnected neural processes, and stained positive for the mature neuronal markers MAP2 and SMI31.

**CELL INFECTIONS**

For glial co-culture infections, 1.5 x $10^5$ cells were infected at an MOI of 5 with HSV-1 KOS diluted in 0.3 mL PBS-GCS. PBS-GCS alone was used for mock infections. Cells were incubated with the inoculum and gently rocked at 37°C for 2 hours. The inoculum was then aspirated, and cells were washed twice with PBS before replacing the growth media. Cellular RNA was isolated 12 hours later using TRIzol reagent (Thermo Fisher Scientific) according to the manufacturer's protocol and quantified using a NanoDrop 1000.

For HSV-2 growth curves, differentiated LUHMES were infected at an MOI=0.1. At 1 hpi, virus was removed and fresh media containing 1% human serum was added to reduce cell-free spread of virus. Virus was collected at each timepoint and quantified by titer on U2OS cells. For Meg3 experiments in LUHMES, cells were nucleofected with expression plasmids at day 2 of differentiation using the Basic Nucleofector Kit for Primary Mammalian Neurons (Lonza VPI-1003) and the Nucleofector 2b device as previously described [118]. pCI-MEG3 was a gift from Anne Klibanski (Addgene plasmid # 44727) [119]. Meg3 overexpression was confirmed by quantitative PCR at day 5 of differentiation. Infections were carried out on day 5 of differentiation. LUHMES were infected in either 96-well or 24-well plates at a multiplicity of infection of 5. After one hour of incubation, the inoculum was aspirated and replaced with fresh differentiation media. Caspase-3 activity was measured at 6 hours post-infection using the fluorometric Caspase-3 Assay Kit (Abcam ab39383) according to the manufacturer's instructions. TUNEL assays were conducted at 6 hours post-infection using the TiterTACS In Situ Detection Kit (R&D Systems #4822-96-K).

**MURINE MODELS OF HSV INFECTION**

Viral stocks were diluted to the appropriate concentration in phosphate-buffered saline containing 1% heat-inactivated serum and 0.1% glucose (PBS-GCS). To control for possible immune stimulation by cell debris in the viral inoculum, stocks for mock infections were prepared by diluting supernatant from mock-infected Vero cells to the same dilution factor as

viral stocks with PBS-GCS. Wild-type C57BL/6J mice were obtained from the Jackson Laboratories (#000664). C57BL/6J NLRP3$^{-/-}$ and ASC$^{-/-}$ mice were obtained from Karen Ridge (Northwestern University) and Christian Stehlik (Northwestern University), respectively, and have been described previously [120,121]. C57BL/6J AIM2$^{-/-}$ mice were obtained from the Jackson Laboratories (#013144).

**Intracranial infections**

Viral inoculum or diluted Vero supernatant were delivered in 10 μL using a positive displacement syringe and 26-gauge needle with a needle guard. The needle was placed through the right parietal bone, lateral to the sagittal suture and equidistant to the lambda and bregma. For survival experiments, mice were weighed daily over the course of the 14-day experimental period and were sacrificed if they lost 30% of their starting weight. For time course tissue titering experiments, mice were infected as described above and sacrificed at the appropriate time point. Brains were collected for viral titering at mortality or the end of the experiment and homogenized in 1 mL DMEM containing penicillin/streptomycin and sonicated.

**Intraperitoneal infections**

Intraperitoneal infections were performed as previously described [122]. A 1000 PFU dose was delivered intraperitoneally in 50 μL. Mice were weighed daily over 14 days and sacrificed if they lost 30% of their starting weight. Organs were collected from each mouse at mortality or the conclusion of the experiment. Each organ was processed for viral titer as described above.

**Stereotaxic infections**

Neonatal and adult C57BL/6J mice (Jackson Laboratories #000664) were stereotaxically infected at P7 and 8-9 weeks of age, respectively. For both adult and neonate infections, $3x10^4$ PFU of HSV-1 strain F was delivered in 0.5 µL to the approximate location of the dentate gyrus using a Hamilton syringe. Neonatal injections were carried out semi-stereotaxically. P7 pups were marked at the nasion, equidistant to each eye, and sedated by placing them on ice for 4 minutes. Once sedated, injection points were marked using a stereotaxic apparatus at the approximate location of the dentate gyri (RC = -1.5 mm, ML = 1.5 mm, DV = 1.5 mm). Injections were carried out manually with a 30 second pause after needle insertion and before withdrawal. For adults, mice were anesthetized with 3% isoflurane and maintained under anesthesia with 2% isoflurane while in the stereotaxic apparatus. Before surgery, mice were given subcutaneous Buprenex at a concentration of 0.1 mg/kg. The top of the head was shaved and scrubbed with Betadine. After exposing the skull, a small hole was drilled at the correct coordinates relative to bregma (RC = -2.0 mm, ML = 1.5 mm, DV = 1.9 mm). The needle was slowly lowered to the injection site and paused for five minutes. 0.5 µL of inoculum was delivered over five minutes. The needle was slowly removed five minutes after injection. The skull was washed with sterile PBS before wound closure with staples. Mice were given meloxicam subcutaneously at a dose of 5 mg/kg at the end of the surgery.

**CYTOKINE QUANTIFICATION**

For brain cytokine quantification, mice were inoculated with 3 x $10^4$ PFU HSV-1 KOS and sacrificed at the appropriate time point. Whole brain homogenates were generated by Dounce homogenization in 1 mL of Tissue Protein Extraction Reagent (Thermo Scientific). IL-1β (BMS6002), IL-18 (BMS618-3), and CCL6 (EMCCL6) ELISA kits (Thermo Fisher) were used according to the manufacturer's instructions.

**FLOW CYTOMETRY**

Mice were inoculated with 3 x $10^4$ PFU HSV-1 KOS or mock-infected and sacrificed by transcardial perfusion with PBS at day 3 post-infection. Brains were dissociated using the Neural Tissue Dissociation Kit (P) (Miltenyi Biotec). For enumeration of infiltrating leukocytes, cells were first treated with TruStain FcX anti-CD16/32 antibody (Fc block-BioLegend; 93) before staining with the following antibodies: Ly6G APC-Cy7 (BioLegend; RB6-8C5), CD11c APC (BioLegend; N418), and CD11b BV421 (BD; M1/70). Flow cytometry was performed on a FACS CantoII (BD Biosciences, San Jose, CA, USA) and analyzed using FlowJo 10.1 software (Ashland, OR, USA).

For fluorescently labeled inhibitor of caspase activity (FLICA) assays, cell suspensions were first incubated with a 1:1000 dilution of Live/Dead Fixable Aqua Dead Cell Stain Kit (Thermo Fisher Scientific) before incubation with the FAM-FLICA reagent according to the manufacturer's protocol (ImmunoChemistry Technologies). Cells were treated with an Fc-blocking reagent (Fc block-BioLegend; 93) and stained with the following antibodies before being analyzed: ACSA-2 PE (Miltenyi Biotec; REA969), CD45 PerCP-Cy 5.5 (BD Biosciences;

30-F11), and CD11b PE-Cy7 (eBioscience; M1/70). Gating of positive populations was based on Fluorescence minus one control (FMO) samples.

**QUANTITATIVE PCR**

Cellular RNA from glial cell infections was reverse transcribed using the RT2 First Strand Kit (QIAGEN) with 0.4 µg RNA per sample. The relative expression of 84 pro-inflammatory cytokines and chemokines was then quantified using the RT2 Profiler PCR Array PAMM-011Z (QIAGEN). Gene expression was analyzed with the RT2 Profiler PCR Array analysis software from the GeneGlobe Data Analysis Center using the ΔΔCt method with a Ct cutoff of 35. Expression was normalized to the housekeeping gene Gapdh. Genes for which fewer than three samples per group had detectable levels of transcript were excluded from analysis. P values were calculated based on a two-tailed Student's t-test of 2-ΔCt values for each gene and $p<0.5$ was considered significant. Relative gene expression was visualized using the freely available online tool Heatmapper [123].

For verification of *Meg3* overexpression in LUHMES, RNA was isolated at day 5 of differentiation using the RNEasy Plus Mini Kit (QIAGEN # 74134) according to the manufacturer's protocol and quantified using a NanoDrop 1000. RNA was reverse transcribed using the High-Capacity cDNA Reverse Transcription Kit (ThermoFisher # 4368814) with 0.5 µg RNA per sample. qRT-PCR was carried out using SYBR Green Master Mix (ThermoFisher #4309155) in 96-well plate format on a StepOnePlus real-time PCR instrument (Applied Biosystems). The following forward and reverse primers were used: for Gapdh, 5'-

TGGTATCGTGGAAGGACTCATGAC-3’ and 5’-ATGCCAGTGAGCTTCCCGTTCAGC-3’; for Meg3, 5’-CAGGATCTGGCATAGAGGAGG-3’ and 5’-GAGGATGCTTGGCAGGAGATGG-3’. The run started with 95°C for 20 s, followed by 40 cycles of the following: 95°C for 3 s, 60°C for 30 s. Results were calculated using the ΔΔCt method with glyceraldehyde-3 phosphate dehydrogenase (Gapdh) used as an endogenous control. Fold gene expression changes were calculated relative to the average of the control vector samples.

**ORGANOTYPIC BRAIN SLICE CULTURES**

Brain slice cultures were prepared from P6-10 neonatal mice as described previously [122]. Membranes with brain slices were placed in six-well plates with 1 mL of filter culture media [50% (vol/vol) minimal essential media, 25% (vol/vol) HBSS, 25% (vol/vol) heat-inactivated horse serum, 0.044% $NaHCO_3$, 2 mM glutamine, 10 U/mL penicillin]. Slices were cultured for 24 hours before being transferred to filter culture media containing either 25 mg/mL clodronate-containing liposomes or an equivalent concentration of empty liposomes (Encapsula NanoSciences). Slices were then cultured for six days in clodronate-containing media or media with empty liposomes with the media changed every two days. After six days in liposome-containing culture, slices were infected with 106 PFU of HSV-1 KOS in 1 mL of PBS-GCS. After two hours, the viral inoculum was aspirated, and membranes were transferred to fresh filter culture media. Media was collected for ELISA analysis at 48 hours post-infection.

## HIPPOCAMPAL TISSUE COLLECTION

At 48 hours post-infection, mice were anesthetized and rapidly decapitated. Brains were extracted and placed in an ice-cold brain block (Ted Pella). Pre-chilled razor blades were used to slice a 2 mm thick coronal section at the site of infection. The section was transferred to a petri dish containing cold Hibernate-A media (Gibco #A1247501) and a 2 mm punch biopsy was used to isolate hippocampal tissue at the site of infection bilaterally. The tissue was transferred to a 2 mL cryotube and immediately flash-frozen in liquid nitrogen. Tubes were stored at -80C until processed for single-nucleus sequencing.

## NUCLEI ISOLATION

Nuclei were isolated from frozen tissue and labeled with hashtag oligos as described previously, with some modifications [124]. RNAse inhibitor (Applied Biosystems; N8080119) was added at a final concentration of 40U/mL to NP40 lysis buffer (NST buffer) and wash buffer. Frozen tissue from each mouse were processed separately by Dounce homogenization in 1 mL of NST buffer (0.1% NP-40 Alternative, 10mM Tris, 146mM NaCl, 1mM CaCl2, 21mM MgCl2), 20 times with a loose pestle followed by 20 times with a tight pestle. 1 mL of wash buffer (10mM Tris, 146mM NaCl, 1mM CaCl2, 21mM MgCl2, 0.01% BSA) was added to the homogenate and mixed before filtering through a 30 μm filter (Miltenyi Biotec; 130-041-407) into a 15 mL conical tube. The Dounce homogenizer was washed three times by adding 1 mL of

wash buffer and filtering through the 30 μm filter. Nuclei were pelleted by centrifugation at 500g for 5 minutes at 4°C in a swinging bucket rotor. The nuclei pellet was resuspended in 200 μL of staining buffer (2%BSA, 0.02%Tween-20, 10mM Tris, 146mM NaCl, 1mM CaCl2, 21mM MgCl2) and filtered through a 20 μm filter (Miltenyi Biotec; 130-101-812) into a LoBind 1.5 mL tube (Eppendorf; 22431081). 10 μL of Fc blocking reagent (Biolegend; 422302) was added to the nuclei suspension and incubated at 4°C for 5 minutes. 1 μg of the corresponding hashtag oligo (Biolegend; TotalSeq™ MAb414) was then added to each sample and incubated at 4°C for 10 minutes. Nuclei were then washed 3 times in 1.2 mL of staining buffer by centrifugation at 500g. Each nuclei sample was resuspended in 200 μL of staining buffer, pooled, and filtered through a 20 μm filter before centrifugation. The pooled nuclei pellet was resuspended in 55 uL of staining buffer for loading onto the 10X Chromium Controller.

**LIBRARY PREPARATION AND SEQUENCING**

Nuclei number and viability were analyzed using Nexcelom Cellometer Auto2000 with AOPI fluorescent staining method. Sixteen thousand nuclei were loaded into the Chromium Controller (10X Genomics, PN-120223) on a Chromium Next GEM Chip G (10X Genomics, PN-1000120), and processed to generate single cell gel beads in the emulsion (GEM) according to the manufacturer's protocol. The cDNA and library were generated using the Chromium Next GEM Single Cell 3' Reagent Kits v3.1 (10X Genomics, PN-1000286) and single Index Kit T Set A (10X Genomics, PN-1000213) according to the manufacturer's manual. The nuclei hashing library was constructed according to BioLegend's published protocol on HTO library preparation

guideline with single index adapters. Quality control for constructed libraries was performed using the Agilent Bioanalyzer High Sensitivity DNA kit (Agilent Technologies, 5067-4626) and Qubit DNA HS assay kit for qualitative and quantitative analysis, respectively. The multiplexed libraries were pooled and sequenced on an Illumina HiSeq 4000 sequencer with 2 × 50 paired-end kits using the following read length: 28 bp Read1 for cell barcode and UMI, and 90 bp Read2 for transcript.

## SINGLE NUCLEUS RNA SEQUENCING ANALYSIS

Raw FASTQ files were processed using the Cell Ranger 6.0.0 pipeline. Reads were aligned to a custom reference genome containing the GRCm38 mouse reference genome with the HSV-1 strain F reference genome appended using the Cell Ranger mkref function13.

### Quality Control

Seurat objects were created from count matrices for each sample using the Seurat v4 package in R [125]. Cells that contained fewer than 200 or more than 2500 unique features were filtered out. Additionally, hashtag oligos for each sample were demultiplexed and analyzed to ensure that each sample contained nuclei from four mice in roughly equal proportions. To do this, hashtag oligo UMI count matrices were generated for each sample using CITE-Seq-Count. Each sample was then demultiplexed and visualized according to the Seurat hashtag oligo demultiplexing vignette.

**snRNA Integration Analysis**

Seurat objects for each sample were separately normalized using the SCTransform function of Seurat and a set of 3000 integration features were selected using the SelectIntegrationFeatures function. After integration, principal component analysis was performed using the RunPCA function with default settings. Clustering was performed using the FindClusters function with a resolution of 0.5. The integrated dataset was plotted on UMAP plots and individual clusters were assigned to known cell types based on canonical marker gene expression.

**Differential gene expression analysis**

For DEG analysis of cell types between conditions, Seurat objects containing only the cell type in question were created using the subset function. Differentially expressed genes were then identified using the FindMarkers function in Seurat. Volcano plots were generated using the R package EnhancedVolcano [126]. Heatmaps were generated using the R package ComplexHeatmap [127]. To define a general antiviral response to HSV-1 in the neonate, DEG analysis was performed for each cell type between the neonate mock and infected samples. Genes were included in the antiviral module if they were differentially expressed in at least one cell type and minimally positively regulated during infection in all cell types (log2FC > 0.1 in all cell types). Cells were assigned an “antiviral” value based on the expression of this gene set using the AddModuleScore function. For identification of age-dependent genes, DEG analysis was performed per cell type between the neonate mock and adult mock samples. Genes that were differentially expressed in neurons, astrocytes, and microglia were included in order to focus on

DEGs applicable to multiple cell types. Genes associated with sex chromosomes or ribosomal RNA were excluded.

**Gene set enrichment analysis**

Lists of differentially expressed genes were sorted according to the direction of regulation and p-value. Genes with p-values of 1 were omitted and gene set enrichment analysis was performed using ClusterProfiler [128]. Gene sets were included if they contained 25 or more genes, 500 or fewer genes, and had a false discovery rate of 0.25 or lower.

**Trajectory analysis**

Count matrices and metadata were extracted from Seurat objects and used as inputs to create Monocle3 objects [129]. Monocle3 objects were then preprocessed using the preprocess_cds and align_cds function. Dimensionality reduction was performed using the reduce_dimension function and clusters were plotted with labels corresponding to the original cell type. Specific cell types were extracted using the choose_cells function and manual selection of the corresponding cluster. Cell-specific objects were clustered using the cluster_cells function, and the trajectory graph was learned using the learn_graph function, with the root node manually selected as the point with the lowest antiviral score, such that pseudotime increases as the antiviral score increases. Pseudotime-correlated genes were identified using the graph_test function and plotted using the plot_genes_in_pseudotime function.

### Receptor-ligand interaction analysis

Neonate mock-infected and HSV-infected samples were analyzed using the R package CellChat [130]. CellChat objects were created using data extracted from Seurat objects. Each sample was processed separately, and communication probabilities were calculated using the 5% truncated mean method. CellChat objects were then merged, and differential interactions were analyzed.

## STATISTICS

All statistics were calculated using GraphPad Prism 9.0 software. For survival experiments, logrank analysis with the Bonferroni adjustment for multiple comparisons was performed. Viral titers and cytokines were analyzed using multiple t-tests with the Holm-Sidak correction for multiple comparisons. FLICA results were analyzed using two-way ANOVA with Tukey's multiple comparison test. qRT-PCR array results were analyzed using the delta-delta Ct method with significant results determined by two-tailed t-tests of $2^{-\Delta Ct}$ values for each gene. Cell enumeration by flow cytometry was analyzed using one-way ANOVA with Dunnett's multiple comparison test. For multiple step growth curves, two-way ANOVA was performed followed by Sidak's multiple comparisons test. For organ titer comparison following death or conclusion of the experiment (bimodal data), organs were categorized as containing virions above the limit of detection or not, and one-way Fisher exact test was performed. For organ titer comparison prior to death, multiple t-tests with Welch correction were performed.

# CHAPTER III: ASC-DEPENDENT INFLAMMASOMES CONTRIBUTE TO IMMUNOPATHOLOGY AND MORTALITY IN HERPES SIMPLEX ENCEPHALITIS*

*(Adapted from Cooper K. Hayes, Douglas R. Wilcox, Yuchen Yang, Grace K. Coleman, Melissa A. Brown, and Richard Longnecker. PLOS Pathogens. 1 February 2021)

## ABSTRACT

Herpes simplex virus encephalitis is the most common cause of sporadic viral encephalitis, and despite targeted antiviral therapy, outcomes remain poor. Although the innate immune system is critical for restricting HSV-1 replication in the brain, there is evidence that prolonged neuroinflammation contributes to HSE pathogenesis. In this study, we investigated the contribution of inflammasomes to disease pathogenesis in a murine model of HSE. Inflammasomes are signaling platforms that activate the pro-inflammatory cytokines IL-1β and IL-18. We found that mice deficient in the inflammasome adaptor protein, ASC, had significantly improved survival and lower levels of IL-1β and IL-18 in the brain. Importantly, this difference in survival was independent of viral replication in the central nervous system. We found that microglia, the resident macrophages of the CNS, are the primary mediators of the ASC-dependent inflammasome response during infection. Using in vitro glial infections and a murine HSE model, we demonstrate that inflammasome activation contributes to the expression of chemokine (C-C motif) ligand 6 (CCL6), a leukocyte chemoattractant. The lower concentration of CCL6 in the brains of $ASC^{-/-}$ mice correlated with lower numbers of infiltrating macrophages during infection. Together, these data suggest that inflammasomes contribute to

pathogenic inflammation in HSE and provide a mechanistic link between glial inflammasome activation and leukocyte infiltration. The contribution of inflammasomes to survival was independent of viral replication in our study, suggesting a promising new target in combating harmful inflammation in HSE.

## INTRODUCTION

Herpes simplex virus type I (HSV-1) is a neurotropic virus and the most common cause of viral encephalitis [69]. Despite antiviral therapy targeted to control viral replication, morbidity and mortality in herpes simplex encephalitis (HSE) remains high [131]. Although the innate immune system is critical for controlling early viral replication [110,122], there is evidence to suggest that excessive neuroinflammation may play a detrimental role during infection. In particular, the prolonged activation of microglia, the resident macrophages in the central nervous system (CNS), and recruitment of infiltrating leukocytes to the brain contribute to pathology in HSE [132,133]. Cytokines and other markers of inflammation are elevated in the cerebrospinal fluid of patients, even months after symptoms have resolved [134]. Taken together, these data suggest that the immune response to HSV in the brain represents a careful balance between controlling viral replication and immune-mediated damage [135], but the specific innate signaling pathways that contribute to this balance are unknown.

Inflammasomes are pro-inflammatory signaling platforms that respond to pathogens and host cell danger signals. Inflammasome activation is initiated by engagement of pattern-recognition receptors (PRRs) and results in the downstream activation of caspase-1, leading to the processing and release of the pro-inflammatory cytokines interleukin-1β (IL-1β) and IL-18,

and a lytic form of cell death called pyroptosis [86]. Canonical inflammasomes, including the NOD-, LRR- and pyrin domain-containing 3 (NLRP3) and absent in melanoma 2 (AIM2) inflammasomes, require the adaptor protein apoptosis-associated speck-like protein containing a caspase activation and recruitment domain (ASC) [86]. The inflammasome signaling pathway is implicated in the pathogenesis of many neurologic diseases, including autoimmune encephalomyelitis, ischemic stroke, and neurodegenerative diseases [136–138].

The role of inflammasomes in the pathogenesis of viral infections is complicated, with inflammasomes shown to be protective in some disease models and detrimental in others [139–143]. Recent work has demonstrated that HSV-1 activates several inflammasomes in vitro and in vivo, including NLRP3 and AIM2 [41,88,89,144,145]. However, these studies have been largely limited to models of intraperitoneal and ocular infection. Intraperitoneal inoculation with high doses of HSV-1 led to higher viral titers in the brains of $NLRP3^{-/-}$ mice, suggesting that the NLRP3 inflammasome may limit neuroinvasion [145]. In a model of herpes stromal keratitis, $NLRP3^{-/-}$ mice demonstrated a more robust early immune response, suggesting that NLRP3 plays an immunomodulatory role in corneal infection [94]. The role that inflammasomes play in HSV infection of the central nervous system, and the specific cell populations that drive this response, are unknown.

In this study, we investigated the contribution of inflammasomes in a murine model of HSE. We found improved survival in $ASC^{-/-}$ mice compared to wild-type (WT), but no difference in survival between $NLRP3^{-/-}$ and $AIM2^{-/-}$ mice. These results corresponded with a decrease in pro-inflammatory cytokines in the brains of $ASC^{-/-}$ mice. Interestingly, this difference in immune response was independent of viral replication. We identified microglia as

key mediators of the inflammasome response during HSE and found that glial inflammasome activation is necessary for the expression of the monocyte chemoattractant CCL6. Accordingly, $ASC^{-/-}$ mice had reduced numbers of infiltrating macrophages during HSE.

## RESULTS

### The inflammasome adaptor protein ASC contributes to mortality during HSE

The role of inflammasomes in the pathogenesis of viral infections depends on both the virus and the target organ host response, with inflammasomes serving a protective role in some disease models and a detrimental one in others [140,143,146]. IL-1β knockout mice exhibit increased susceptibility to infection in an intranasal model of HSE [90]. Therefore, we hypothesized that inflammasome knockout mice would also be more susceptible to disease in a model of herpes simplex encephalitis. Direct intracranial inoculation of HSV-1 in a murine model of HSE was used to prevent any confounding impact of peripheral replication on neuroinvasiveness. WT, $NLRP3^{-/-}$, $AIM2^{-/-}$, and $ASC^{-/-}$ mice were infected and monitored for survival over 14 days. WT mice began to succumb to disease on day 4 post-infection with a mean survival time of 9.9 days, and 52.9% survived to the experimental endpoint (Fig 1A). Notably, $ASC^{-/-}$ mice had significantly improved survival compared to WT, with 93.3% of $ASC^{-/-}$ mice surviving until the experimental endpoint and a mean survival time of 13.4 days. $NLRP3^{-/-}$ and $AIM2^{-/-}$ mice did not have statistically significant differences in survival compared to WT mice (71.4% and 36.4%, respectively). This suggests that although the individual inflammasome sensor components NLRP3 and AIM2 are dispensable for HSE survival, the common inflammasome adaptor ASC contributes to mortality.

A possible explanation for the improved survival in $ASC^{-/-}$ mice is that ASC-dependent inflammasomes directly affect HSV-1 replication in the CNS. To test this, we infected WT, $NLRP3^{-/-}$, and $ASC^{-/-}$ mice and determined viral replication in brain tissue at various time points until average time to mortality. No difference in viral titer was found at 1-, 3-, or 4-days post-infection, indicating that neither NLRP3 nor ASC contribute to controlling HSV-1 replication in the CNS (Fig 1B). These data suggest that differences in mortality between WT and $ASC^{-/-}$ mice are due to the immunomodulatory function of ASC, rather than by affecting viral replication. Following inflammasome-mediated activation of caspase-1, pro-IL-1β and IL-18 are cleaved to their activated forms to serve as the downstream mediators of the inflammasome signaling pathway. To determine the contribution of ASC-dependent inflammasomes to IL-1β and IL-18 production in HSE, we assayed mice early after infection and prior to mortality (days 1 and 3). As expected, IL-1β was low in the brains of uninfected mice but rose sharply in WT mice at days 1 and 3 post-infection (Fig 1C). $ASC^{-/-}$ mice had significantly lower IL-1β levels than WT at both time points, suggesting that ASC-dependent inflammasomes are essential for IL-1β production during HSE. $NLRP3^{-/-}$ mice expressed higher levels of IL-1β than WT at day 3 post-infection. This result suggests that NLRP3 does not contribute to IL-1β production in the brain, and may actually play an immunomodulatory role to regulate IL-1β production, as previously shown in ocular HSV-1 infection [94]. IL-18 concentrations followed a similar pattern, although $ASC^{-/-}$ mice had significantly higher levels than WT at the uninfected baseline (Fig 1D). At days 1 and 3 post-infection, WT mice had significantly higher levels of brain IL-18 than $NLRP3^{-/-}$ and $ASC^{-/-}$ mice, demonstrating that ASC-dependent inflammasomes are also essential for IL-18 production during HSE.

**Microglial ASC-dependent inflammasomes are activated during HSE**

We next sought to determine which cell types in the CNS mediate the ASC-dependent inflammasome response during HSE. Microglia are resident macrophages of the CNS and are known to secrete IL-1β under pro-inflammatory conditions [147]. Additionally, microglia have been identified as key contributors to the inflammasome response in a model of traumatic brain injury [148]. Thus, we hypothesized that microglia and infiltrating leukocytes would be the primary cell types with active inflammasome complexes during HSE. To test this hypothesis, we utilized a fluorescently labeled inhibitor of caspase activity (FLICA) assay combined with traditional flow cytometric analysis to label cells with active caspase-1. The FAM-FLICA reagent is a membrane-permeable probe that irreversibly binds to activated caspase, selectively labeling cells with activated inflammasomes. At day 3 post-infection, single-cell suspensions of dissociated brain cells were labeled with the FAM-FLICA reagent and fluorescent antibodies to identify resident CD45mid CD11b+ microglia and CD45mid ACSA-2+ astrocytes, as well as infiltrating CD45hi CD11b+ leukocytes.

Microglia exhibited robust inflammasome activation during infection as evidenced by the representative flow cytometry histograms depicting FAM-FLICA intensity from WT and $ASC^{-/-}$ mice either mock-infected or infected with HSV-1 (Fig 2A). The percentage of microglia that were FAM-FLICA+ increased significantly in both WT and $ASC^{-/-}$ mice during infection, although the percentage of FAM-FLICA+ microglia was significantly lower in infected $ASC^{-/-}$ mice compared to WT (Fig 2B). Because FAM-FLICA intensity is directly correlated with the quantity of activated caspase-1, we also measured the mean fluorescence intensity (MFI) of

FAM-FLICA in each group of mice and saw a similar increase in microglia from infected WT mice. Of note, the MFI did not significantly increase in infected $ASC^{-/-}$ microglia compared to mock infected cells (Fig 2C). Caspase-1 activity in $ASC^{-/-}$ microglia was not completely abrogated, suggesting that ASC-independent non-canonical inflammasome pathways are also activated during infection. Surprisingly, caspase-1 activity in the infiltrating CD11b+ leukocyte populations from both WT and $ASC^{-/-}$ mice did not increase during infection (Fig 2B). Astrocytes also had low levels of caspase-1 activity that did not increase with infection (Fig 2B). These data demonstrate that microglia are the key drivers of ASC-dependent inflammasome activity during HSE.

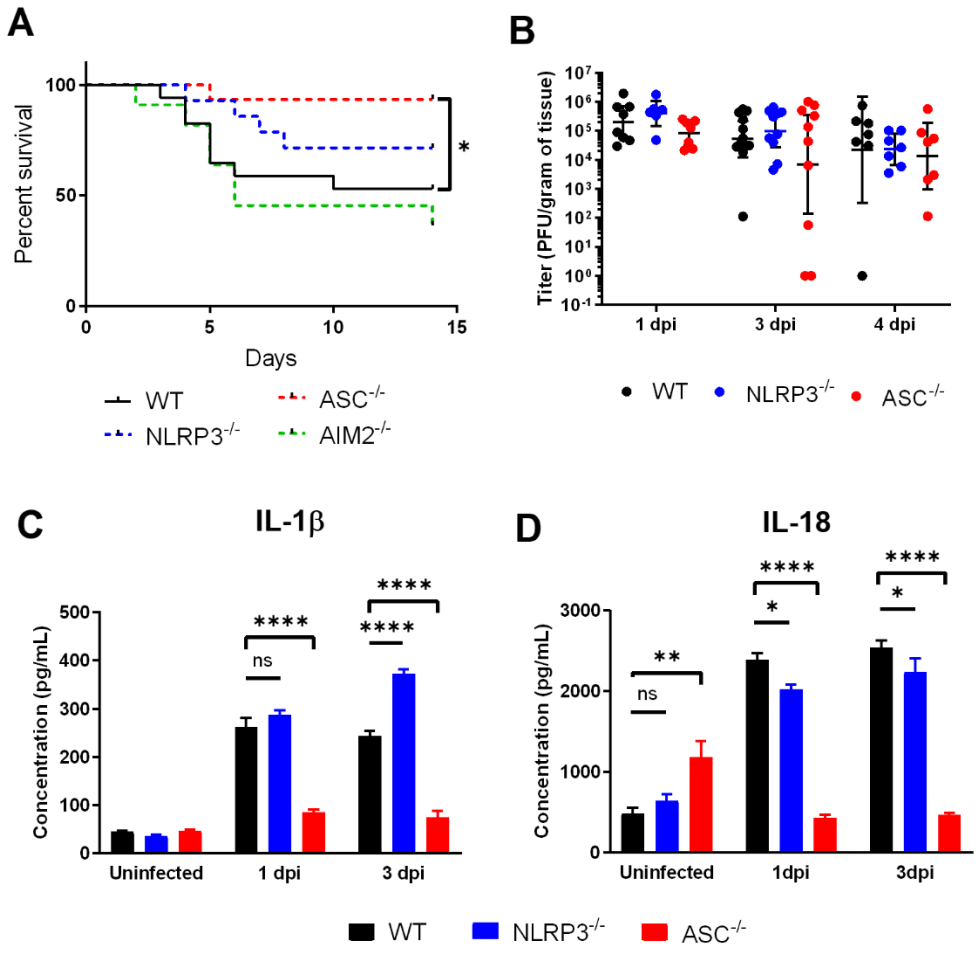
A
Percent survival
100
50
0
0
5
10
15
Days
*
WT
ASC-/-
NLRP3-/-
AIM2-/-
B
Titer (PFU/gram of tissue)
1 dpi
3 dpi
4 dpi
WT
NLRP3-/-
ASC-/-
C
IL-1β
Concentration (pg/mL)
500
400
300
200
100
0
ns
****
****
****
Uninfected
1 dpi
3 dpi
D
IL-18
Concentration (pg/mL)
3000
2000
1000
0
**
ns
****
*
****
*
Uninfected
1dpi
3dpi
WT
NLRP3-/-
ASC-/-

**Figure 1. ASC-dependent inflammasomes contribute to the pathogenesis of HSV-1 encephalitis.**

(A) Survival curve of WT (n=17), NLRP3-/- (n=14), AIM2-/- (n=11), and ASC-/- (n=15) mice infected intracranially with 3x104 PFU HSV-1 KOS. Results are combined from seven inoculations. (B) Whole brain titers of infected WT, NLRP3-/-, and ASC-/- mice at days 1, 3, and 4 post-infection (n = 7-12 per group, 8 inoculations). (C) Whole brain IL-1β and (D) IL-18 from WT, NLRP3-/-, and ASC-/- mice either before infection or at days 1 and 3 post-infection (n = 4-5 per group). Values are expressed as means ± SEM (**P < 0.01, ***P < 0.001, ****P < 0.0001).

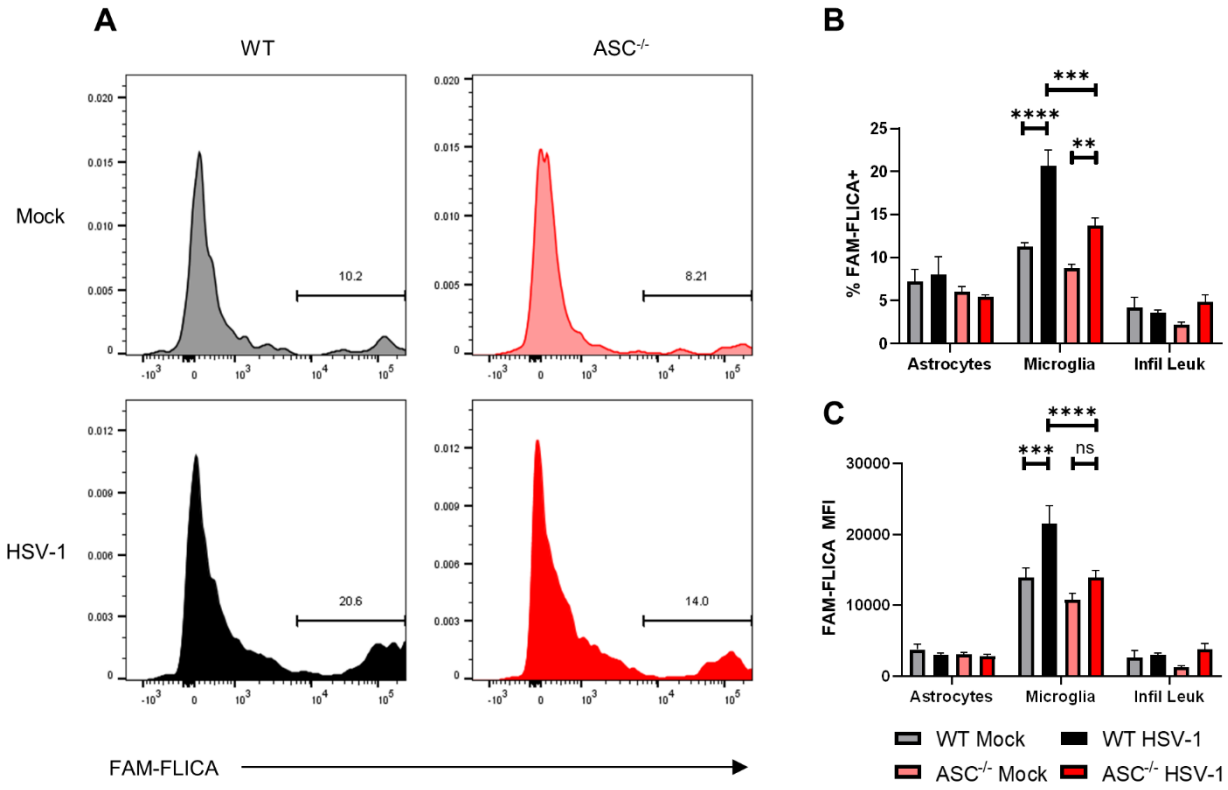
A
WT
ASC-/-
Mock
HSV-1
10.2
8.21
20.6
14.0
FAM-FLICA
B
% FAM-FLICA+
***
****
**
Astrocytes
Microglia
Infil Leuk
C
FAM-FLICA MFI
****
***
ns
WT Mock
WT HSV-1
ASC-/- Mock
ASC-/- HSV-1

**Figure 2. Microglial ASC-dependent inflammasomes are activated during HSE.**

Cell-specific caspase-1 activity was analyzed by flow cytometry and FLICA assay at day 3 post-infection following intracranial inoculation of 3 x 106 PFU HSV-1 KOS. (A) Representative flow cytometry histograms of CD45midCD11b+ microglia from mock-infected or HSV-1-infected WT and ASC-/- mice stained with FLICA reagent to quantify active caspase-1. Percentages of each cell type that are FLICA+ (B) or FAM-FLICA mean fluorescence intensity (C) in astrocytes, microglia, and CD11b+ infiltrating leukocytes (n = 3-4 mice per group). After excluding multiplets and dead cells, cells were gated using the following strategy: astrocytes CD45lo/ACSA-2+, microglia CD45mid/CD11b+, infiltrating leukocytes CD45hi/CD11b+. Values are expressed as means ± SEM (**P < 0.01, ***P < 0.001, ****P < 0.0001). Results are representative of two independent experiments.

**IL-1β production is microglia-dependent in an organotypic brain slice culture model of HSV encephalitis**

We demonstrated that microglia isolated from HSV-infected brains have increased caspase-1 activity (Fig 2). To validate the importance of microglia in inflammasome activation and IL-1β production during HSE we used an organotypic brain slice culture model of HSV-1 infection. Our group and others have previously used brain slice cultures (BSCs) to model HSV-1 encephalitis, and they are amenable to selective microglia depletion using clodronate liposomes [122,149].

Brain slices were obtained from WT mice and allowed to recover in culture for 24 hours before incubation with media containing either clodronate-containing liposomes or an equivalent concentration of empty liposomes as a control (Fig 3A). After six days of incubation with clodronate, depletion of microglia was confirmed by flow cytometry (Fig 3B). Slices were then either infected with HSV-1 or mock-infected with vehicle control and incubated for 48 hours, a time point previously determined to be associated with peak viral titer in brain slice cultures [122]. We collected culture media and quantified IL-1β by ELISA. Consistent with our prior results, IL-1β levels sharply rose after HSV-1 infection in BSCs without microglial depletion (Fig 3C). IL-1β did not increase during infection in microglia-depleted BSCs and was significantly lower at baseline than non-depleted BSCs, demonstrating that inflammasome activation and IL-1β release depend on microglia in a model of HSE (Fig 3C).

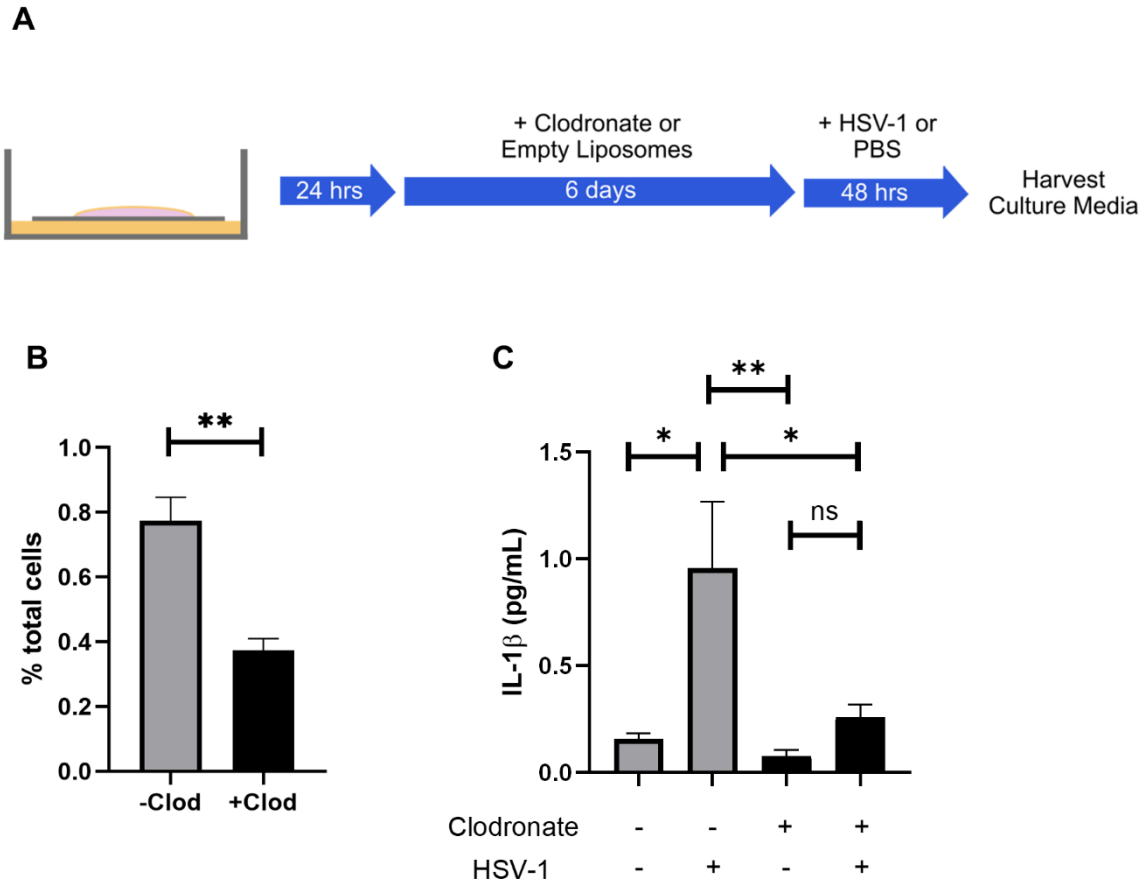
A
+ Clodronate or
Empty Liposomes
+ HSV-1 or
PBS
24 hrs
6 days
48 hrs
Harvest
Culture Media
B
**
% total cells
1.0
0.8
0.6
0.4
0.2
0.0
-Clod
+Clod
C
**
*
*
ns
IL-1β (pg/mL)
1.5
1.0
0.5
0.0
Clodronate - - + +
HSV-1 - + - +

**Figure 3. IL-1β production is microglia-dependent in an organotypic brain slice culture model of HSV encephalitis.**

Microglia were depleted from organotypic brain slice cultures by incubation with clodronate-filled liposomes and IL-1β production was quantified after HSV-1 infection. (A) Diagram of experimental set-up. Slices were allowed to settle for 24 hours in culture before incubation with either clodronate-filled or empty liposomes. Slices were then infected with $10^6$ PFU HSV-1 KOS and culture media was collected at 48 hour post-infection. (B) Microglia quantification by flow cytometry after 6 days of clodronate or empty liposome treatment (n = 4 slices per group). (C) Protein levels of IL-1β as quantified by ELISA (n = 3 slices per group). Values are expressed as means ± SEM (*$P < 0.05$, **$P < 0.01$).

**Glial inflammasome activation drives expression of the monocyte chemokine CCL6 during HSV-1 infection**

Our findings demonstrated that ASC-dependent inflammasomes increase mortality in HSE, and that microglia are the main contributors to inflammasome activity in the brain during HSV infection. To better understand the inflammasome-dependent immune signaling mechanisms in microglia that contribute to immunopathology in HSE, we screened for ASC-dependent pro-inflammatory cytokines and chemokines and validated their expression in vivo. Although microglia were identified to be the key inflammasome mediators in vivo (Fig 2, Fig 3), the innate immune response to HSV-1 has been shown to involve cross-talk between both microglia and astrocytes [150]. Therefore, we used a mixed glial cell culture model to screen for cytokines and chemokines that are induced by astrocytic or microglial inflammasome signaling. Microglia and astrocytes were isolated from WT and $ASC^{-/-}$ mice and co-cultures were established with $ASC^{-/-}$ astrocytes, $ASC^{-/-}$ microglia, or both. After in vitro HSV-1 infection, gene expression was determined by quantitative real-time PCR array. Two genes, *Ccl6* and *Il1rn*, were significantly downregulated in at least one of the culture conditions containing $ASC^{-/-}$ cells compared to cultures with only WT cells (Fig 4). *Ccl6* gene expression in $ASC^{-/-}$ astrocytes and $ASC^{-/-}$ microglia cultures was significantly lower than in the WT astrocyte and microglia cultures (Fig 5A). Thus, both astrocytic and microglial ASC contribute to CCL6 expression in vitro. The chemokine CCL6 is a monocyte chemoattractant [151,152]. The gene *Il1rn* was also downregulated in all three culture conditions with $ASC^{-/-}$ astrocytes and/or microglia (Fig 5B). *Il1rn* encodes the IL-1 receptor antagonist, IL-1RA, that acts as a negative regulator of IL-1β

activity [153]. As a negative regulator, the expression of *Il1rn* is likely tightly linked to inflammasome activity, explaining its reduced expression in these cultures.

To validate the role of ASC in CCL6 expression in vivo, we measured CCL6 concentrations in the brains of either uninfected WT and $ASC^{-/-}$ mice or at days 1 and 3 post-infection. Similar to IL-18 concentrations (Fig 1D), CCL6 was slightly higher in uninfected $ASC^{-/-}$ mice compared to WT (Fig 5C). CCL6 was not significantly different between WT and $ASC^{-/-}$ mice at day 1 post-infection, but by day 3 post-infection CCL6 levels were lower in $ASC^{-/-}$ mice compared to WT mice (Fig 5C). Although early CCL6 expression does not depend on ASC, increased expression of this chemokine is ASC-dependent later in infection.

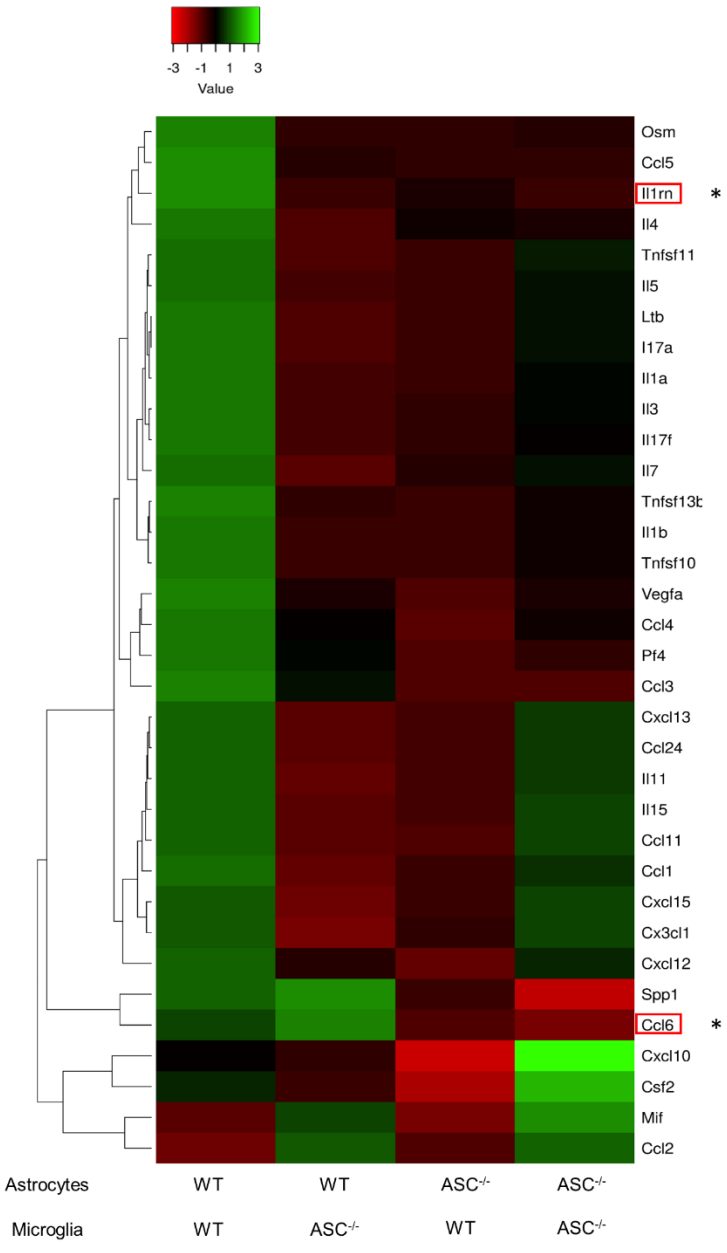
-3 -1 1 3
Value
Osm
Ccl5
Il1rn
*
Il4
Tnfsf11
Il5
Ltb
Il17a
Il1a
Il3
Il17f
Il7
Tnfsf13b
Il1b
Tnfsf10
Vegfa
Ccl4
Pf4
Ccl3
Cxcl13
Ccl24
Il11
Il15
Ccl11
Ccl1
Cxcl15
Cx3cl1
Cxcl12
Spp1
Ccl6
*
Cxcl10
Csf2
Mif
Ccl2
Astrocytes WT WT ASC-/- ASC-/-
Microglia WT ASC-/- WT ASC-/-

**Figure 4. Normalized relative gene expression in glial co-cultures.**

Heat map of z-score normalized relative gene expression of pro-inflammatory cytokines and chemokines for each culture condition. *Ccl6* and *Il1rn* are highlighted as having significant differences between groups.

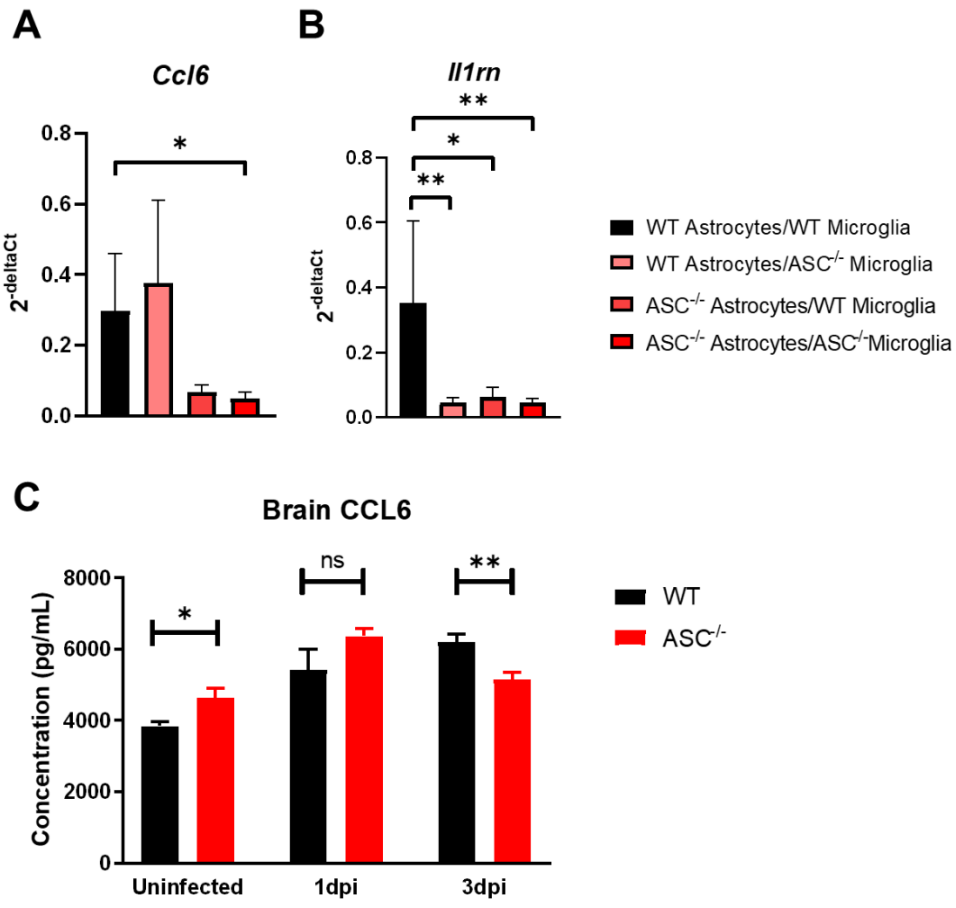
A
Ccl6
2-deltaCt
0.8
0.6
0.4
0.2
0.0
*
B
Il1rn
2-deltaCt
**
*
**
WT Astrocytes/WT Microglia
WT Astrocytes/ASC-/- Microglia
ASC-/- Astrocytes/WT Microglia
ASC-/- Astrocytes/ASC-/-Microglia
C
Brain CCL6
Concentration (pg/mL)
8000
6000
4000
2000
0
*
ns
**
Uninfected
1dpi
3dpi
WT
ASC-/-

**Figure 5. Glial inflammasome activation drives expression of the monocyte chemokine CCL6 during HSV-1 infection.**

Glial co-cultures were infected at an MOI of 5 and cellular RNA was isolated at 12 hours post-infection. Relative gene expression of (A) Ccl6 and (B) Il1rn in glial co-cultures (n = 3-4 per group). (C) CCL6 protein levels from the brains of either uninfected or infected mice at days 1 and 3 post-infection (n = 4-5 per group). Values for gene expression are expressed as means ± SD and values for CCL6 levels are expressed as means ± SEM (*P < 0.05, **P < 0.01).

**ASC-dependent inflammasomes promote macrophage infiltration of the CNS during HSE**

Leukocyte infiltration into the brain has been shown to be important for controlling replication of HSV-1, yet the infiltration of CXCR3+ monocytes and T cells has been associated with detrimental inflammation in HSE [154,155]. We demonstrated that $ASC^{-/-}$ mice have lower CCL6 concentrations at day 3 post-infection. Based on this finding, we hypothesized that $ASC^{-/-}$ mice have reduced CNS infiltration of leukocytes at that time point. We examined several immune cell types including total infiltrating CD45hi cell populations, macrophages, neutrophils, dendritic cells (DCs), and CD4+ and CD8+ T cells. Absolute numbers of total CD45hi cells (Fig 6A), neutrophils, DCs, and both CD4+ and CD8+were reduced in $ASC^{-/-}$ mice (Figs 6B-D) although the differences did not reach statistical significance. Notably, absolute numbers of infiltrating macrophages were significantly reduced in $ASC^{-/-}$ compared to WT mice infected with HSV-1, suggesting that ASC-dependent inflammasomes drive the infiltration of this particular cell type (Figs 6E-F). Consistent with our survival and cytokine expression data, there was no difference in macrophage infiltration between WT and $NLRP3^{-/-}$ mice (Fig 6F). The significantly increased infiltration of macrophages in WT mice is consistent with the elevated CCL6 levels found at day 3 post-infection in Fig 5D. These results demonstrate that ASC is critical for the recruitment of macrophages into the CNS during HSE.

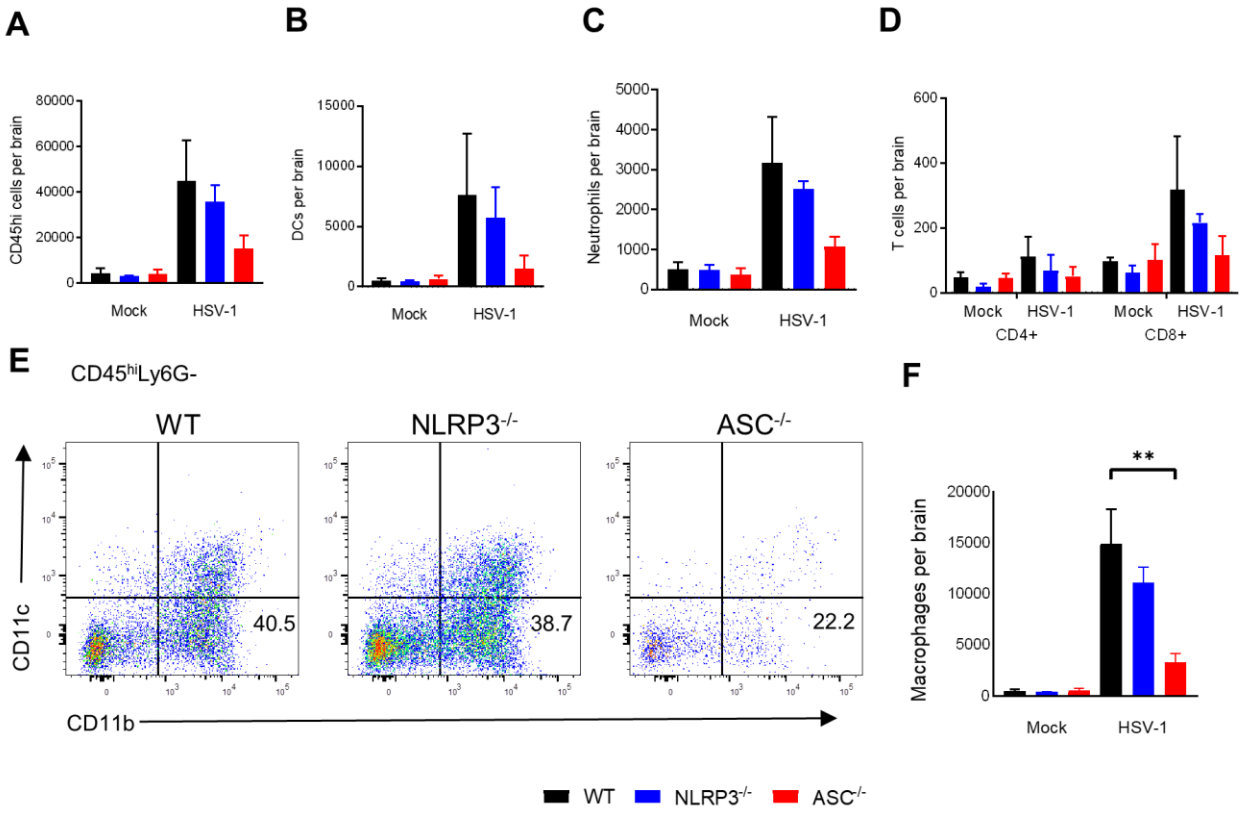
A
CD45hi cells per brain
80000
60000
40000
20000
0
Mock
HSV-1
B
DCs per brain
15000
10000
5000
0
Mock
HSV-1
C
Neutrophils per brain
5000
4000
3000
2000
1000
0
Mock
HSV-1
D
T cells per brain
600
400
200
0
Mock
HSV-1
Mock
HSV-1
CD4+
CD8+
E
CD45hiLy6G-
WT
NLRP3-/-
ASC-/-
CD11c
CD11b
40.5
38.7
22.2
F
Macrophages per brain
**
20000
15000
10000
5000
0
Mock
HSV-1
WT
NLRP3-/-
ASC-/-

**Figure 6. ASC-dependent inflammasomes promote leukocyte migration into the CNS during HSV-1 encephalitis.**

Infiltrating leukocytes in the brain were analyzed by flow cytometry in WT, NLRP3-/-, and ASC-/- mice at day 3 post-infection after intracranial inoculation with 3 x 106 PFU HSV-1 KOS. Total CD45hi cells (A), dendritic cells (B), neutrophils (C), CD4+ and CD8+ T cells (D). Representative FACS plots of CD11c and CD11b expression within CD45hi and Ly6G- cells. Macrophages are gated as CD11b+ and CD11c- (E). Absolute numbers of macrophages (F) calculated from numbers of total cells at day 3 post-infection (n = 5, 3 replicates for myeloid cells; n = 3-4, 2 replicates for T cells). After excluding multiplets, cell types were gated within the CD45hi population using the following gating strategy: macrophages/monocytes Ly6G-/CD11c-/CD11b+, dendritic cells Ly6G-/CD11c+, neutrophils Ly6G+/CD11b+/CD11c-, T cells CD3+/CD4+ or CD3+/CD8+. No significant decrease was observed between WT and ASC-/- mice for total CD45hi, DCs, neutrophils, or T cells. Values are expressed as means ± SEM (**P < 0.01).

## DISCUSSION

We report that the inflammasome adaptor protein, ASC, contributes to mortality in a murine model of HSE. By contrast, mice deficient in the inflammasome sensor components NLRP3 and AIM2 did not differ in survival from WT mice. We demonstrated that ASC-dependent inflammasomes contribute to mortality without affecting viral replication. ASC was also critical for the generation of the pro-inflammatory cytokines IL-1β and IL-18, suggesting that ASC-dependent inflammasomes are the primary contributors to the release of these cytokines during HSE. We identified microglia as the primary mediators of the inflammasome response in vivo and in an organotypic brain slice culture model of HSV-1 infection. Using both in vitro infections of glial cultures and our in vivo HSE model, we found that expression of the macrophage chemoattractant CCL6 depends on ASC-dependent inflammasomes. Finally, reduced CCL6 in $ASC^{-/-}$ mice was associated with decreased infiltration of macrophages to the CNS during infection.

ASC is the key adaptor for canonical inflammasomes, acting as a bridge between the sensor and procaspase-1 through its PYD (pyrin domain) and CARD (caspase activation and recruitment domain) domains, respectively [156]. HSV-1 infection in vitro has been shown to activate several of these inflammasomes that act through ASC, including NLRP3, AIM2, and IFI16 [41,89,144], but the extent to which these contribute to disease in the CNS were unknown. The role of inflammasomes in HSV-1 pathogenesis in vivo has been largely limited to murine models of corneal HSV-1 infection. Prior studies found that corneal infection of $NLRP3^{-/-}$ mice results in more severe immunopathogenesis [94], and that corneal HSV-1 infection induces the NLRP3, NLRP12, and IFI16 inflammasomes [157]. A previous study found that IL-1β-deficient

mice were more susceptible in an intranasal model of HSV-1 infection [90]. This discrepancy is likely due to the route of infection, with IL-1β being important for preventing neuroinvasion or restricting peripheral replication in the nasal mucosa but detrimental once the virus has gained access to the CNS. In an intracranial model of HSE, our study suggests that multiple ASC-dependent inflammasomes contribute to pathogenesis by driving excessive neuroinflammation in the CNS, but that neither NLRP3 or AIM2 alone account for differences in survival or cytokine production. Interestingly, NLRP3 deficiency resulted in higher levels of IL-1β in the brain later in infection, suggesting a regulatory role for NLRP3 in modifying caspase-1 activity rather than simply increasing IL-1β activation in response to an immune stimulus. Our study suggests a complex immunomodulatory role for ASC in regulating multiple inflammasomes in the brain, without a dominant PRR component.

Importantly, our study identified microglia as key mediators of the inflammasome response in HSE, adding to mounting data that microglia contribute to pathology in HSV-1 CNS infection [158]. We also demonstrated downregulation of the chemokine CCL6 in cultures of $ASC^{-/-}$ glia and in the brains of $ASC^{-/-}$ mice at day 3 post-infection. Interestingly, CCL6 was elevated in both WT and $ASC^{-/-}$ mice at day 1 post-infection. Taken together, these results suggest that after initial activation early in infection, ASC-dependent inflammasomes significantly influence immune cell infiltration later in infection by regulating CCL6 production and contribute to a prolonged neuroinflammatory response. CCL6 has been described as a monocyte chemoattractant through its putative receptor, CC-type chemokine receptor 1 (CCR1) [151,152]. Few studies have examined CCL6 in the brain, but it has been reported to be expressed in rat microglia and not astrocytes [159]. In a murine model of Venezuelan equine

encephalitis virus, more virulent strains of the virus induce greater expression of CCL6 in the brain and subsequent infiltration of mononuclear cells into the parenchyma [160]. These studies are consistent with our finding of reduced macrophage infiltration in the brain in $ASC^{-/-}$ mice, coinciding with reduced levels of CCL6, and may represent a common mechanism of adaptive immune cell recruitment to the brain following neurotropic virus infection. Together, our findings suggest that microglial inflammasome activation may serve as a key link between the early innate immune response to HSV-1 and prolonged neuroinflammation through the recruitment of infiltrating leukocytes.

Although components of the innate immune system are critical for controlling HSV-1 replication in the brain [110,122], our study found that ASC-dependent inflammasomes do not contribute to controlling viral replication. Improved survival in $ASC^{-/-}$ mice in the setting of decreased inflammatory markers, with no influence on viral replication, indicates that inflammasomes are immunopathogenic in HSE. These results are consistent with studies demonstrating a key role for inflammasomes in driving neuroinflammation in response to other viral CNS infections [146,161,162]. In HSV-1 infection, neuronal damage can be caused by both viral replication and pathologic inflammation, which can also ultimately promote excitotoxicity, pyroptosis, and necroptosis [132,163]. As a result, the host response to infection represents a careful balance between an appropriate immune response and prolonged neuroinflammation. Immunopathology is clinically apparent through the standard use of acyclovir, an anti-viral therapeutic targeted to control HSV replication, which has significantly reduced mortality but not neurologic morbidity following HSV encephalitis [72]. This suggests that the host immune response significantly impacts neurologic outcomes in HSE beyond the direct detrimental effects

of viral replication. Our data suggest that targeting inflammasome activation in HSE may shift the balance to a less detrimental immune response and improve outcomes after HSV infection. Current antiviral therapy for HSV-1 is targeted to viral replication, but adjunctive corticosteroid treatment has been suggested to counteract immunopathology [164]. However, rational targeting of immune pathways offers the possibility of preventing harmful inflammation without impairing viral clearance, offering a synergistic approach to the treatment of a diverse spectrum of viral illnesses. Targeting inflammasome components has been explored in both neuroinflammatory disorders and pre-clinical models of viral disease. For example, the IL-1 receptor antagonist, anakinra, has been shown to be effective in improving outcomes in mouse models of Zika virus-induced placental dysfunction and Chikungunya virus arthritis [165,166]. Anakinra has also been used to treat patients with Behcet's disease, an inflammatory disorder with CNS involvement [167], and has been demonstrated to cross the blood-brain barrier in humans [168]. This drug, and others that similarly target IL-1 signaling, may represent a better strategy to selectively target harmful inflammation during HSV-1 infection. Our study suggests that targeting the inflammasome response could prevent harmful inflammation with the potential to improve survival independent of viral clearance in HSE.

# CHAPTER IV: SINGLE-NUCLEUS RNA SEQUENCING UNCOVERS AGE-DEPENDENT SUSCEPTIBILITY TO HSV-1


## ABSTRACT

Herpes simplex encephalitis is a devastating illness that results in significant morbidity and mortality even with prompt antiviral therapy. Neonates are more susceptible to herpes simplex encephalitis than adults, suggesting that developmental factors contribute to increased risk and severity of disease. We used single-nucleus RNA sequencing of brain tissue from adult and neonatal mice infected with HSV-1 to identify host factors that contribute to this difference in susceptibility. Surprisingly, we found that adult cells do not express higher levels of antiviral transcripts at baseline, and neonates can generate robust antiviral responses during infection. Instead, we found that the long noncoding RNA Meg3 is expressed at higher levels in the neonatal brain and inhibits host cell apoptosis during HSV-1 infection. Our study highlights a potential role for the developmental state of a cell to influence viral susceptibility outside of traditional antiviral gene expression.


## INTRODUCTION

The newborn brain is significantly more susceptible to a range of pathogens compared to the adult brain, including herpes simplex virus type I (HSV-1), the most commonly identified cause of sporadic encephalitis [169,170]. HSV-1 infection in adults is common and is typically asymptomatic or associated with self-limiting disease [169]. By contrast, half of neonatal HSV-1 disease progresses to central nervous system (CNS) or disseminated disease, resulting in

significant morbidity and mortality even with prompt antiviral therapy [171]. The exact mechanism responsible for this difference in susceptibility is unknown, but differences in the host immune response and developmental state are likely contributors [135].

Our previous work has focused on important age-dependent differences in the innate immune response to HSV infection. At the center of this difference is a dampened type-I interferon (IFN) response in the neonatal brain that results in failure to effectively clear replicating virus [110,135]. As a key part of the innate immune response, the type I IFN response is initiated through recognition of pathogen-associated molecular patterns (PAMPs), leading to the elaboration of type I IFNs. These cytokines signal in a paracrine or autocrine manner to induce an antiviral state in nearby cells. The importance of the type I IFN response in limiting herpes simplex encephalitis (HSE) is underscored by genetic studies demonstrating increased susceptibility to HSE in neonates with inborn errors of type I IFN signaling [100,102–104,172–174]. However, these rare genetic causes of increased susceptibility do not account for the overwhelmingly higher incidence of HSE in neonates, suggesting that other developmental factors must be at play.

Recently, the advent of single-cell RNA sequencing (scRNA-seq) has allowed for the study of cell type specific responses to viral infections [175–179]. We have recently shown that coordination between astrocytes and microglia is essential for mounting a complete immune response to HSV-1 in the CNS [180,181]. These studies focused on genetic knockouts of innate immune components, but an unbiased analysis of intercellular communication during HSE is needed. Using a murine model of HSE, we undertook single-nucleus RNA sequencing (snRNA-seq) of infected CNS tissue from both neonatal and adult mice. In this study, we present the first

unbiased analysis of the coordinated host immune response across all major CNS cell types during HSE. We found that neonatal mice were overwhelmingly more susceptible to HSV-1 infection in the CNS, and that neonates were capable of mounting a robust antiviral response despite this susceptibility. Surprisingly, we found that neonates and adults do not have different levels of expression of antiviral transcript at baseline. By analyzing baseline gene expression differences between neonates and adults, we identified the imprinted long noncoding RNA (lncRNA) maternally expressed 3 (*Meg3*) as expressed at higher levels in all neonatal cell types. Here we show that this developmentally regulated gene inhibits apoptosis, the last line of defense against viral replication, during HSV-1 infection. This finding highlights the potential for age-dependent susceptibility to infection to arise from the developmental state of a cell, rather than solely from differences in the immune response.

## RESULTS

### The neonatal brain is more susceptible across all cell types to HSV-1 infection than in the adult

To study the age-dependent host response to HSV-1 infection in the brain, we performed snRNA-seq analysis of hippocampi isolated from either neonatal (7-day-old) or adult (8-9-week-old) C57BL/6 mice. Mouse hippocampi were either infected with HSV-1 or mock-infected and tissue was collected and flash frozen at 48 hours post infection (Fig 7A). This time point was chosen to emphasize the early innate immune response to infection while avoiding significant tissue destruction by the virus. Nuclei from four mice per experimental condition were labeled

with hashtag oligos (HTOs) to ensure that each sample was representative of nuclei from multiple individuals (Fig 8). After quality control, the total dataset consisted of 15,904 cells.

To interrogate cell type specific responses to infection in both age groups, we performed integrated scRNA-seq analysis to build a unified dataset consisting of all four experimental groups. Clustering of the integrated dataset revealed 31 clusters (Fig 9). Each cluster was manually assigned to one of 12 cell types based on canonical marker gene expression. The integrated dataset consists of neurons, astrocytes, microglia, oligodendrocyte precursor cells (OPCs), oligodendrocytes, neural progenitor cells (NPCs), endothelial cells, mural cells, ependymal cells, choroidal epithelial cells, vascular and leptomeningeal cells (VLMCs), and Cajal-Retzius cells (Fig 7B). Each cell type was found in all four experimental groups, although age-dependent differences in cell proportions were apparent (Fig 7C). Neurons represented a significantly higher proportion of cells found in neonatal samples compared to adult, consistent with developmentally-regulated neuronal apoptosis occurring postnatally [182]. By contrast, astrocytes and oligodendrocytes were found in higher proportions in the adult samples. The relative sparsity of oligodendrocytes in the neonatal samples is consistent with postnatal myelinogenesis taking place during the first three weeks of murine development [183], as OPCs were abundant in this age group.

We next examined the ability for HSV-1 to infect CNS cells and its tropism in neonates and adults. By aligning sequencing reads to the HSV-1 genome, we were able to classify individual cells as infected, bystander (uninfected but derived from infected tissue), and naïve. Consistent with previous findings, adult brains were notably resistant to infection, with HSV-1 transcript being sparsely found in each cell type (Fig 7D). By contrast, neonatal brains were very

susceptible to infection, with transcript being abundantly expressed in every cell type (Fig 7E). The proportion of total cells infected in neonatal brain tissue was significantly higher than in the adult (mean of 65.9% vs 3.4%) (Fig 7F). These findings are consistent with previously reported age-dependent differences in susceptibility to HSV-1 in the CNS [111,184].

Although it was expected that more cells would be infected in the neonatal brain, it was unknown whether the difference could be explained by an age-dependent difference in tropism, or whether all cell types in the neonate are universally more susceptible to HSV-1. Differences in the makeup of the infected cell population between the two age groups were apparent (Fig 7G), but these data did not take into account the age-dependent difference in cell type composition (Fig 7C). To answer this question, we calculated an infectivity index for each cell type by dividing the percentage of infected cells from a given cell type by the proportion with which that cell type was present in the sample. This normalized infectivity ratio allows for the comparison of tropism between neonate and adult samples with different compositions of cell types. Infectivity indices greater than 1 indicate that a cell type was infected more often than would be expected based on its abundance in the sample, and vice versa. Among the top six most abundant cell types in the dataset, there was no difference in the infectivity index between neonates and adults (Fig 7H). In each of these cell types, the infectivity index was close to 1 for both neonatal and adult samples. These data suggest that rather than an age-specific tropism for a particular cell type, neonatal CNS cells are universally more susceptible to HSV-1 infection than in the adult.

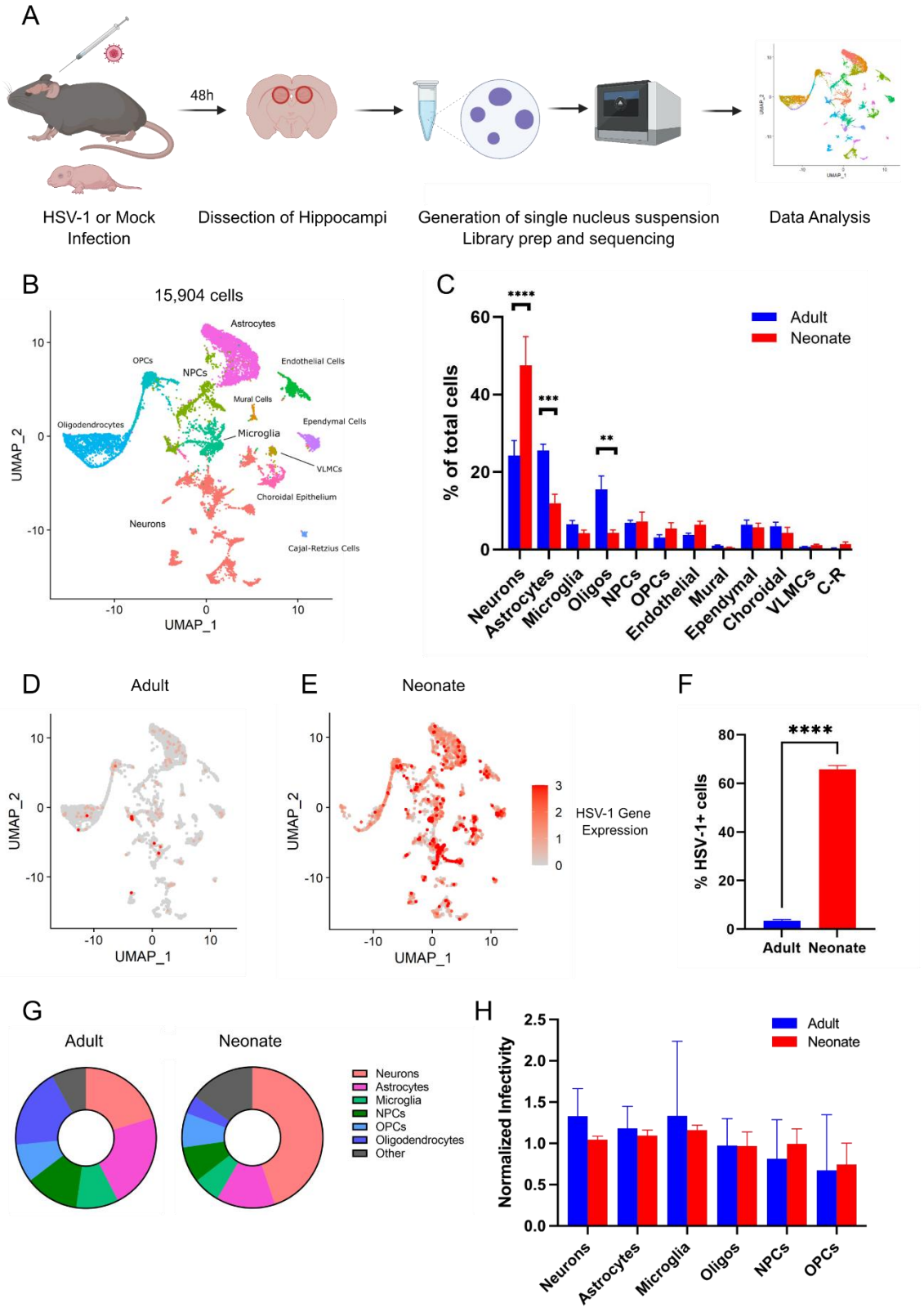
A
48h
HSV-1 or Mock Infection
Dissection of Hippocampi
Generation of single nucleus suspension
Library prep and sequencing
Data Analysis
B
15,904 cells
Astrocytes
Endothelial Cells
OPCs
NPCs
Mural Cells
Oligodendrocytes
Ependymal Cells
Microglia
VLMCs
Choroidal Epithelium
Neurons
Cajal-Retzius Cells
UMAP_1
UMAP_2
C
Adult
Neonate
% of total cells
****
***
**
Neurons
Astrocytes
Microglia
Oligos
NPCs
OPCs
Endothelial
Mural
Ependymal
Choroidal
VLMCs
C-R
D
Adult
E
Neonate
HSV-1 Gene Expression
F
% HSV-1+ cells
****
Adult
Neonate
G
Adult
Neonate
Neurons
Astrocytes
Microglia
NPCs
OPCs
Oligodendrocytes
Other
H
Adult
Neonate
Normalized Infectivity
Neurons
Astrocytes
Microglia
Oligos
NPCs
OPCs

**Figure 7. The neonatal brain is more susceptible across all cell types to HSV-1 infection than in the adult.**

(A) Schematic of experimental design. Adult (8–9-week-old) or neonatal (7 day-old) mice were stereotaxically inoculated with 3x104 PFU HSV-1 strain F bilaterally into the hippocampi or mock infected. At 48 hours post-infection, hippocampal tissue was isolated and nuclei suspensions were generated. Sequencing libraries were prepared using the 10X Genomics Chromium Next GEM Single Cell 3' Kit and sequenced using an Illumina HiSeq 4000 sequencer. Created with BioRender.com (B) Integrated dataset of 15,904 cells with clusters assigned to known CNS cell types using canonical marker gene expression. (C) Proportions of cell types found in adult or neonatal nuclei samples (n=8 mice per age group). UMAP plots of HSV-1 gene expression in adult (D) and neonatal (E) CNS nuclei. (F) Percentage of total infected cells in adult and neonatal samples. (G) Composition of infected cells in adult and neonatal samples. (H) Normalized infectivity of common CNS cell types in neonates and adults. For each sample, the percentage of infected cells from a given cell type was normalized to the proportion with which that cell type was present in the sample. Values greater than 1 correspond to cell types that are overrepresented among infected cells, and vice versa (n=4 mice per group). Values are expressed as means ± SEM (**P < 0.01, ***P < 0.001, ****P < 0.0001).

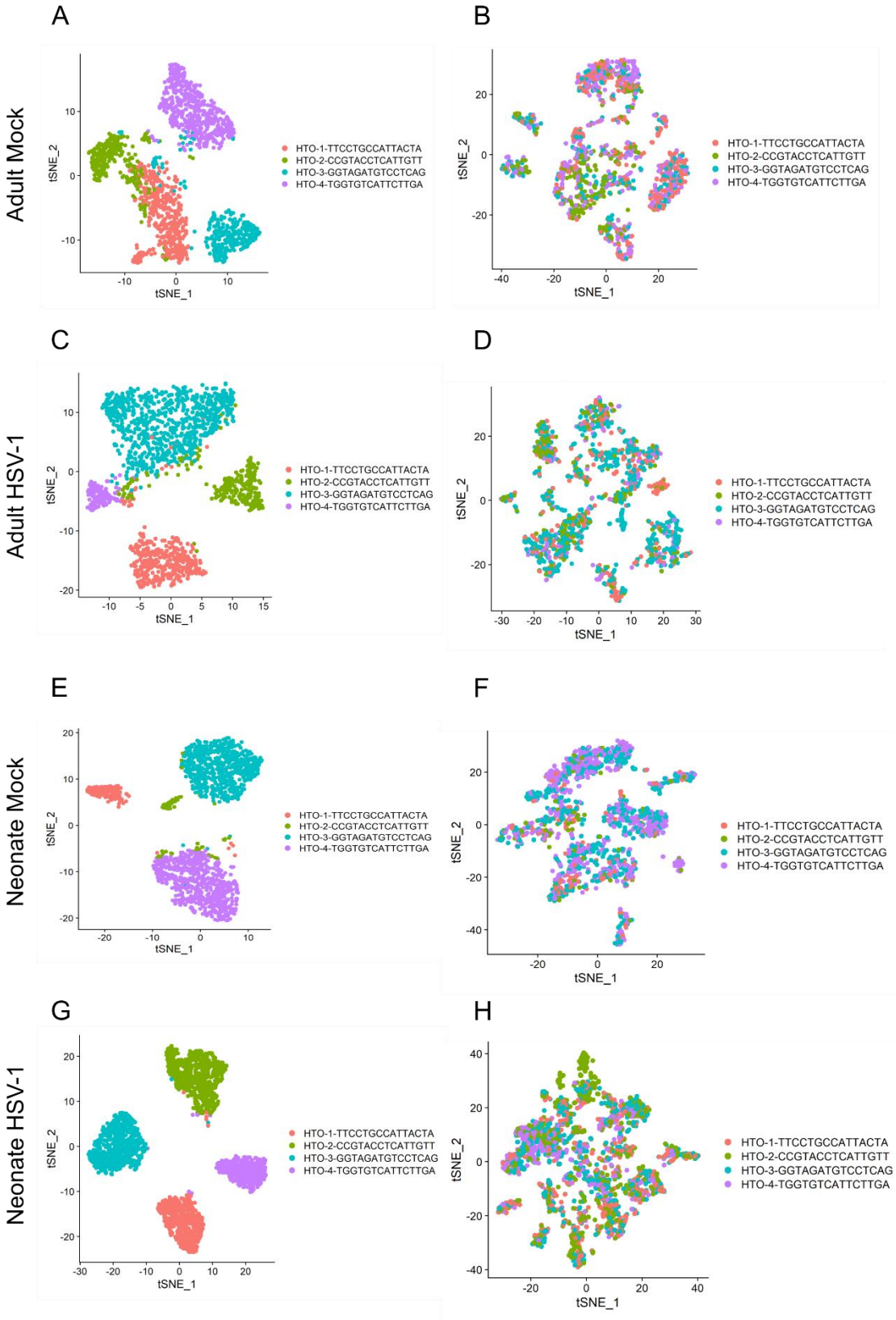
A
B
C
D
E
F
G
H
Adult Mock
Adult HSV-1
Neonate Mock
Neonate HSV-1
tSNE_1
tSNE_2
HTO-1-TTCCTGCCATTACTA
HTO-2-CCGTACCTCATTGTT
HTO-3-GGTAGATGTCCTCAG
HTO-4-TGGTGTCATTCTTGA

**Figure 8. HTO demultiplexing of single nucleus RNA sequencing samples.**

tSNE plots of adult mock (A, B), adult HSV-1 (C, D), neonate mock (E, F), and neonate HSV-1 (G, H) samples clustered by either HTO label or gene expression.

A

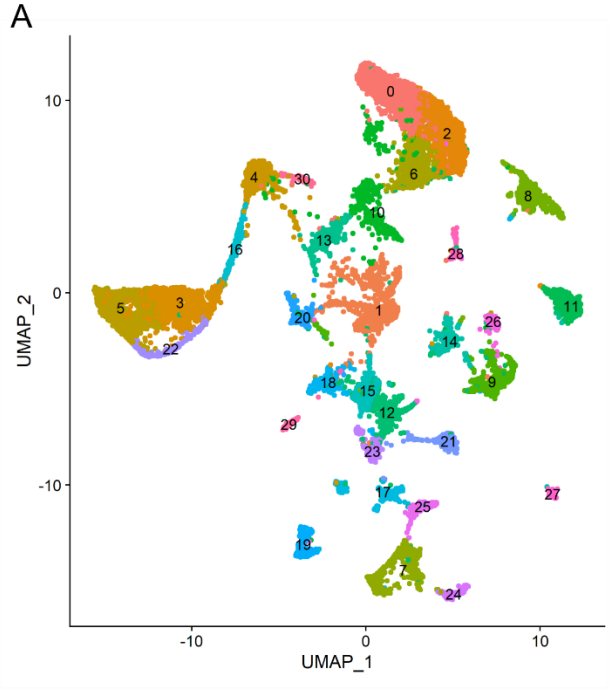
UMAP_2
UMAP_1
10
0
-10
-10
0
10

B

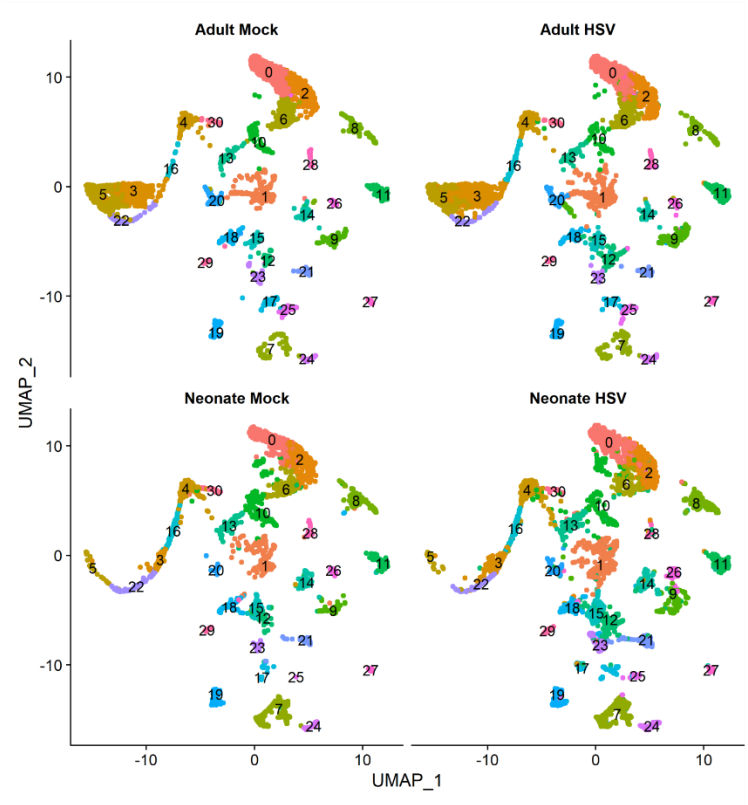
Adult Mock
Adult HSV
Neonate Mock
Neonate HSV
UMAP_2
UMAP_1
10
0
-10
-10
0
10

**Figure 9. Integrated dataset before cell type assignment.**

(A) UMAP plot of the integrated dataset before assignment of cell types. 31 clusters are shown.

(B) UMAP plots of the integrated dataset separated by experimental group.

**Defining the global anti-HSV-1 response in the neonatal brain**

The relative resistance of adult cells to HSV-1 infection presented a challenge in comparing the host response between the two age groups. Overall, neonatal mice had a strong response to infection in virtually all cell types. By comparison, the response in adults was hardly detectable in many cell types (Fig 10). This difference in magnitude of response is likely due to the greatly reduced number of infected cells in adult mice, although an intrinsic difference in response cannot be ruled out. In order to both better understand the features of this robust neonatal response, as well as to examine the baseline antiviral state of both neonates and adults, we set out to define a set of genes that constitute a global anti-HSV-1 response across diverse CNS cell types. To do this, we performed differentially expressed gene (DEG) analysis between the infected neonate sample and the mock-infected neonate sample for each cell type. Candidate genes were included in the antiviral module if they were differentially upregulated in at least one cell type (adjusted p-value $< 0.05$) and minimally upregulated in all cell types ($\log2FC > 0.1$) in the HSV-1 infected cells compared to mock. In all, 54 genes met these criteria, and their expression is shown in Fig 11A.

We next assigned each cell an antiviral score based on the average expression of these 54 genes, allowing us to assess the antiviral state of any cell in the dataset. Comparing the antiviral scores of each cell type in neonates shows a robust upregulation of this module in all cell types during infection (Fig 11B). Many of the genes found in the antiviral module are unsurprisingly interferon-stimulated genes (ISGs). We performed gene ontology analysis to identify enriched pathways in this module. Consistent with a general antiviral response, the top enriched GO term was “defense response to virus” (Fig 11C). Prominent ISGs found in the module include *Ifih1*,

*Rnf213*, and *Eif2ak2*. *Ifih1*, which encodes the antiviral protein melanoma differentiation-associated protein 5 (MDA5), is a RIG-I like receptor (RLR) that recognizes double-stranded RNA byproducts of HSV replication in order to initiate interferon activation [185,186]. *Rnf213*, encoding ring finger protein 213 (RNF213), was a previously poorly characterized ISG but has recently been shown to have anti-HSV-1 effects [187]. Finally, *Eif2ak2* encodes protein kinase R (PKR), another double-stranded RNA sensor that shuts down host translation upon activation [77,188]. Despite the increase in susceptibility of neonates to HSV-1 infection, neonatal cells are clearly capable of initiating a robust innate immune response during HSE.

Neurons, astrocytes, and microglia represent three of the most abundant cell types in our samples and are targets of HSV-1 infection (Fig 7). Differential gene expression analysis of these three cell types in neonatal mice demonstrated upregulation of several genes that are part of the global antiviral module (Figs 11D-F). In order to better understand the gene expression pathways that are up or downregulated during infection, we performed gene set enrichment analysis (GSEA) of these cell types. The top five enriched gene sets upregulated in all three cell types are involved in the innate immune response, consistent with a global antiviral response (Figs 11G-H, 12). Surprisingly, several suppressed gene sets in both neurons and astrocytes were related to cilia (Figs 11G-H, 12). In the mature brain, both astrocytes and neurons contain a single primary cilium that detects extracellular signals. Primary cilia are key modulators of sonic hedgehog signaling, which is essential for normal CNS development and adult neurogenesis [189]. Thus, neonatal HSV-1 infection may disrupt important developmental pathways in addition to direct damage caused by the virus.

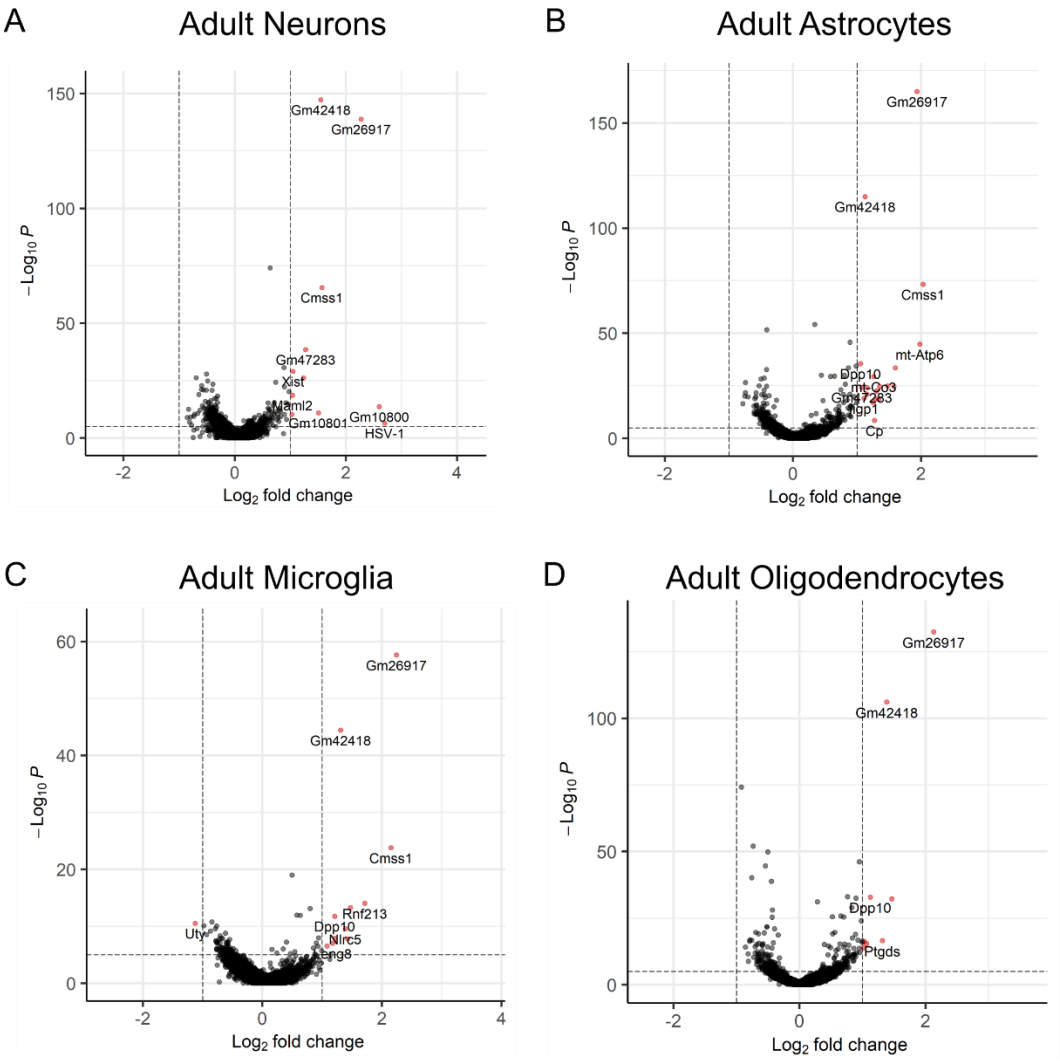
A
Adult Neurons
Gm42418
Gm26917
Cmss1
Gm47283
Xist
Maml2
Gm10801
Gm10800
HSV-1
−Log10 P
Log2 fold change
B
Adult Astrocytes
Gm26917
Gm42418
Cmss1
mt-Atp6
Dpp10
mt-Co3
Gm47283
Itgp1
Cp
−Log10 P
Log2 fold change
C
Adult Microglia
Gm26917
Gm42418
Cmss1
Rnf213
Dpp10
Nlrc5
Epg8
Uty
−Log10 P
Log2 fold change
D
Adult Oligodendrocytes
Gm26917
Gm42418
Dpp10
Ptgds
−Log10 P
Log2 fold change

**Figure 10. Differentially expressed gene analysis in adult mice.**

Volcano plots of differentially expressed genes for neurons (A), astrocytes (B), microglia (C), and oligodendrocytes (D) between the adult HSV-1 and adult mock samples.

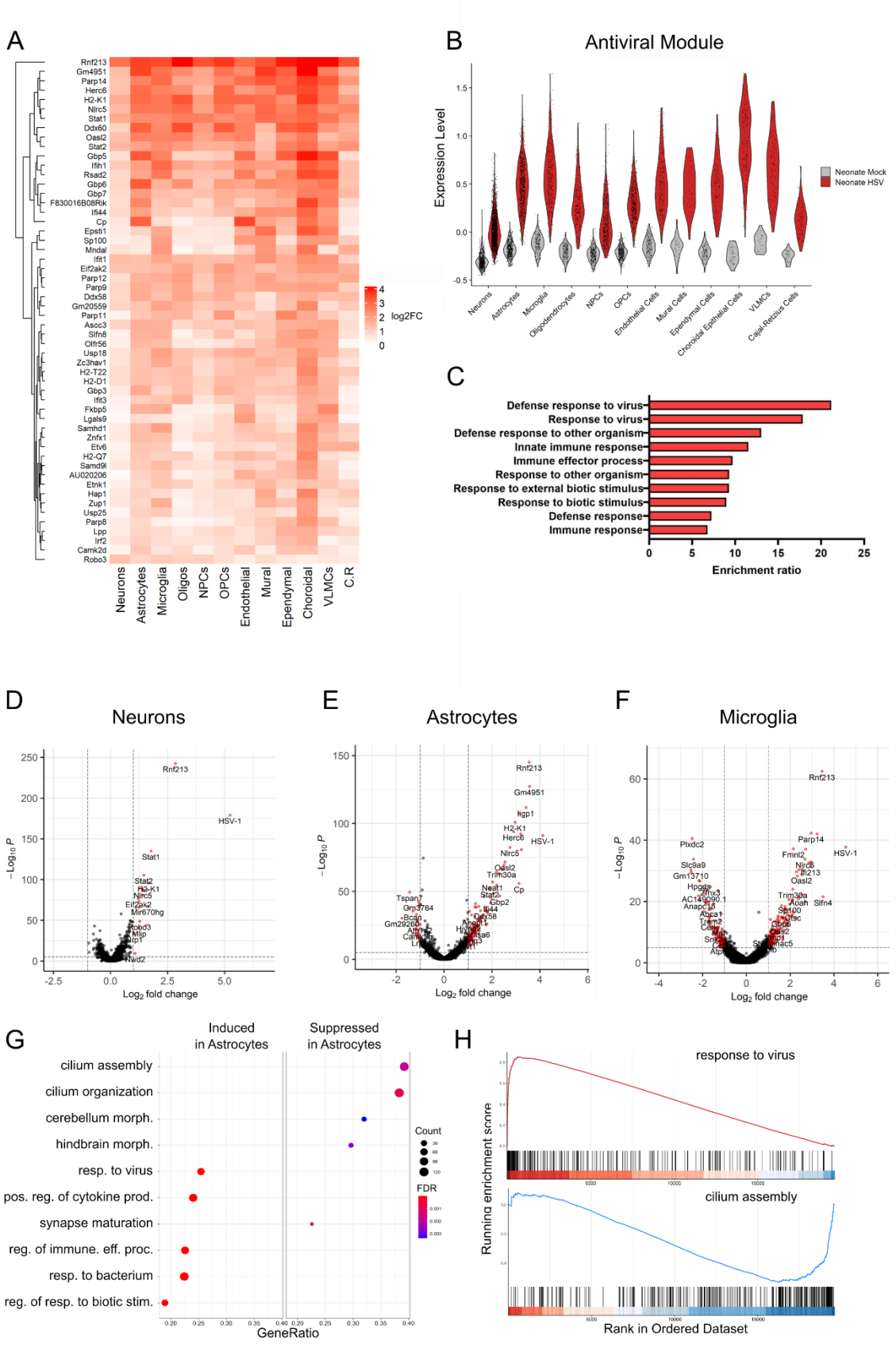
A
Rnf213
Gm4951
Parp14
Herc6
H2-K1
Nlrc5
Stat1
Ddx60
Oasl2
Stat2
Gbp5
Ifih1
Rsad2
Gbp6
Gbp7
F830016B08Rik
Ifi44
Cp
Epsti1
Sp100
Mndal
Ifit1
Eif2ak2
Parp12
Parp9
Ddx58
Gm20559
Parp11
Ascc3
Slfn8
Olfr56
Usp18
Zc3hav1
H2-T22
H2-D1
Gbp3
Ifit3
Fkbp5
Lgals9
Samhd1
Znfx1
Etv6
H2-Q7
Samd9l
AU020206
Etnk1
Hap1
Zup1
Usp25
Parp8
Lpp
Irf2
Camk2d
Robo3
log2FC
Neurons
Astrocytes
Microglia
Oligos
NPCs
OPCs
Endothelial
Mural
Ependymal
Choroidal
VLMCs
C.R
B
Antiviral Module
Expression Level
Neonate Mock
Neonate HSV
Neurons
Astrocytes
Microglia
Oligodendrocytes
NPCs
OPCs
Endothelial Cells
Mural Cells
Ependymal Cells
Choroidal Epithelial Cells
VLMCs
Cajal-Retzius Cells
C
Defense response to virus
Response to virus
Defense response to other organism
Innate immune response
Immune effector process
Response to other organism
Response to external biotic stimulus
Response to biotic stimulus
Defense response
Immune response
Enrichment ratio
D
Neurons
E
Astrocytes
F
Microglia
Log2 fold change
G
Induced in Astrocytes
Suppressed in Astrocytes
cilium assembly
cilium organization
cerebellum morph.
hindbrain morph.
resp. to virus
pos. reg. of cytokine prod.
synapse maturation
reg. of immune. eff. proc.
resp. to bacterium
reg. of resp. to biotic stim.
Count
FDR
GeneRatio
H
response to virus
cilium assembly
Running enrichment score
Rank in Ordered Dataset

**Figure 11. Defining the global anti-HSV-1 response in the neonatal brain.**

(A) Heatmap of 54 genes selected as part of the global anti-HSV-1 response in the neonatal brain (B) Violin plot of antiviral module expression in individual cell types in the neonate mock or infected neonate samples. Dots represent individual cells. (C) Gene ontology analysis of antiviral module genes. The top 10 significantly enriched gene ontology terms are plotted. Volcano plots of differentially expressed genes between neonatal HSV-1-infected and mock-infected neurons (D), astrocytes (E), and microglia (F). (G) Gene set enrichment analysis of differentially expressed genes between neonatal HSV-1-infected and mock-infected astrocytes. The top 5 enriched upregulated and suppressed pathways are shown. (H) Gene set enrichment plots of the "response to virus" and "cilium assembly" gene sets in astrocytes.

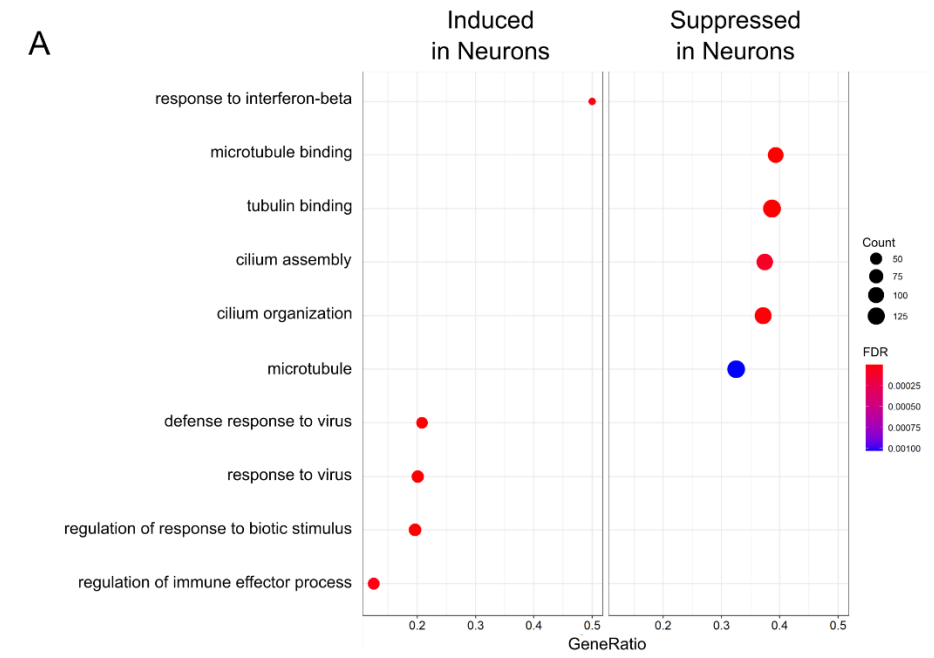
A
Induced in Neurons
Suppressed in Neurons
response to interferon-beta
microtubule binding
tubulin binding
cilium assembly
cilium organization
microtubule
defense response to virus
response to virus
regulation of response to biotic stimulus
regulation of immune effector process
0.2
0.3
0.4
0.5
GeneRatio
Count
50
75
100
125
FDR
0.00025
0.00050
0.00075
0.00100

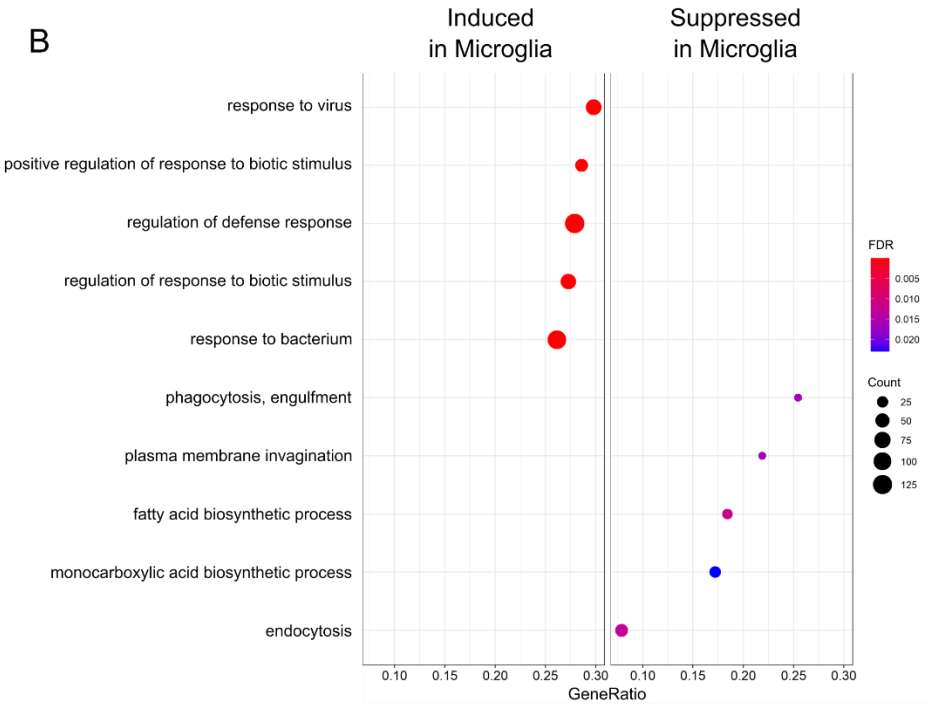
B
Induced in Microglia
Suppressed in Microglia
response to virus
positive regulation of response to biotic stimulus
regulation of defense response
regulation of response to biotic stimulus
response to bacterium
phagocytosis, engulfment
plasma membrane invagination
fatty acid biosynthetic process
monocarboxylic acid biosynthetic process
endocytosis
0.10
0.15
0.20
0.25
0.30
GeneRatio
FDR
0.005
0.010
0.015
0.020
Count
25
50
75
100
125

**Figure 12. Gene set enrichment analysis of the neonatal response to infection in neurons and microglia.**

Dot plots of the top 5 induced and suppressed gene sets in neonatal neurons (A) and microglia (B).

**Neonatal microglia and astrocytes take on distinct and complementary proinflammatory states during HSE**

We have previously shown that the coordination between microglia and astrocytes is important for a complete immune response during HSE [180,181]. In order to assess the complete response of both of these cell types, we performed trajectory analysis of neonatal microglia and astrocytes using Monocle3 to identify genes that are associated with transition to an antiviral state [129]. After unsupervised trajectory learning, the starting node of the trajectory was chosen based on proximity to cells with low antiviral scores. Importantly, the trajectory line and pseudotime values closely follow an increase in antiviral score, indicating that our analysis identified genes associated with the development of an antiviral state (Figs 13A-B, 14). As microglia transitioned to an antiviral state, they upregulated several proinflammatory cytokines and chemokines, including *Ccl3*, *Ccl5*, and *Tnf* (Fig 13C). It was initially unknown whether the antiviral response would be mediated by infected cells, bystander cells, or both. Among proinflammatory microglia, both infected and bystander cells were responsible for cytokine upregulation (Fig 13C). While microglia moved along the antiviral trajectory, they also downregulated several genes known to be associated with anti-inflammatory microglia, including *Mrc1*, *Tgfb1*, and *Trem2* (Fig 13D). Astrocytes also transitioned to a proinflammatory state, upregulating the cytokines and chemokines *Ccl7*, *Cxcl1*, and *Il6* (Fig 13E). These results highlight the importance of coordination of glia-specific responses in antiviral immunity.

**The host response to HSV-1 in the neonatal brain involves coordination between diverse cell types**

While glia have demonstrated importance in the response to HSV-1, we were also interested in better understanding the complete repertoire of cell-to-cell communication in the CNS during infection. To do this, we performed ligand-receptor interaction inference using the R toolkit CellChat [130]. By analyzing basal signaling in the neonate mock-infected sample and comparing it to the HSV-infected sample we were able to identify several differences in both the number of interactions between cell types and the strength of those interactions (Fig 14A). We identified several significant signaling pathways that were exclusive to either the mock-infected or HSV-infected samples (Fig 14B). Among the upregulated pathways during infection were several cytokine and chemokine signaling pathways, including CXCL, TNF, and CCL signaling (Fig 14B). We chose to analyze these pathways further by examining the cell types involved and the specific ligand-receptor interactions at play. Most CNS cell types were found to be producers of CXCL chemokines during infection, including microglia, astrocytes, NPCs, VLMCs, and choroidal epithelial cells (Fig 14C). Interestingly, the primary targets of CXCL signaling were endothelial cells through the atypical chemokine receptor 1 (ACKR1) receptor (Fig 14C). As an atypical chemokine receptor, ACKR1 is present at endothelial junctions and is essential for translocation of chemokines across the blood-brain barrier in order to recruit circulating leukocytes [190]. TNF signaling was exclusively mediated by microglia, consistent with our trajectory analysis results (Fig 14D). A large portion of this signaling was autocrine through the TNF receptor 2 (TNFR2), consistent with previous reports of upregulation of TNFR2 by microglia in response to pro-inflammatory stimuli [191]. A significant proportion of TNF

signaling was targeted to vascular cells through both the TNF receptor 1 (TNFR1) and TNFR2 (Fig 14D). Finally, CCL chemokines were primarily produced by astrocytes, microglia, VLMCs, and choroidal epithelial cells (Fig 14E). The primary targets of CCL signaling were microglia and endothelial cells through CCR5 and ACKR1, respectively (Fig 14E).

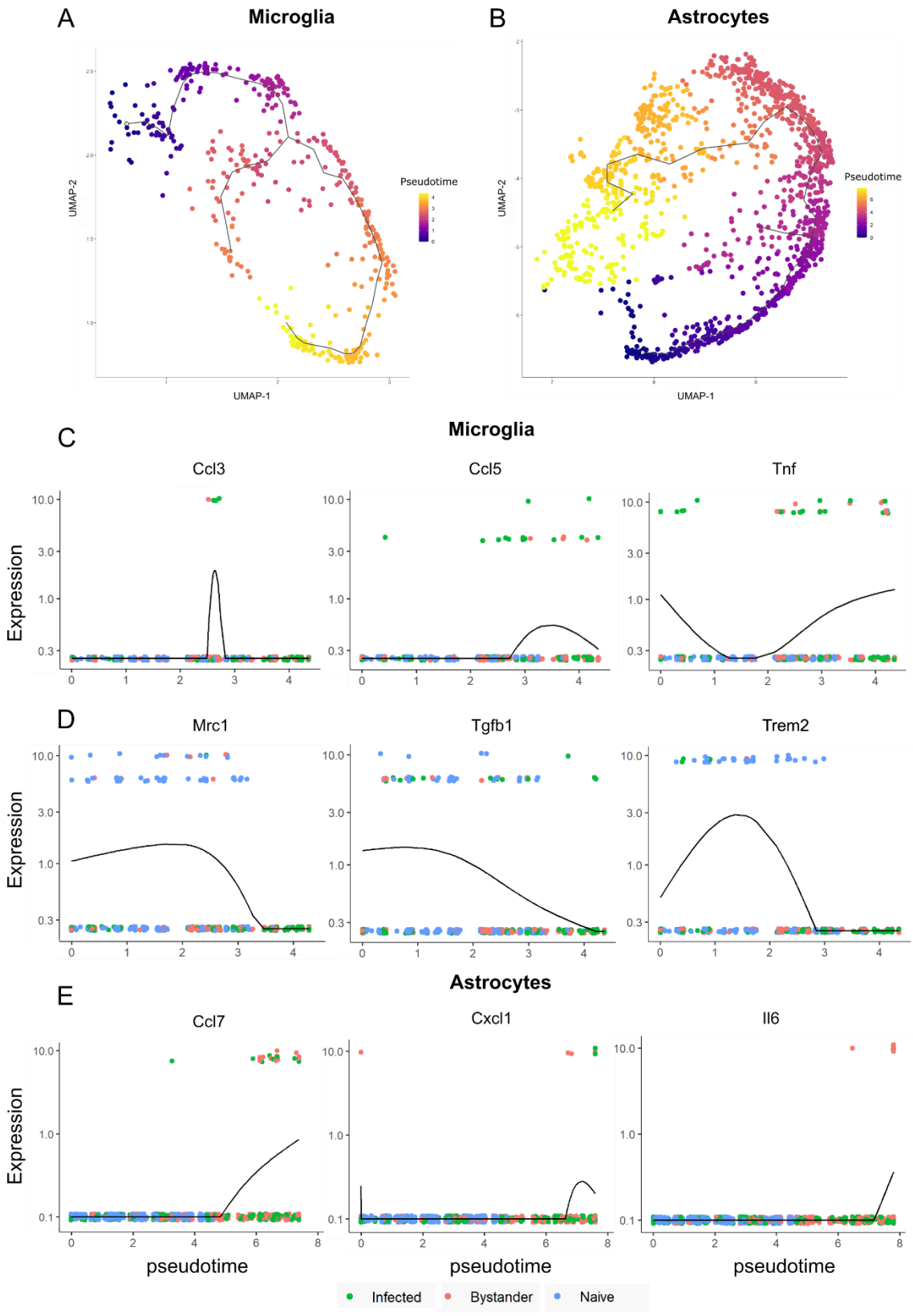
A
Microglia
UMAP-2
UMAP-1
Pseudotime
B
Astrocytes
UMAP-2
UMAP-1
Pseudotime
C
Microglia
Ccl3
Ccl5
Tnf
Expression
D
Mrc1
Tgfb1
Trem2
Expression
E
Astrocytes
Ccl7
Cxcl1
Il6
Expression
pseudotime
pseudotime
pseudotime
Infected
Bystander
Naive

**Figure 13. Microglia and astrocytes take on distinct and complementary proinflammatory states during HSV-1 infection.**

UMAP plots of microglia (A) and astrocytes (B) from mock infected and HSV-1 infected neonates. The learned trajectory is shown as a black line and colors denote pseudotime. Trajectory analysis of proinflammatory (C) and anti-inflammatory (D) genes significantly associated with pseudotime in microglia. (E) Trajectory analysis of proinflammatory genes significantly associated with pseudotime in astrocytes. Dot colors denote infection status. Infected cells are those containing HSV-1 transcript. Bystander cells come from infected mice but do not contain HSV-1 transcript. Naïve cells come from mock infected mice.

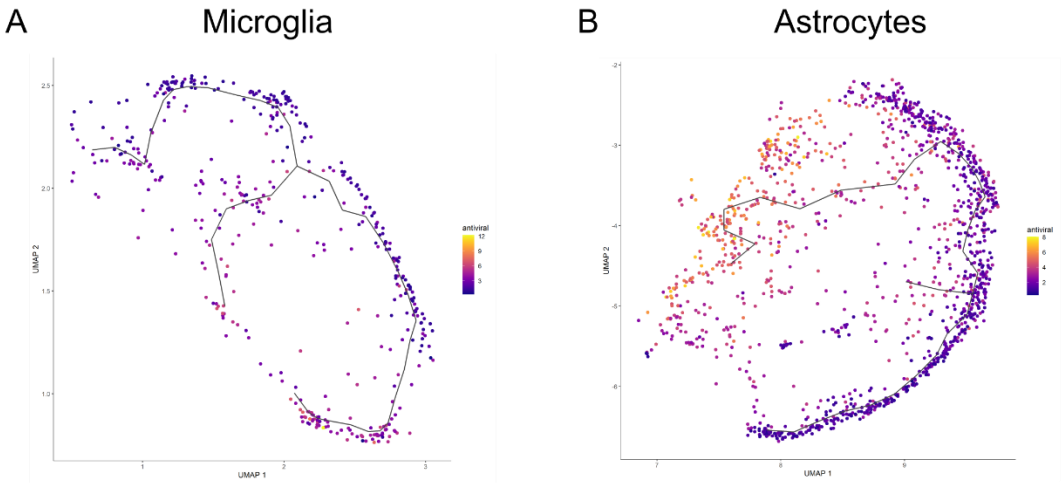
A
Microglia
B
Astrocytes
UMAP 1
UMAP 2
antiviral

**Figure 14. Trajectory analysis of astrocytes and microglia with antiviral module score.**

UMAP plots of neonatal microglia (A) and astrocytes (B) with the learned trajectory line overlayed. Color indicates antiviral module score.

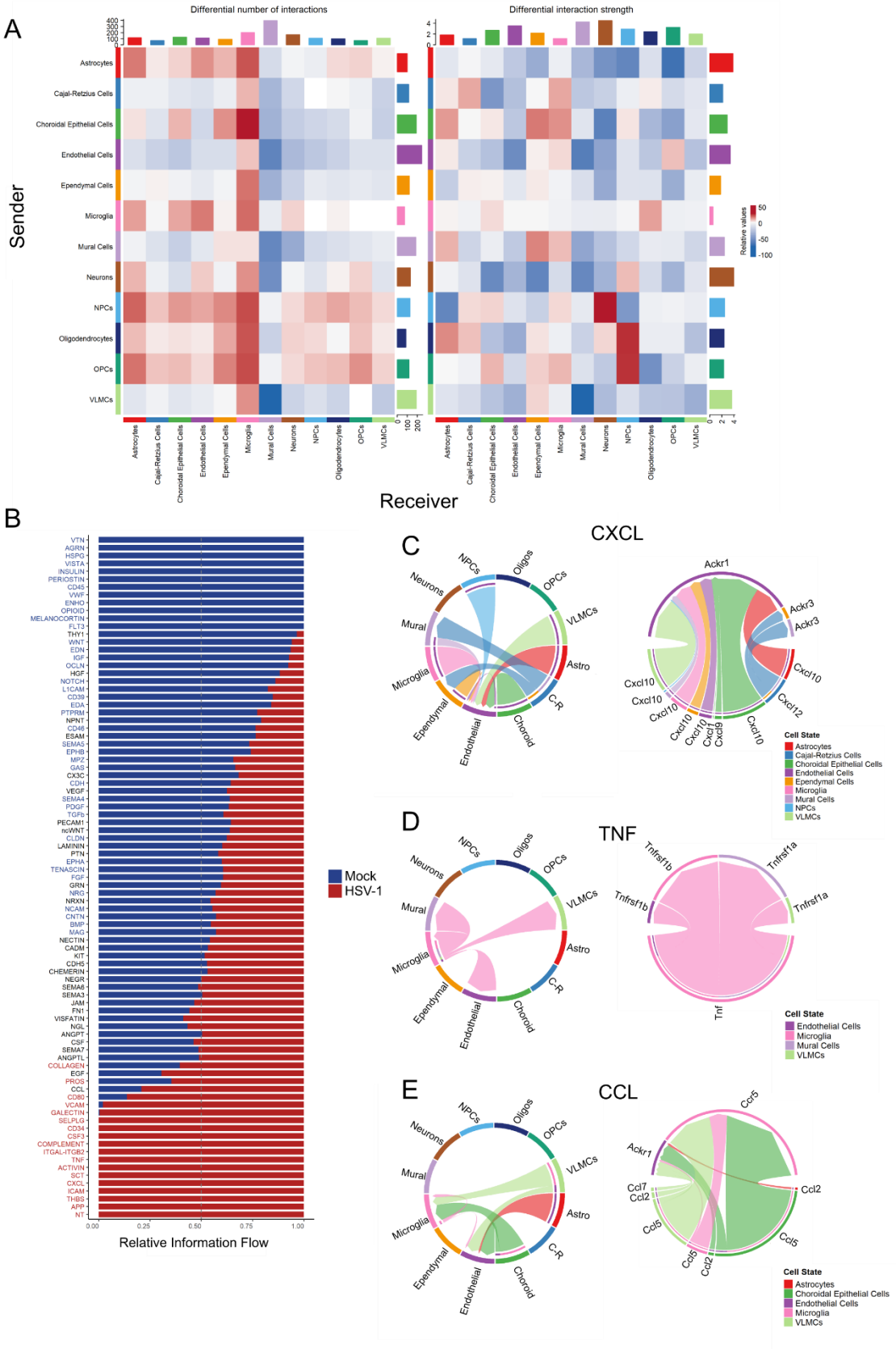
A
Differential number of interactions
Differential interaction strength
Sender
Receiver
Relative values
Astrocytes
Cajal-Retzius Cells
Choroidal Epithelial Cells
Endothelial Cells
Ependymal Cells
Microglia
Mural Cells
Neurons
NPCs
Oligodendrocytes
OPCs
VLMCs
B
Mock
HSV-1
Relative Information Flow
C
CXCL
D
TNF
E
CCL
Cell State

**Figure 15. The host response to HSV-1 in the neonatal brain involves coordination between diverse cell types.**

(A) Heatmap of differential cell-to-cell ligand-receptor communication between the HSV-1-infected neonatal cells and the mock-infected neonatal cells. Ligand-expressing cells are represented vertically, and receptor-expressing cells are represented horizontally. Left heatmap represents differential number of interactions and right heatmap represents differential strength of interactions between the two groups. Red represents increased interaction number or strength in the HSV-1-infected group; blue represents a decrease. (B) Relative information flow of various ligand-receptor pathways in the HSV-1-infected and mock-infected neonatal groups. Chord diagrams of CXCL (C), TNF (D), and CCL (E) signaling pathways. The left diagram shows the relevant cell types involved in each pathway; the right diagram shows the corresponding ligand-receptor pairs involved in each pathway.

**The long noncoding RNA Meg3 is expressed at higher levels in the neonatal CNS**

Despite mounting a robust antiviral response during infection involving the coordination between several cell types, neonatal CNS cells were still strikingly more susceptible to HSV-1 infection. Interestingly, antiviral module scores did not vary between adult and neonatal mock-infected cells, suggesting that baseline antiviral gene expression alone does not account for differences in susceptibility (Fig 17A). Due to the universal increase in susceptibility of neonatal cells, we sought to identify broadly differentially expressed genes at baseline between the adult mock-infected and neonate mock-infected samples. After performing DEG analysis of each cell type, genes were included if they were differentially expressed in neurons, astrocytes, and microglia. In total, we identified 26 genes that were expressed at higher levels in neonates and 12 genes expressed at higher levels in adults (Fig 17B). Importantly, none of the antiviral genes included in the antiviral module were present in this set of genes. One gene, the lncRNA *Meg3*, was differentially expressed at higher levels in neonates in every cell type except VLMCs (Fig 17B). *Meg3* is an imprinted gene that has been implicated in development, immunomodulation, and control of apoptosis [192–194]. We therefore chose to focus on a potential role for *Meg3* in increasing neonatal susceptibility.

Overall, *Meg3* expression was highest in neurons of both age groups (Fig 17C), although significantly more so in neonates. While neonates had high expression in all cell types, adults retained moderate expression of *Meg3* only in neurons and Cajal-Retzius cells (Fig 17C). We confirmed this difference in expression in situ using RNAscope. In the hippocampus, adults showed modest expression of *Meg3* only in the pyramidal layers, with little to no expression in the stratum radiatum (Fig 17D). By contrast, neonates had high expression of *Meg3* throughout

all structures, with high concentrations in the pyramidal layers (Fig 17D). When normalized to hippocampal area, neonates had approximately 2.5-fold increased expression of *Meg3* compared to adults (Fig 17E).

**The long noncoding RNA Meg3 inhibits apoptosis during HSV-1 infection in vitro**

We next wanted to identify the functional significance of higher *Meg3* expression in neonatal HSV-1 susceptibility. We used Lund human mesencephalic (LUHMES) cells, a human embryonic neural progenitor cell line that can be differentiated and supports HSV-1 replication, to assess the effect of *Meg3* overexpression in vitro [115,116]. LUHMES were nucleofected with either a *Meg3* overexpression vector or a control vector at day 2 of differentiation and infected with HSV-1 at day 5 of differentiation, at which point they are morphologically neuronal (Fig 18A). We confirmed that nucleofected LUHMES had robust expression of *Meg3* at the time of HSV-1 infection by quantitative real-time PCR (qRT-PCR) (Fig 18B). We next assessed the ability of *Meg3* to modulate apoptosis during HSV-1 infection using two different measures of apoptotic cells. At 6 hours post-infection, we found that HSV-1 infection alone was sufficient to dramatically reduce caspase-3 activity below baseline levels, consistent with known anti-apoptotic effects of various HSV-1 proteins [195–197] (Fig 18C). The mock-infected *Meg3* overexpressing cells also had a nonsignificant decrease in caspase-3 activity, and the HSV-1-infected Meg3 overexpressing cells had significantly reduced capase-3 activity compared to baseline (Fig 18C). We also measured apoptosis using terminal deoxynucleotidyl transferase dUTP nick end labeling (TUNEL) at 6 hours post-infection. We found that *Meg3* overexpression alone was sufficient to reduce TUNEL activity compared to baseline (Fig 18D). Importantly,

*Meg3* overexpression reduced TUNEL activity during HSV-1 infection, suggesting that high *Meg3* expression in neonates may prevent infected cells from undergoing programmed cell death (Fig 18D).

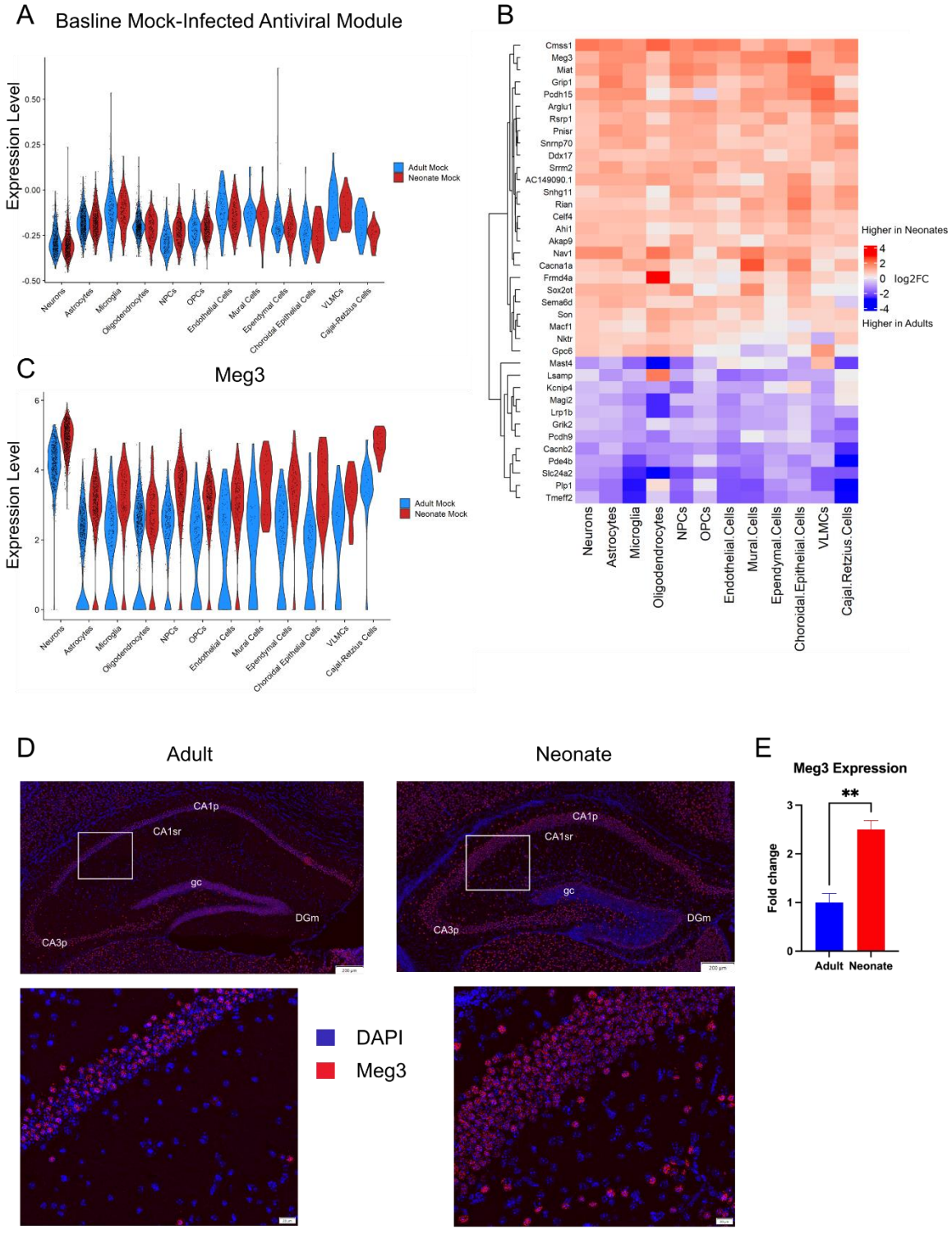
A
Basline Mock-Infected Antiviral Module
Expression Level
Adult Mock
Neonate Mock
Neurons
Astrocytes
Microglia
Oligodendrocytes
NPCs
OPCs
Endothelial Cells
Mural Cells
Ependymal Cells
Choroidal Epithelial Cells
VLMCs
Cajal-Retzius Cells
B
Higher in Neonates
log2FC
Higher in Adults
C
Meg3
D
Adult
Neonate
CA1p
CA1sr
gc
DGm
CA3p
DAPI
Meg3
E
Meg3 Expression
Fold change
Adult
Neonate

**Figure 16. The long noncoding RNA *Meg3* is expressed at higher levels in the neonatal CNS.**

(A) Violin plot of antiviral module expression in the adult mock and neonate mock samples. Dots represent individual cells. (B) Heatmap of 31 genes found to be differentially expressed at baseline in the neonate mock and adult mock samples. (C) Violin plot of *Meg3* expression in adult mock and neonate mock samples. (D) Representative RNAscope images of *Meg3* expression in hippocampal sections from uninfected adult and neonatal mice. Labeled regions: pyramidal layer of CA1 (CA1p), stratum radiatum of CA1 (CA1sr), granule cell layer of dentate gyrus (gc), molecular layer of dentate gyrus (DGm), pyramidal layer of CA3 (CA3p). (E) Relative expression of *Meg3* as quantified by normalizing fluorescence signal to the total hippocampal area (n=4 mice per age group). Values are expressed as means ± SEM (**P < 0.01).

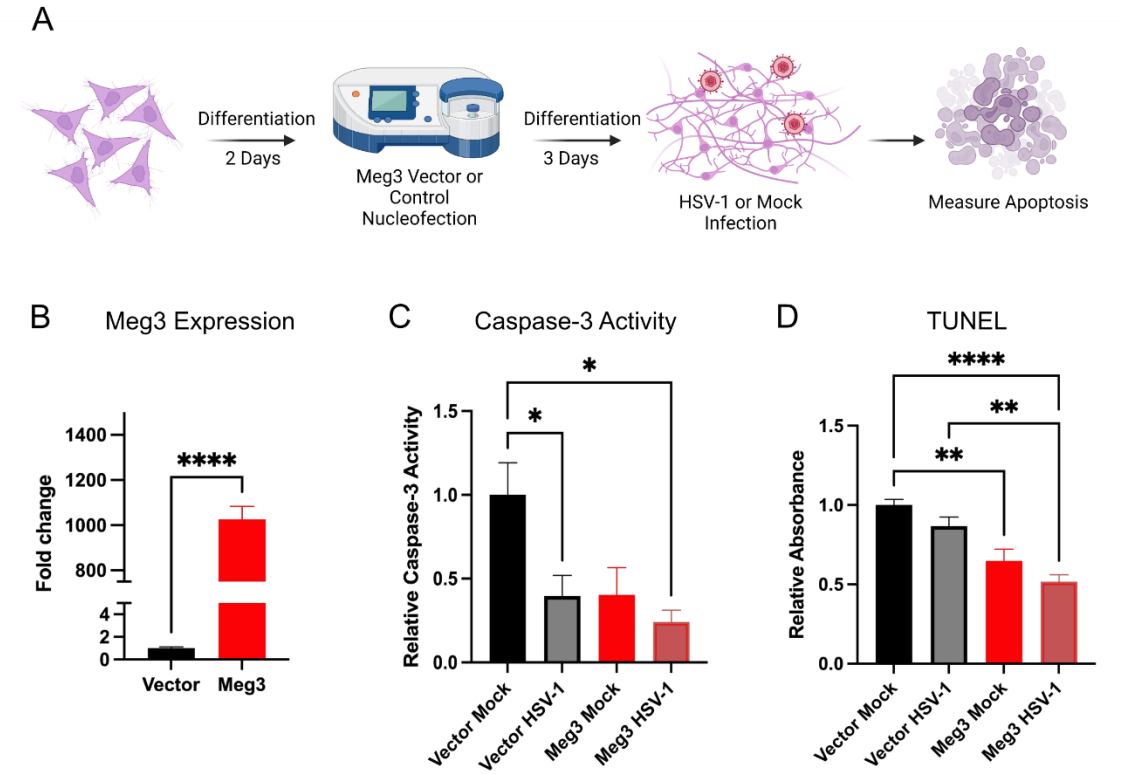
A
Differentiation
2 Days
Meg3 Vector or
Control
Nucleofection
Differentiation
3 Days
HSV-1 or Mock
Infection
Measure Apoptosis
B
Meg3 Expression
Fold change
1400
1200
1000
800
4
2
0
****
Vector
Meg3
C
Caspase-3 Activity
Relative Caspase-3 Activity
1.5
1.0
0.5
0.0
*
*
Vector Mock
Vector HSV-1
Meg3 Mock
Meg3 HSV-1
D
TUNEL
Relative Absorbance
1.5
1.0
0.5
0.0
****
**
**
Vector Mock
Vector HSV-1
Meg3 Mock
Meg3 HSV-1

**Figure 17. The long noncoding RNA Meg3 inhibits apoptosis during HSV-1 infection in vitro.**

(A) Schematic of experimental design. LUHMES were nucleofected with either the *Meg3* overexpression plasmid or the control plasmid on day 2 of differentiation. Cells were infected on day 5 of differentiation. Created with BioRender.com (B) Relative expression of *Meg3* in LUHMES cells at day 5 of differentiation nucleofected with either a *Meg3* overexpression vector or an empty vector. LUHMES were nucleofected at day 2 of differentiation and RNA was collected at day 5 for qPCR analysis (n=4 per condition). (C) Relative caspase-3 activity of LUHMES at 6 hours post-infection. LUHMES were infected on day 5 of differentiation and caspase-3 activity was normalized to the vector mock control (n=3-4 per group). (D) Relative TUNEL staining of LUHMES at 6 hours post-infection (n=4-5 per group). Values are expressed as means ± SEM (*P < 0.05, **P < 0.01, ****P < 0.0001).

## DISCUSSION

Neonates are overwhelmingly more susceptible to severe HSV-1 infection than adults. Using an intracranial model of infection that bypasses peripheral barriers to the CNS, we found that this difference in susceptibility is recapitulated in the murine brain. Given the same infectious dose, all neonatal cell types were infected at higher levels than in the adult. We have previously shown that HSV-1 displays tropism towards several CNS cell types in the adult [198]. In this study, we found no difference in cell tropism between the two age groups, suggesting that the developmental state of each cell type is a critical factor in its susceptibility to viral infection. To our knowledge, this is the most complete account of HSV-1 tropism in either the neonatal or adult CNS. A limitation of this aspect of our study is that HSV-1 infection was determined by the presence of viral transcript, leaving open the possibility of abortive rather than productive infection. Further study is needed to determine the extent to which abortive infection takes place in HSE.

The apparent resistance of adult cells to infection presented a challenge in qualitatively comparing neonatal and adult antiviral responses. We chose to initially focus on defining the neonatal response due to the sheer number of infected cells. Despite traditionally being thought of as having a dampened immune system, we demonstrated that neonates could mount detectable gene expression changes in response to HSV-1 infection. We defined a set of genes that are broadly upregulated across all cell types, consisting of several interferon-stimulated genes. All neonatal cell types were capable of taking on an antiviral state, raising the question of why this response is not protective. One possibility was that neonatal cells are not primed at baseline to restrict viral replication, but we found that antiviral module scores were similar at baseline

between the two age groups. We turned our attention to baseline differences in gene expression in an attempt to identify developmentally regulated genes that may influence viral replication. Interestingly, several long noncoding RNAs were found to be expressed at higher levels in neonates, including *Meg3*, *Snhg11*, and *Sox2ot*. While we chose to focus on the role of *Meg3* in increasing susceptibility to infection, we are interested in further exploring the significance of other lncRNAs in the context of HSV-1 infection.

*Meg3* has been best characterized as a tumor suppressor through its induction of p53, although several other functions are becoming more clear [119]. Knockout of the maternal *Meg3* allele is embryonic lethal in mice, highlighting its importance in normal development [194,199,200]. Little is known about the function of *Meg3* in neurodevelopment, but *Meg3* is known to interact with polypyrimidine tract-binding protein 1 (PTBP1) [201]. PTBP1 is an RNA-binding protein found at high levels in the nuclei of neural stem cells during development and promotes stemness and represses neuronal differentiation [202]. Ramos, et. al. found that another lncRNA, *Pnky*, is able to regulate neural stem cell differentiation through its interaction with PTBP1 [203]. In this way, *Meg3* may similarly regulate differentiation of CNS cells. Further study is needed to elucidate the mechanistic role of *Meg3* in neural development.

Extensive programmed cell death in the developing brain is physiologic and necessary for establishing the proper size of progenitor populations and proper neuronal connectivity [204]. The higher expression of *Meg3* in the neonatal brain and the importance of postnatal apoptosis regulation led us to examine whether *Meg3* might play a role in this process and inadvertently make neonatal cells less prone to shutting down HSV-1 replication. We found that *Meg3* overexpression inhibits apoptosis in LUHMES during infection. HSV-1 has evolved several

mechanisms to inhibit apoptosis in host cells, highlighting the importance this pathway in halting viral replication [195,196,205]. HSV-1 has also been shown to induce apoptosis in hippocampal cultures and in adult human cases of HSE [163]. We are currently investigating the mechanistic underpinnings of regulation of apoptosis by *Meg3* during HSE. Our study indicates that developmental regulation of apoptosis may have unintended consequences for susceptibility to viral infection.

# CHAPTER V: HSV-2 VARIATION CONTRIBUTES TO NEUROVIRULENCE DURING NEONATAL INFECTION*

*(Adapted from Cooper K. Hayes, Christopher K. Villota, Fiona B. McEnany, Stacey Cerón, David A. Leib, Richard Longnecker, Matthew D. Weitzman, and Lisa N. Akhtar. The Journal of Infectious Diseases. 22 April, 2022.)


## ABSTRACT

Herpes simplex virus (HSV) infection of the neonatal brain causes severe encephalitis and permanent neurologic deficits. However, infants infected with HSV at the time of birth follow varied clinical courses, with approximately half of infants experiencing only external infection of the skin rather than invasive neurologic disease. Understanding the cause of these divergent outcomes is essential to developing neuroprotective strategies. To directly assess the contribution of viral variation to neurovirulence, independent of human host factors, we evaluated clinical HSV isolates from neonates with different neurologic outcomes in neurologically-relevant in vitro and in vivo models. We found that isolates taken from neonates with encephalitis are more neurovirulent in human neuronal culture and mouse models of HSV encephalitis, as compared to isolates collected from neonates with skin-limited disease. These findings suggest that inherent characteristics of the infecting HSV strain contribute to disease outcome following neonatal infection.

## INTRODUCTION

Each year approximately 14,000 infants are infected with herpes simplex virus (HSV) in the perinatal period [206], typically due to maternal genital infection and shedding of HSV-1 or HSV-2 at the time of birth. Infected infants follow different clinical courses [207,208]. About half will experience only non-invasive disease affecting the skin, eyes, and mouth (SEM disease). However, 30% will experience invasive infection of the central nervous system (CNS disease), with another 15% experiencing invasive systemic infection (disseminated disease) with CNS involvement. While treatment of all HSV-infected neonates with acyclovir has dramatically decreased deaths [209], survivors of invasive CNS disease often experience permanent neurologic deficits [210–212]. The personal and societal costs of this lost developmental potential, over the lifetime of these individuals, cannot be overstated.

The factors that promote HSV infection of the neonatal brain are not well understood. This knowledge gap has prevented the development of neuroprotective therapeutic strategies. Previous studies have investigated the causes of HSV encephalitis in adults and older children, and have shown that individuals with rare host defects in specific innate immune pathways may be predisposed to CNS infection [105,172]. However, the vast majority of HSV encephalitis in adults and older children is not explained by a known host immune defect [213], and no such host defect has been shown to contribute to HSV encephalitis in neonates. In fact, the epidemiology of neonatal disease, with more than 45% of HSV-infected neonates experiencing CNS involvement, makes it unlikely that host genetics alone could account for invasive forms of infection.

Viral variants that impact virulence and disease outcomes have been identified for several pathogens including influenza [214], HIV [215], and others. These viral genotype-to-disease-

phenotype comparisons have classically been addressed in small RNA genomes with high levels of variability, while the large DNA genomes of herpesviruses have been considered less diverse. However, the recent work of our lab and others has shown that herpesvirus genetic variation exists between hosts, as well as within a given host [216–222]. These data provide rationale for assessing the contribution of HSV genetic variation to clinical manifestations and disease severity in neonatal infection.

We previously examined HSV-2 isolates from a cohort of neonates with diverse disease manifestations [216]. CNS disease-associated isolates displayed enhanced viral cell-to-cell spread through epithelial cell culture, as compared to virus isolated during SEM disease. These more virulent isolates also contained specific viral genetic variations in HSV proteins known to impact cell-to-cell spread and neurovirulence in animal models of encephalitis. These associations led us to hypothesize that enhanced ability of the virus to spread cell-to-cell, and potentially neuron-to-neuron, may underlie CNS pathogenesis and impact clinical outcome. Here we directly assessed the neurovirulence of neonatal HSV-2 isolates in a series of neurologically-relevant in vitro and in vivo models. We show that clinical HSV-2 isolates, in the absence of host variation, are sufficient to recapitulate the relative neurovirulence observed in the human neonatal patient. These findings suggest that inherent characteristics of the infecting HSV strain contribute to disease outcome following neonatal infection.

## RESULTS

### CNS-derived HSV-2 exhibits enhanced spread in human neuronal cultures

To determine whether HSV-2 isolated from neonates with neurologic versus non-neurologic clinical outcomes demonstrated enhanced spread in human neuronal cultures, we focused on isolates at opposite ends of the clinical spectrum. CNS11 was isolated directly from the CSF of a neonate with severe encephalitis and poor neurologic outcome, while SEM02 was isolated from the skin of a neonate with skin-limited disease and no long-term impairment (Table 1) [115]. Each was used to infect differentiated LUHMES cells (Fig 18A) [116,117]. Cells were infected at a low multiplicity of infection (MOI = 0.1) to assess differences over multiple rounds of viral replication and spread through the neuronal network (Fig 18B, C). For 72 hours post-infection (hpi) the extent of neuron-to-neuron spread was measured either quantitatively by titer (Fig 18B), or qualitatively by immunofluorescence (Fig 18C). Infectious virions recovered were similar at 2, 6, and 12 hpi, confirming that equivalent amounts of each virus were present following the initial infection, and after a single cycle of replication (Fig 18B). However, by 72 hpi, after multiple rounds of replication and spread, CNS11 achieved statistically higher viral loads than SEM02. Next, infected LUHMES were fixed at 24, 48, and 72 hpi and subjected to immunocytochemistry analysis using antibodies directed against total HSV (Fig 18C). By 48 hpi a greater number of infected cells arose from each single infectious focus of CNS11 as compared to SEM02. By 72 hpi CNS11 consumed each culture and often resulted in the breakdown of neuronal processes. These data showed that both viruses were competent to enter neurons, replicate with equal kinetics during early infection, and achieve a productive, spreading infection within neuronal cultures. However, the neurologic disease-associated isolate CNS11 exhibited

enhanced spread as compared to the skin-limited SEM02, indicating a potential advantage in a neurologic environment.

**Table 1. Clinical and experimental characteristics of each neonatal HSV-2 isolate.**

| Neonatal Patient | | | | Mouse | |
|---|---|---|---|---|---|
| Clinical isolate | Disease(s) at diagnosis | Sample source | Morbidity score | Death - IC (%) | Death - IP (%) |
| SEM18 | SEM | SKIN | | 1/9 (11%) | 0/6 (0%) |
| SEM13 | SEM | SKIN | | 5/9 (56%) | 0/10 (0%) |
| SEM02 | SEM | SKIN | | 5/9 (56%) | 1/11 (9%) |
| DISS14 | DISS + CNS | CSF | 2 | 6/9 (67%) | 2/12 (17%) |
| CNS03 | CNS | SKIN | 4 | 7/9 (78%) | 1/6 (17%) |
| DISS29 | DISS + CNS | SKIN | 3 | 8/9 (89%) | 0/6 (0%) |
| CNS12 | CNS | SKIN | 4 | 9/9 (100%) | 1/6 (17%) |
| CNS17 | CNS | SKIN | 4 | 9/9 (100%) | 0/6 (0%) |
| CNS11 | CNS | CSF | 4 | 9/9 (100%) | 6/11 (55%) |

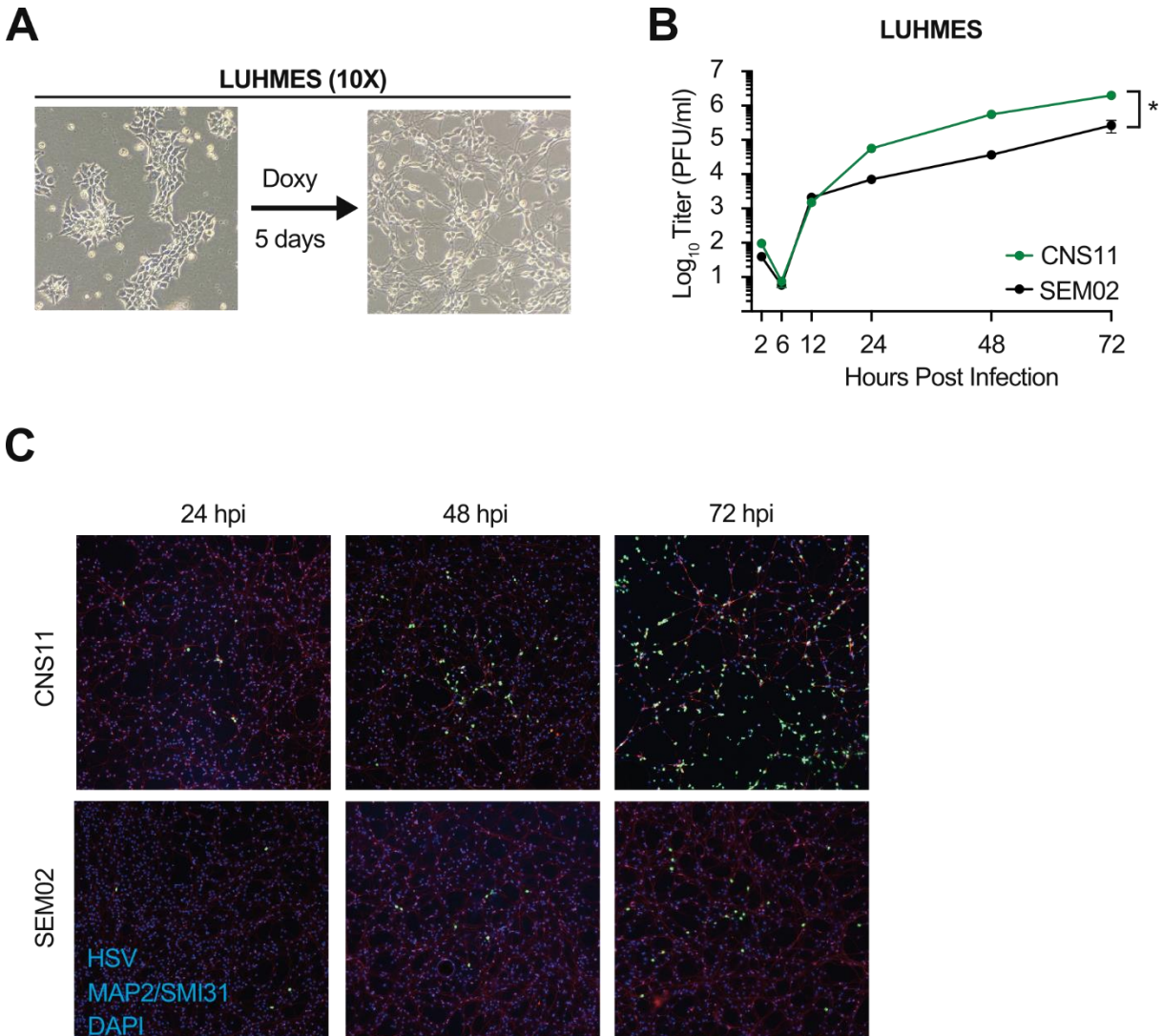
A
LUHMES (10X)
Doxy
5 days
B
LUHMES
Log10 Titer (PFU/ml)
7
6
5
4
3
2
1
*
CNS11
SEM02
2 6 12 24 48 72
Hours Post Infection
C
24 hpi
48 hpi
72 hpi
CNS11
SEM02
HSV
MAP2/SMI31
DAPI

**Figure 18. CNS-derived HSV-2 exhibits enhanced spread in human neuronal cultures.** (A) Human LUHMES were differentiated for 5 days in the presence of doxycycline (doxy) to produce neuron-like cells. 10X images of replicating vs. terminally differentiated cells are shown. (B, C) Differentiated LUHMES were infected at MOI=0.1 and samples were harvested at each time point. (B) Virus was quantified by titer. Triplicate data are shown as mean +/- SEM. *p=0.01. (C) In parallel experiments, HSV-positive cells (green) were evaluated by immunofluorescence. Neuronal processes are counterstained with MAP2 and SMI31 (red), and cell nuclei with DAPI (blue). 5x images are shown. Images are representative of results from 3 independent experiments.

**CNS-derived HSV-2 promotes neurologic disease following murine peripheral inoculation**

These in vitro data suggested CNS11 may promote neurologic infection via an increased ability to enter or spread within the CNS. Therefore, we tested its in vivo neurologic phenotypes following peripheral inoculation. First, intraperitoneal infections were performed in adult mice which result in presumed hematogenous dissemination of virus [122,223]. After 2 weeks, only 9% of animals infected with the skin-derived SEM02 had died, as compared to 55% of animals infected with the CNS-derived CNS11 (Fig 19A). All animals that died had high viral loads within the brain at the time of death (Fig 19B). However, significantly more animals developed neurologic infection following inoculation with CNS11 as compared to SEM02 (73% vs. 9%; Fig 19B), with nearly half of CNS11-infected animals experiencing infection only within the brain following hematogenous dissemination (Fig 19B). These data indicate that CNS11 is able to enter or replicate within the CNS following peripheral inoculation more readily than SEM02 and suggest a possible preference for the CNS relative to other organs.

**CNS-derived HSV-2 promotes neurologic disease following murine intracranial inoculation**

Evaluation of peripheral models of infection provides clinical relevance but does not distinguish between a viral advantage in entry verses replication within the CNS. To determine whether CNS11 was more neurovirulent than SEM02 in the absence of peripheral barriers to CNS entry, we assessed these HSV-2 isolates following direct intracranial inoculation of adult mice [111,180,184]. All mice infected with CNS11 died by 9 days post-infection (dpi) as compared to half of those infected with SEM02 (Fig 20A). Notably, CNS11-infected animals achieved consistently high viral loads within the brain at the time of death (Fig 20B). By contrast, animals

who survived direct intracranial injection of SEM02 were able to clear infectious virus from the brain by the conclusion of the experiment (Fig 20B). To further define the kinetics of viral replication and clearance following intracranial infection, we performed inoculations with either virus and harvested brain tissue over time (Fig 20C,D). SEM02 viral load lagged behind CNS11 at 3 and 5 dpi (Fig 20C). To specifically assess the time course of SEM02 clearance from the brain, we infected animals with SEM02 and harvested brain tissue over a later time course from animals predicted to survive based on percentage of weight loss at 7 dpi. All predicted survivors were able to clear virus between 9 and 12 dpi (Fig 20D).

Next, intracranial infections were performed in 7-day-old mice to determine whether CNS11 and SEM02 also produced different neurologic phenotypes in neonatal animals. Infection with CNS11 resulted in rapid death of all animals by 4 dpi (Fig 21A), and uniformly high viral loads within the brain at the time of death (Fig 21B). In this neonatal model, SEM02 also resulted in the death of all infected animals but occurred statistically later than in those infected with CNS11 (Fig 21A). Interestingly, several SEM02-infected animals had no detectable virus within the brain at the time of death (Fig 21B), mimicking the clearance of SEM02 seen in the adult model. Overall, neonatal brains contained approximately 10-fold more infectious virus at the time of death as compared to adult brains infected with the same amount of input virus (Fig 20B, 21B).

These data showed that CNS11 consistently resulted in neurologic infection and death once peripheral barriers to CNS entry were breached, while SEM02 virions were often cleared from the brain. Notably, viral clearance late in infection led to survival in adult animals, but not in neonatal animals. This suggests a role for virus-independent mortality, perhaps due to an

overwhelming immune response necessary for viral clearance that cannot be tolerated by the neonatal brain.

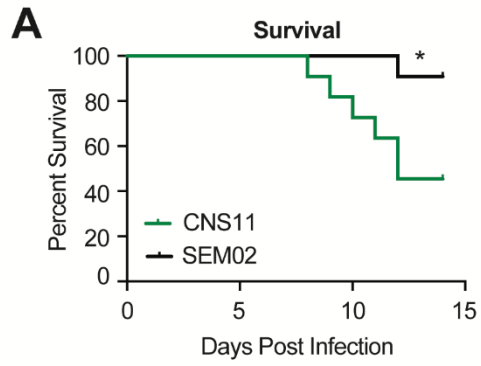


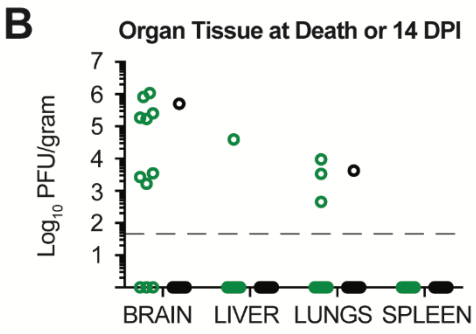


| | # Organs with PFU Detected | | | | # Animals with PFU Detected | | | | |
|---|---|---|---|---|---|---|---|---|---|
| | | | | | Brain Only | Brain + Peripheral Organs | PFU Detected in Brain | No PFU Detected in Brain | |
| **CNS11** | 8/11 | 1/11 | 3/11 | 0/11 | 5/11 | 3/11 | 8/11 | 3/11 | ** |
| **SEM02** | 1/11 | 0/11 | 1/11 | 0/11 | 0/11 | 1/11 | 1/11 | 10/11 | |

**Figure 19. CNS-derived HSV-2 promotes neurologic disease following intraperitoneal inoculation in adult mice.**

Adult mice were injected intraperitoneally with 1000 PFU HSV-2 (n=11 mice/virus over 2 independent experiments) and monitored daily for survival (A); *p=0.02. Virus was quantified in brain, liver, lung, and spleen tissue at the time of death or completion of the experiment (B). Grey dashed line represents limit of detection. Organs and animals are categorized by presence or absence of detectable virions; **p=0.004.

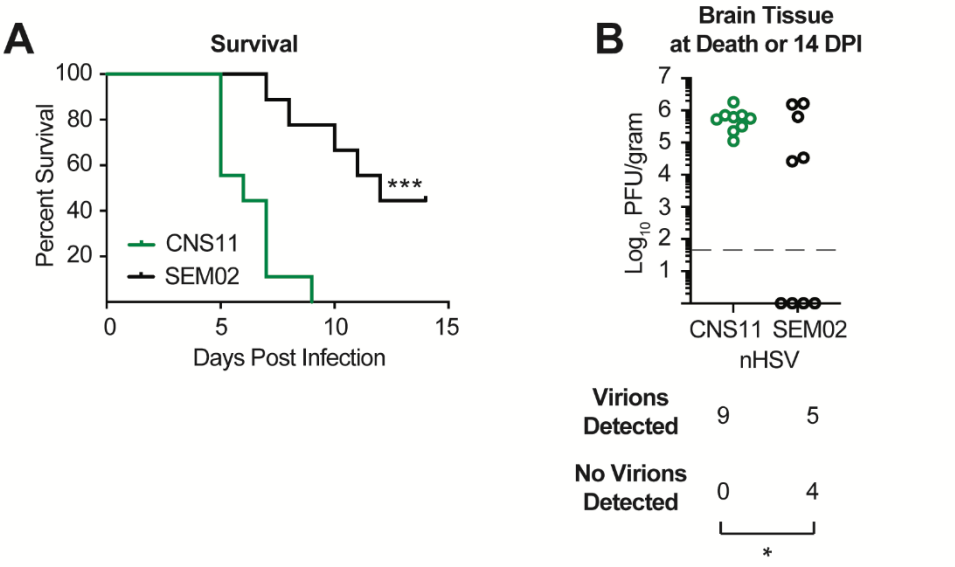
A
Survival
Percent Survival
100
80
60
40
20
0
5
10
15
Days Post Infection
CNS11
SEM02
***
B
Brain Tissue
at Death or 14 DPI
Log10 PFU/gram
7
6
5
4
3
2
1
CNS11
SEM02
nHSV
Virions Detected
9
5
No Virions Detected
0
4
*

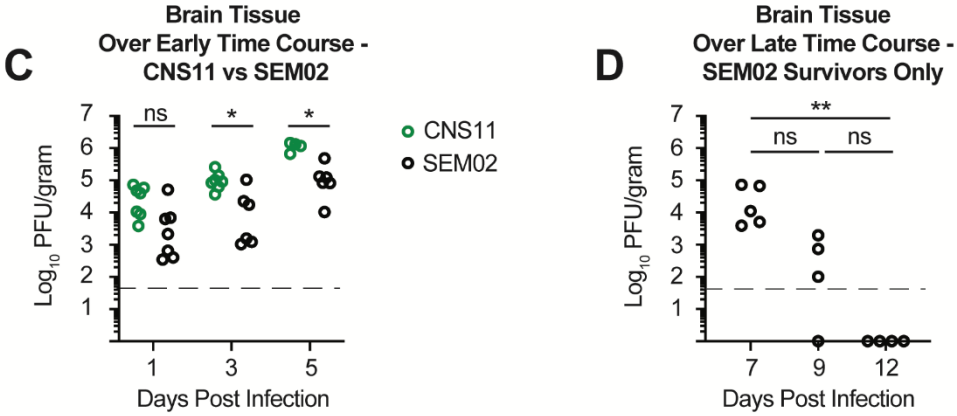
C
Brain Tissue
Over Early Time Course -
CNS11 vs SEM02
Log10 PFU/gram
ns
*
*
1
3
5
Days Post Infection
CNS11
SEM02
D
Brain Tissue
Over Late Time Course -
SEM02 Survivors Only
Log10 PFU/gram
**
ns
ns
7
9
12
Days Post Infection

**Figure 20. CNS-derived HSV-2 promotes neurologic disease following intracranial inoculation in adult mice.**

Adult mice were injected intracranially with 1000 PFU HSV-2 (n=9 mice/virus over 2 independent experiments) and monitored daily for survival (A); ***p=0.0002. Virus was quantified in brain tissue by titer (B) at the time of death or conclusion of the experiment. Grey dashed line represents limit of detection. Animals are categorized by presence or absence of detectable virions in brain; *p=0.04. Mice were also sacrificed over time (n=4-7 mice/virus at each timepoint over 2 independent experiments), and viral load within the brain quantified (C,D); *p<0.05.

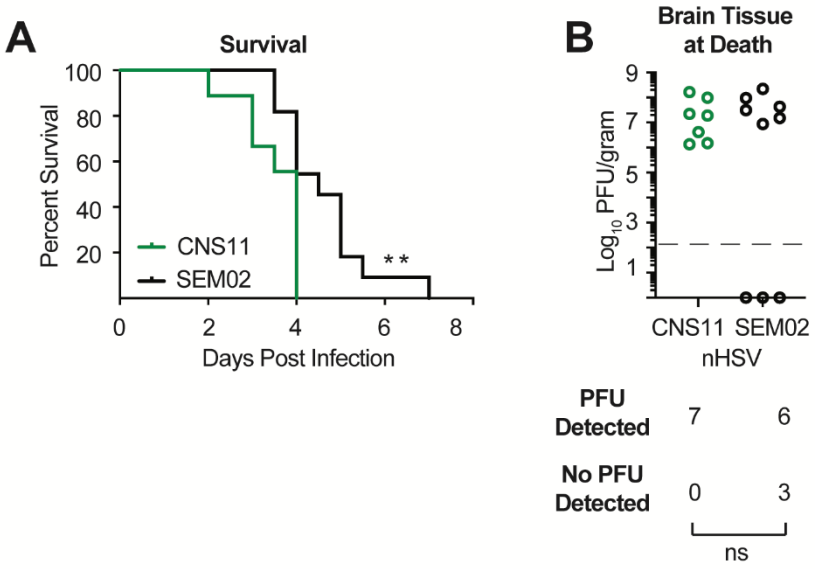
A
Survival
Percent Survival
100
80
60
40
20
CNS11
SEM02
**
0
2
4
6
8
Days Post Infection
B
Brain Tissue at Death
Log10 PFU/gram
9
7
5
3
1
CNS11
SEM02
nHSV
PFU Detected
7
6
No PFU Detected
0
3
ns

**Figure 21. CNS-derived HSV-2 promotes neurologic disease following intracranial inoculation in neonatal mice.**

Neonatal mice were injected intracranially with 1000 PFU HSV-2 (n=9-11 mice/virus over 3 independent experiments) and monitored daily for survival (A); **p=0.01. Virus was quantified in brain tissue by titer at the time of death (B). Grey dashed line represents limit of detection. Animals are categorized by presence or absence of detectable virions in brain.

**Multiple HSV-2 strains isolated from neonates with CNS disease exhibit superior neurovirulence**

These experiments evaluating the in vivo phenotype of two HSV-2 strains isolated from neonates on opposite ends of the clinical neurologic spectrum suggest that inherent viral differences can contribute to neurovirulence. To determine if the ability of a particular virus to recapitulate clinical disease manifestations in a murine model is more generalizable, we subjected 7 additional HSV-2 isolates collected from neonates with differing severity of disease (Table 1) [216] to intracranial infection of adult mice (Fig 22A,B). In addition to CNS11, CNS12, CNS17, and DISS29 caused severe neurologic morbidity in their human source patients (Table 1). All of these HSV-2 isolates caused significant mortality and high CNS viral loads following murine intracranial infection (Fig 22A,B).

In addition to SEM02, SEM13 and SEM18 were collected from neonates with skin-limited disease (Table 1). These isolates resulted in significantly lower rates of mortality and higher rates of viral clearance from the brain (Fig 22A,B). Notably, DISS14 caused disseminated disease with CNS involvement in its human source patient, but only mild neurologic morbidity (Table 1). This HSV-2 isolate resulted in intermediate disease following murine intracranial infection (Fig 22A,B).

These data showed that virus alone, independent of host factors, can recapitulate the relative neurovirulence observed in a human neonatal host. While the neurologic outcome of neonatal HSV-2 infection is almost certainly multifactorial, these data indicate that viral variation contributes to clinical outcome.

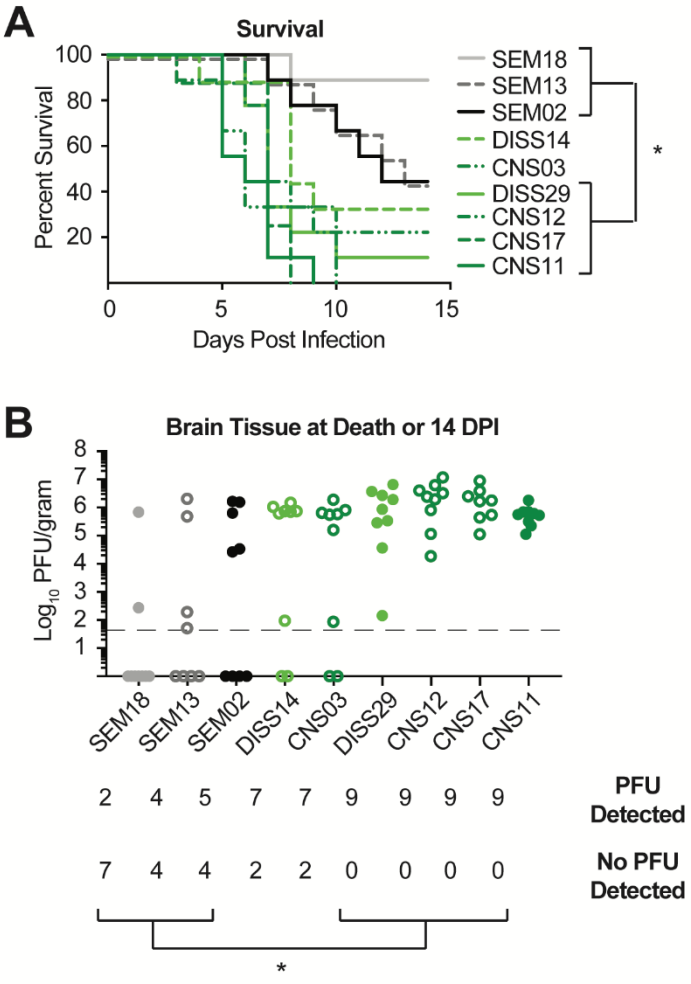
A
Survival
Percent Survival
100
80
60
40
20
0
5
10
15
Days Post Infection
SEM18
SEM13
SEM02
DISS14
CNS03
DISS29
CNS12
CNS17
CNS11
*
B
Brain Tissue at Death or 14 DPI
Log10 PFU/gram
8
7
6
5
4
3
2
1
SEM18
SEM13
SEM02
DISS14
CNS03
DISS29
CNS12
CNS17
CNS11
2 4 5 7 7 9 9 9 9
PFU Detected
7 4 4 2 2 0 0 0 0
No PFU Detected
*

**Figure 22. Multiple HSV-2 strains isolated from neonates with CNS disease exhibit superior neurovirulence.**

Adult mice were infected intracranially with 1000 PFU HSV-2 (n=9 mice/virus) and monitored daily for survival (A); *$p<0.02$. Virus was quantified in brain tissue by titer (B) at the time of death or conclusion of the experiment. Grey dashed line represents limit of detection. Animals are categorized by presence or absence of detectable virions in brain; *$p<0.05$.

## DISCUSSION

Neonatal HSV infection results in widely disparate neurologic outcomes which are often assumed to be driven by human host variation. We utilized a series of neurologically-relevant in vitro and in vivo models to evaluate the neurovirulence of clinical HSV-2 isolates in the absence of human host variation. We found that CNS disease-associated isolates were significantly more likely to cause neurologic infection and death as compared to skin-limited isolates in multiple murine models of encephalitis, in both adult and neonatal animals, performed in multiple laboratories with separately grown viral stocks. Our results suggest an inherent difference in the potential for a given HSV-2 strain to cause invasive neurologic disease in the human neonate.

This study represents the largest set of HSV isolates obtained from neonates that have been evaluated genotypically [216], and the data presented here provide an important link to neurologic phenotype. We previously identified several viral variations in HSV-2 proteins associated with cell-to-cell spread which were unique to isolates cultured directly from the CSF (gK, gI, gG, US2, and UL8), and other variations associated with CNS disease (UL24), or disseminated disease (UL20) more broadly. However, this analysis could only assess for genotype-to-human-phenotype links driven by multifactorial clinical outcomes, or sample characteristics of unknown significance such as location of virus collection. The current study provides additional data, allowing for comparative genomic analysis of the most neurovirulent isolates, unbiased by host or clinical characteristics. For example, we can compare the previously described genic regions to identify amino acid variations that occur only in isolates causing significantly greater animal mortality (CNS11, CNS12, CNS17, and DISS29) as compared to SEM isolates (Fig 22A). This analysis reveals two new variations of potential importance (Fig

23): one unique variation occurs in the thymidine kinase (UL23), and another in the capsid protein VP5 (UL19). Both proteins have been previously shown to be important for neurovirulence [224–226]. Use of this method to identify additional monogenic associations in intergenic and highly repetitive regions of the viral genome not previously analyzed, and to identify polygenic links, is ongoing.

In addition to these genomic links, evaluation of viral phenotype in multiple models of encephalitis provides further insights. Notably, all CNS-disease associated isolates tested exhibited neurovirulence, regardless of whether the isolate was obtained from the CSF or skin of the patient. This suggests that inherent characteristics of the infecting strain drive neurovirulence, rather than these features being selected for in the viral population only after entry and replication within the human neonatal brain. Our results also identified nuanced differences between neurovirulent strains. While CNS11 exhibited an advantage in establishing CNS infection in all murine models of encephalitis, the neurovirulence of other CNS disease-associated isolates was dependent on the route of inoculation. These results highlight the importance of peripheral barriers to CNS infection and suggest that multiple viral factors may contribute to the capacity for neurologic disease by different mechanisms, either independently or in combination.

It is important to note that human clinical disease outcome is almost certainly multifactorial, including viral virulence, route of infection, viral dose, gestational age, host immune competence, and presence of maternal antibody, among other factors. Our data indicate that when other factors are controlled for, viral variation alone is sufficient to reproduce the relative neurovirulence observed in human patient, suggesting it is an important contributor.

Notably, while neonates often experience severe neurologic outcomes, their mothers who are presumably genitally infected with the same viral strain do not – although notable rare exceptions involving dual mother-child fatality do exist [217,227]. It is possible that inherent neurovirulent characteristics are revealed preferentially in neonates because peripheral barriers are more routinely breached. This may occur in the setting of increased blood brain barrier permeability associated with gestational age, or penetration of epithelial barriers with scalp electrode placement during birth monitoring, both known risk factors for neonatal CNS infection [98,211]. Our results also showed increased viral load following intracranial infection of neonatal animals as compared to adult animals, as well as death of neonates even following viral clearance. These data may indicate an exaggerated immune response as a contributor to neonatal mortality, and suggest that a complete evaluation of the neuroimmune response elicited by various viruses would provide valuable insights on how age-specific differences contribute to poor neonatal outcomes. Understanding which viral strains have the greatest inherent potential for harm, and ultimately the mechanism by which this occurs, could lead clinicians to provide longer courses of antiviral treatment or suppression in specific circumstances, or target a dysregulated neuroimmune response to provide therapeutic benefit [228]. This unique approach utilizes natural forward genetics and clinical observations, which are then further refined by animal modeling, to elucidate the key virus-host interactions in the neonatal brain that determine clinical outcome.

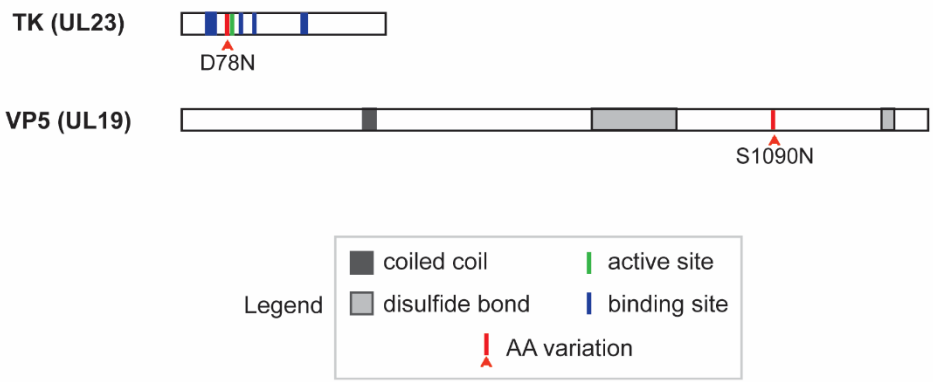
TK (UL23)
D78N
VP5 (UL19)
S1090N
Legend
coiled coil
disulfide bond
active site
binding site
AA variation

**Figure 23. Coding variations shared by neonatal HSV-2 isolates producing the highest rates of mortality and neurologic infection following murine intracranial inoculation.**

The domain structure is shown for each HSV-2 protein. Red arrows and text labels indicate protein-coding variations discussed in the text.

# CHAPTER VI: DISCUSSION

This thesis focused on two critical determinants of herpes simplex encephalitis outcomes: the host response and viral genetic variation. First, I studied the importance of the host inflammasome pathway in contributing to harmful inflammation in the course of HSE (Chapter III). Throughout the course of this thesis, I made extensive use of murine models of HSE due to the natural ability of HSV to infect mice and the ease of altering both host and viral factors to study their effects. At the onset of this project, we were unsure whether inflammasomes would be protective or harmful in HSE. We found that while individual inflammasome pattern recognition receptors were dispensable for affecting HSE mortality, the inflammasome adaptor protein ASC contributes to mortality and neuroinflammation. This suggests that in vivo, HSV-1 activates more than one redundant inflammasomes. Importantly, the activation of inflammasomes and the downstream inflammation did not contribute to the control of viral replication. Thus, we identified a host response pathway that could potentially be targeted without unintended effects on helpful immune responses. Throughout my thesis studies, I have studied in particular detail the responses of glia in mediating the innate immune response to HSV-1. In Chapter III, I identified microglia, the resident macrophages of the CNS, as the key mediators of the inflammasome response in HSE. Although a microglial response was found to be detrimental in this study, microglia themselves are essential in protecting against HSV infection [229]. This highlights the importance of balance in the host response during HSE between effective clearance of virus and excessive neuroinflammation. The potential to target detrimental neuroinflammation while simultaneously inhibiting viral replication with traditional antiviral therapy is exciting. Since publishing this study, other groups have confirmed the

importance of microglia in mediating the inflammasome response during HSV-1 infection [230,231].

While Chapter III focused on a specific pathway and its role in HSE, I wanted to use an unbiased method to examine not only the adult host response to infection, but also the neonatal response and their differences. In Chapter IV, I used single-nucleus RNA sequencing to characterize the host response during HSE. In this study, I used stereotaxic delivery of the viral inoculum to the same site in both age groups in order to compare identical cell type responses. I found that all neonatal cell types were more susceptible to HSV-1 than adult cells, indicating that an age-dependent cell tropism is not responsible for the increased susceptibility in this age group. I found that despite being more susceptible, neonates mount a robust but ineffective antiviral response to infection. Neonatal astrocytes and microglia took on distinct proinflammatory states, with both infected and bystander cells responding to infection. Central to this response was the elaboration of proinflammatory cytokines and chemokines. In Chapter III, I identified the chemokine CCL6 as a key mediator downstream of inflammasome signaling. In Chapter IV, I used ligand-receptor interaction analysis to examine the complete repertoire of cytokine and chemokine networks in the neonatal brain. I found that most CNS cell types participate in these pathways in one way or another. For example, CXCL chemokines were found to be produced by most cell types during infection and signaled primarily through the endothelial cell ACKR1 receptor. This result highlights the importance of a coordinated response from many cell types to recruit infiltrating leukocytes to the CNS during infection. Surprisingly, I found that baseline antiviral transcript levels were similar between neonates and adults. I therefore turned our attention to developmentally regulated genes that could indirectly promote or inhibit viral

replication. Interestingly, I identified several lncRNAs that are expressed at higher levels in the neonatal brain. One of these, the maternally-expressed gene *Meg3* was found at higher levels in nearly every cell type. I found that overexpression of *Meg3* resulted in inhibition of apoptosis in LUHMES during infection. This discovery suggests that developmentally-regulated genes other than antiviral factors could contribute to age-dependent susceptibility. The role of lncRNAs in herpesvirus pathogenesis is an emerging field in need of further study. Kaposi's sarcoma-associated herpesvirus (KSHV) is known to dysregulate several lncRNAs, including *Meg3*, in order to promote oncogenesis [232]. The lncRNA nuclear paraspeckle assembly transcript 1 (NEAT1) is upregulated during HSV-1 infection and important for recruitment of STAT3 to viral promoters [233]. Similarly, the lncRNA *U90926* is upregulated during HSV-1 infection and has been shown to increase viral DNA replication and proliferation [234]. A more complete understanding of the regulatory effects of lncRNAs during HSE is needed and is currently under investigation in our lab.

Finally, in Chapter V, I studied how genetic variation in clinical isolates of HSV-2 contributes to neurovirulence in mouse models of HSE. As a DNA virus, HSV has a relatively low mutation rate. Therefore, the focus has traditionally been on host factors that contribute to virulence during neonatal HSV infection. This study is the first to use a forward genetics approach to take clinical isolates from patients with varying disease courses and validate that the genetic makeup of the virus itself contributes to that course. By characterizing the neurovirulence phenotype of each isolate in mice, we can reexamine genomic variation that is common to either mild or severe isolates to identify mutations with clinical relevance. This approach allows for natural viruses, rather than lab strains, to inform us about factors that are important for causing

human disease. Future studies will focus on expanding the range of clinical isolates and their real-world disease courses to better understand factors that are critical for each step of virus life cycle.

# REFERENCES


1. Bradley H, Markowitz LE, Gibson T, McQuillan GM. Seroprevalence of Herpes Simplex Virus Types 1 and 2—United States, 1999–2010. J Infect Dis. 2014;209: 325–333. doi:10.1093/infdis/jit458

2. Pebody R, Andrews N, Brown D, Gopal R, de Melker H, Francois G, et al. The seroepidemiology of herpes simplex virus type 1 and 2 in Europe. Sex Transm Infect. 2004;80: 185–191. doi:10.1136/sti.2003.005850

3. Knipe DM, Howley P. Fields Virology. Lippincott Williams & Wilkins; 2013.

4. Pinninti SG, Kimberlin DW. Neonatal herpes simplex virus infections. Semin Perinatol. 2018;42: 168–175. doi:10.1053/j.semperi.2018.02.004

5. Grünewald K, Desai P, Winkler DC, Heymann JB, Belnap DM, Baumeister W, et al. Three-Dimensional Structure of Herpes Simplex Virus from Cryo-Electron Tomography. Science. 2003;302: 1396–1398. doi:10.1126/science.1090284

6. Kieff ED, Bachenheimer SL, Roizman B. Size, Composition, and Structure of the Deoxyribonucleic Acid of Herpes Simplex Virus Subtypes 1 and 2. J Virol. 1971;8: 125–132.

7. Poffenberger KL, Roizman B. A noninverting genome of a viable herpes simplex virus 1: presence of head-to-tail linkages in packaged genomes and requirements for circularization after infection. J Virol. 1985;53: 587–595.

8. Wadsworth S, Jacob RJ, Roizman B. Anatomy of herpes simplex virus DNA. II. Size, composition, and arrangement of inverted terminal repetitions. J Virol. 1975;15: 1487–1497.

9. McGeoch DJ, Rixon FJ, Davison AJ. Topics in herpesvirus genomics and evolution. Virus Res. 2006;117: 90–104. doi:10.1016/j.virusres.2006.01.002

10. Lycke E, Hamark B, Johansson M, Krotochwil A, Lycke J, Svennerholm B. Herpes simplex virus infection of the human sensory neuron. An electron microscopy study. Arch Virol. 1988;101: 87–104. doi:10.1007/BF01314654

11. Milne RSB, Nicola AV, Whitbeck JC, Eisenberg RJ, Cohen GH. Glycoprotein D Receptor-Dependent, Low-pH-Independent Endocytic Entry of Herpes Simplex Virus Type 1. J Virol. 2005 [cited 9 Feb 2022]. doi:10.1128/JVI.79.11.6655-6663.2005

12. Nicola AV, Hou J, Major EO, Straus SE. Herpes Simplex Virus Type 1 Enters Human Epidermal Keratinocytes, but Not Neurons, via a pH-Dependent Endocytic Pathway. J Virol. 2005;79: 7609–7616. doi:10.1128/JVI.79.12.7609-7616.2005

13. Nicola AV, McEvoy AM, Straus SE. Roles for Endocytosis and Low pH in Herpes Simplex Virus Entry into HeLa and Chinese Hamster Ovary Cells. J Virol. 2003;77: 5324–5332. doi:10.1128/JVI.77.9.5324-5332.2003

14. Nicola AV, Straus SE. Cellular and Viral Requirements for Rapid Endocytic Entry of Herpes Simplex Virus. J Virol. 2004;78: 7508–7517. doi:10.1128/JVI.78.14.7508-7517.2004

15. Wittels M, Spear PG. Penetration of cells by herpes simplex virus does not require a low pH-dependent endocytic pathway. Virus Res. 1991;18: 271–290. doi:10.1016/0168-1702(91)90024-P

16. Kristensson K, Lycke E, Röyttä M, Svennerholm B, Vahlne A 1986. Neuritic Transport of Herpes Simplex Virus in Rat Sensory Neurons in vitro. Effects of Substances Interacting with Microtubular Function and Axonal Flow [Nocodazole, Taxol and Erythro-9-3-(2-hydroxynonyl)adenine]. J Gen Virol. 67: 2023–2028. doi:10.1099/0022-1317-67-9-2023

17. Sodeik B, Ebersold MW, Helenius A. Microtubule-mediated Transport of Incoming Herpes Simplex Virus 1 Capsids to the Nucleus. J Cell Biol. 1997;136: 1007–1021.

18. Newcomb WW, Cockrell SK, Homa FL, Brown JC. Polarized DNA Ejection from the Herpesvirus Capsid. J Mol Biol. 2009;392: 885–894. doi:10.1016/j.jmb.2009.07.052

19. Honess RW, Roizman B. Regulation of Herpesvirus Macromolecular Synthesis I. Cascade Regulation of the Synthesis of Three Groups of Viral Proteins 1. J Virol. 1974;14: 8–19.

20. Honess RW, Roizman B. Regulation of herpesvirus macromolecular synthesis: sequential transition of polypeptide synthesis requires functional viral polypeptides. Proc Natl Acad Sci U S A. 1975;72: 1276–1280.

21. Gibson W, Roizman B. Proteins Specified by Herpes Simplex Virus VIII. Characterization and Composition of Multiple Capsid Forms of Subtypes 1 and 2. J Virol. 1972;10: 1044–1052.

22. Mettenleiter TC. Herpesvirus Assembly and Egress. J Virol. 2002 [cited 9 Mar 2022]. doi:10.1128/JVI.76.4.1537-1547.2002

23. Skepper JN, Whiteley A, Browne H, Minson A. Herpes simplex virus nucleocapsids mature to progeny virions by an envelopment --> deenvelopment --> reenvelopment pathway. J Virol. 2001;75: 5697–5702. doi:10.1128/JVI.75.12.5697-5702.2001

24. Stackpole CW. Herpes-Type Virus of the Frog Renal Adenocarcinoma. J Virol. 1969;4: 75–93. doi:10.1128/jvi.4.1.75-93.1969

25. Zaichick SV, Bohannon KP, Hughes A, Sollars PJ, Pickard GE, Smith GA. The Herpesvirus VP1/2 Protein Is an Effector of Dynein-Mediated Capsid Transport and Neuroinvasion. Cell Host Microbe. 2013;13: 10.1016/j.chom.2013.01.009. doi:10.1016/j.chom.2013.01.009

26. Deshmane SL, Fraser NW. During latency, herpes simplex virus type 1 DNA is associated with nucleosomes in a chromatin structure. J Virol. 1989;63: 943–947. doi:10.1128/JVI.63.2.943-947.1989

27. Kubat NJ, Tran RK, McAnany P, Bloom DC. Specific histone tail modification and not DNA methylation is a determinant of herpes simplex virus type 1 latent gene expression. J Virol. 2004;78: 1139–1149. doi:10.1128/jvi.78.3.1139-1149.2004

28. Efstathiou S, Minson AC, Field HJ, Anderson JR, Wildy P. Detection of herpes simplex virus-specific DNA sequences in latently infected mice and in humans. J Virol. 1986;57: 446–455.

29. Umbach JL, Kramer MF, Jurak I, Karnowski HW, Coen DM, Cullen BR. MicroRNAs expressed by herpes simplex virus 1 during latent infection regulate viral mRNAs. Nature. 2008;454: 780–783. doi:10.1038/nature07103

30. Cliffe AR, Wilson AC. Restarting Lytic Gene Transcription at the Onset of Herpes Simplex Virus Reactivation. J Virol. 2017;91: e01419-16. doi:10.1128/JVI.01419-16

31. Smith G. Herpesvirus Transport to the Nervous System and Back Again. Annu Rev Microbiol. 2012;66: 10.1146/annurev-micro-092611–150051. doi:10.1146/annurev-micro-092611-150051

32. Longnecker R, Roizman B. Clustering of Genes Dispensable for Growth in Culture in the S Component of the HSV-1 Genome. Science. 1987;236: 573–576. doi:10.1126/science.3033823

33. Dogrammatzis C, Waisner H, Kalamvoki M. "Non-Essential" Proteins of HSV-1 with Essential Roles In Vivo: A Comprehensive Review. Viruses. 2020;13: 17. doi:10.3390/v13010017

34. Boutell C, Sadis S, Everett RD. Herpes simplex virus type 1 immediate-early protein ICP0 and is isolated RING finger domain act as ubiquitin E3 ligases in vitro. J Virol. 2002;76: 841–850. doi:10.1128/jvi.76.2.841-850.2002

35. Alandijany T, Roberts APE, Conn KL, Loney C, McFarlane S, Orr A, et al. Distinct temporal roles for the promyelocytic leukaemia (PML) protein in the sequential regulation of intracellular host immunity to HSV-1 infection. PLoS Pathog. 2018;14: e1006769. doi:10.1371/journal.ppat.1006769

36. Chelbi-Alix MK, de Thé H. Herpes virus induced proteasome-dependent degradation of the nuclear bodies-associated PML and Sp100 proteins. Oncogene. 1999;18: 935–941. doi:10.1038/sj.onc.1202366

37. Cai W, Astor TL, Liptak LM, Cho C, Coen DM, Schaffer PA. The herpes simplex virus type 1 regulatory protein ICP0 enhances virus replication during acute infection and reactivation from latency. J Virol. 1993;67: 7501–7512.

38. Halford WP, Schaffer PA. ICP0 Is Required for Efficient Reactivation of Herpes Simplex Virus Type 1 from Neuronal Latency. J Virol. 2001;75: 3240–3249. doi:10.1128/JVI.75.7.3240-3249.2001

39. Duffy C, LaVail JH, Tauscher AN, Wills EG, Blaho JA, Baines JD. Characterization of a UL49-Null Mutant: VP22 of Herpes Simplex Virus Type 1 Facilitates Viral Spread in Cultured Cells and the Mouse Cornea. J Virol. 2006;80: 8664–8675. doi:10.1128/JVI.00498-06

40. Tanaka M, Kato A, Satoh Y, Ide T, Sagou K, Kimura K, et al. Herpes Simplex Virus 1 VP22 Regulates Translocation of Multiple Viral and Cellular Proteins and Promotes Neurovirulence. J Virol. 2012;86: 5264–5277. doi:10.1128/JVI.06913-11

41. Maruzuru Y, Ichinohe T, Sato R, Miyake K, Okano T, Suzuki T, et al. Herpes Simplex Virus 1 VP22 Inhibits AIM2-Dependent Inflammasome Activation to Enable Efficient Viral Replication. Cell Host Microbe. 2018;23: 254-265.e7. doi:10.1016/j.chom.2017.12.014

42. Chou J, Roizman B. Herpes simplex virus 1 gamma(1)34.5 gene function, which blocks the host response to infection, maps in the homologous domain of the genes expressed during growth arrest and DNA damage. Proc Natl Acad Sci U S A. 1994;91: 5247–5251.

43. Chou J, Kern ER, Whitley RJ, Roizman B. Mapping of Herpes Simplex Virus-1 Neurovirulence to γ134.5, a Gene Nonessential for Growth in Culture. Science. 1990;250: 1262–1266. doi:10.1126/science.2173860

44. Chou J, Roizman B. The gamma 1(34.5) gene of herpes simplex virus 1 precludes neuroblastoma cells from triggering total shutoff of protein synthesis characteristic of programed cell death in neuronal cells. Proc Natl Acad Sci U S A. 1992;89: 3266–3270.

45. Whitley RJ, Kern ER, Chatterjee S, Chou J, Roizman B. Replication, establishment of latency, and induced reactivation of herpes simplex virus gamma 1 34.5 deletion mutants in rodent models. J Clin Invest. 1993;91: 2837–2843.

46. He B, Chou J, Liebermann DA, Hoffman B, Roizman B. The carboxyl terminus of the murine MyD116 gene substitutes for the corresponding domain of the gamma(1)34.5 gene of herpes simplex virus to preclude the premature shutoff of total protein synthesis in infected human cells. J Virol. 1996;70: 84–90.

47. He B, Gross M, Roizman B. The γ134.5 protein of herpes simplex virus 1 complexes with protein phosphatase 1α to dephosphorylate the α subunit of the eukaryotic translation initiation factor 2 and preclude the shutoff of protein synthesis by double-stranded RNA-activated protein kinase. Proc Natl Acad Sci U S A. 1997;94: 843–848.

48. Orvedahl A, Alexander D, Tallóczy Z, Sun Q, Wei Y, Zhang W, et al. HSV-1 ICP34.5 Confers Neurovirulence by Targeting the Beclin 1 Autophagy Protein. Cell Host Microbe. 2007;1: 23–35. doi:10.1016/j.chom.2006.12.001

49. Wilcox DR, Wadhwani NR, Longnecker R, Muller WJ. Differential reliance on autophagy for protection from HSV encephalitis between newborns and adults. PLoS Pathog. 2015;11: e1004580. doi:10.1371/journal.ppat.1004580

50. Ma Y, Jin H, Valyi-Nagy T, Cao Y, Yan Z, He B. Inhibition of TANK Binding Kinase 1 by Herpes Simplex Virus 1 Facilitates Productive Infection. J Virol. 2012;86: 2188–2196. doi:10.1128/JVI.05376-11

51. Verpooten D, Ma Y, Hou S, Yan Z, He B. Control of TANK-binding Kinase 1-mediated Signaling by the γ134.5 Protein of Herpes Simplex Virus 1. J Biol Chem. 2009;284: 1097–1105. doi:10.1074/jbc.M805905200

52. Jing X, He B 2005. Characterization of the triplet repeats in the central domain of the γ134·5 protein of herpes simplex virus 1. J Gen Virol. 86: 2411–2419. doi:10.1099/vir.0.81033-0

53. Mao H, Rosenthal KS. Strain-Dependent Structural Variants of Herpes Simplex Virus Type 1 ICP34.5 Determine Viral Plaque Size, Efficiency of Glycoprotein Processing, and Viral Release and Neuroinvasive Disease Potential. J Virol. 2003;77: 3409–3417. doi:10.1128/JVI.77.6.3409-3417.2003

54. Ravi V, Kennedy PG, MacLean ARY 1998. Functional analysis of the herpes simplex virus type 2 strain HG52 RL1 gene: the intron plays no role in virulence. J Gen Virol. 79: 1613–1617. doi:10.1099/0022-1317-79-7-1613

55. Tang S, Guo N, Patel A, Krause PR. Herpes Simplex Virus 2 Expresses a Novel Form of ICP34.5, a Major Viral Neurovirulence Factor, through Regulated Alternative Splicing. J Virol. 2013;87: 5820–5830. doi:10.1128/JVI.03500-12

56. Korom M, Davis KL, Morrison LA. Up to Four Distinct Polypeptides Are Produced from the γ34.5 Open Reading Frame of Herpes Simplex Virus 2. J Virol. 2014;88: 11284–11296. doi:10.1128/JVI.01284-14

57. Bernstein DI, Bellamy AR, Hook EW, Levin MJ, Wald A, Ewell MG, et al. Epidemiology, Clinical Presentation, and Antibody Response to Primary Infection With Herpes Simplex Virus Type 1 and Type 2 in Young Women. Clin Infect Dis Off Publ Infect Dis Soc Am. 2013;56: 344–351. doi:10.1093/cid/cis891

58. Xu F, Sternberg MR, Kottiri BJ, McQuillan GM, Lee FK, Nahmias AJ, et al. Trends in Herpes Simplex Virus Type 1 and Type 2 Seroprevalence in the United States. JAMA. 2006;296: 964–973. doi:10.1001/jama.296.8.964

59. Ross JD, Smith IW, Elton RA. The epidemiology of herpes simplex types 1 and 2 infection of the genital tract in Edinburgh 1978-1991. Genitourin Med. 1993;69: 381–383.

60. Roberts CM, Pfister JR, Spear SJ. Increasing proportion of herpes simplex virus type 1 as a cause of genital herpes infection in college students. Sex Transm Dis. 2003;30: 797–800. doi:10.1097/01.OLQ.0000092387.58746.C7

61. Jin F, Prestage GP, Mao L, Kippax SC, Pell CM, Donovan B, et al. Transmission of herpes simplex virus types 1 and 2 in a prospective cohort of HIV-negative gay men: the health in men study. J Infect Dis. 2006;194: 561–570. doi:10.1086/506455

62. Douglas RG, Couch RB. A Prospective Study of Chronic Herpes Simplex Virus Infection and Recurrent Herpes Labialis in Humans. J Immunol. 1970;104: 289–295.

63. Oliver L, Wald A, Kim M, Zeh J, Selke S, Ashley R, et al. Seroprevalence of herpes simplex virus infections in a family medicine clinic. Arch Fam Med. 1995;4: 228–232. doi:10.1001/archfami.4.3.228

64. Johnson RE, Nahmias AJ, Magder LS, Lee FK, Brooks CA, Snowden CB. A Seroepidemiologic Survey of the Prevalence of Herpes Simplex Virus Type 2 Infection in the United States. N Engl J Med. 1989;321: 7–12. doi:10.1056/NEJM198907063210102

65. Annunziato PW, Gershon A. Herpes simplex virus infections. Pediatr Rev. 1996;17: 415–423; quiz 424.

66. McMillan JA, Weiner LB, Higgins AM, Lamparella VJ. Pharyngitis associated with herpes simplex virus in college students. Pediatr Infect Dis J. 1993;12: 280–284. doi:10.1097/00006454-199304000-00004

67. Spruance SL, Overall JC, Kern ER, Krueger GG, Pliam V, Miller W. The Natural History of Recurrent Herpes Simplex Labialis. N Engl J Med. 1977;297: 69–75. doi:10.1056/NEJM197707142970201

68. Corey L, Adams HG, Brown ZA, Holmes KK. Genital herpes simplex virus infections: clinical manifestations, course, and complications. Ann Intern Med. 1983;98: 958–972. doi:10.7326/0003-4819-98-6-958

69. George BP, Schneider EB, Venkatesan A. Encephalitis Hospitalization Rates and Inpatient Mortality in the United States, 2000-2010. PLoS ONE. 2014;9: e104169. doi:10.1371/journal.pone.0104169

70. Whitley R, Arvin A, Prober C, Burchett S, Corey L, Powell D, et al. A controlled trial comparing vidarabine with acyclovir in neonatal herpes simplex virus infection. Infectious Diseases Collaborative Antiviral Study Group. N Engl J Med. 1991;324: 444–449. doi:10.1056/NEJM199102143240703

71. Whitley RJ, Soong S, Dolin R, Galasso GJ, Ch'ien LT, Alford CA. Adenine Arabinoside Therapy of Biopsy-Proved Herpes Simplex Encephalitis. N Engl J Med. 1977;297: 289–294. doi:10.1056/NEJM197708112970601

72. Kimberlin DW, Lin C-Y, Jacobs RF, Powell DA, Corey L, Gruber WC, et al. Safety and Efficacy of High-Dose Intravenous Acyclovir in the Management of Neonatal Herpes Simplex Virus Infections. Pediatrics. 2001;108: 230–238. doi:10.1542/peds.108.2.230

73. Takeda K, Akira S. TLR signaling pathways. Semin Immunol. 2004;16: 3–9. doi:10.1016/j.smim.2003.10.003

74. Wu J, Chen ZJ. Innate immune sensing and signaling of cytosolic nucleic acids. Annu Rev Immunol. 2014;32: 461–488. doi:10.1146/annurev-immunol-032713-120156

75. Ning S, Pagano JS, Barber GN. IRF7: activation, regulation, modification and function. Genes Immun. 2011;12: 399–414. doi:10.1038/gene.2011.21

76. Liu S, Cai X, Wu J, Cong Q, Chen X, Li T, et al. Phosphorylation of innate immune adaptor proteins MAVS, STING, and TRIF induces IRF3 activation. Science. 2015;347: aaa2630. doi:10.1126/science.aaa2630

77. Taddeo B, Luo TR, Zhang W, Roizman B. Activation of NF-kappaB in cells productively infected with HSV-1 depends on activated protein kinase R and plays no apparent role in blocking apoptosis. Proc Natl Acad Sci U S A. 2003;100: 12408–12413. doi:10.1073/pnas.2034952100

78. Shuai K, Horvath CM, Huang LH, Qureshi SA, Cowburn D, Darnell JE. Interferon activation of the transcription factor Stat91 involves dimerization through SH2-phosphotyrosyl peptide interactions. Cell. 1994;76: 821–828. doi:10.1016/0092-8674(94)90357-3

79. Krug A, Luker GD, Barchet W, Leib DA, Akira S, Colonna M. Herpes simplex virus type 1 activates murine natural interferon-producing cells through toll-like receptor 9. Blood. 2004;103: 1433–1437. doi:10.1182/blood-2003-08-2674

80. Jacquemont B, Roizman B. RNA synthesis in cells infected with herpes simplex virus. X. Properties of viral symmetric transcripts and of double-stranded RNA prepared from them. J Virol. 1975;15: 707–713. doi:10.1128/JVI.15.4.707-713.1975

81. Leoni V, Gianni T, Salvioli S, Campadelli-Fiume G. Herpes Simplex Virus Glycoproteins gH/gL and gB Bind Toll-Like Receptor 2, and Soluble gH/gL Is Sufficient To Activate NF-κB. J Virol. 2012;86: 6555–6562. doi:10.1128/JVI.00295-12

82. Li X-D, Wu J, Gao D, Wang H, Sun L, Chen ZJ. Pivotal Roles of cGAS-cGAMP Signaling in Antiviral Defense and Immune Adjuvant Effects. Science. 2013;341: 10.1126/science.1244040. doi:10.1126/science.1244040

83. Johnson KE, Bottero V, Flaherty S, Dutta S, Singh VV, Chandran B. IFI16 Restricts HSV-1 Replication by Accumulating on the HSV-1 Genome, Repressing HSV-1 Gene Expression, and Directly or Indirectly Modulating Histone Modifications. PLoS Pathog. 2014;10: e1004503. doi:10.1371/journal.ppat.1004503

84. Gill N, Deacon PM, Lichty B, Mossman KL, Ashkar AA. Induction of innate immunity against herpes simplex virus type 2 infection via local delivery of Toll-like receptor ligands correlates with beta interferon production. J Virol. 2006;80: 9943–9950. doi:10.1128/JVI.01036-06

85. Leib DA, Harrison TE, Laslo KM, Machalek MA, Moorman NJ, Virgin HW. Interferons Regulate the Phenotype of Wild-type and Mutant Herpes Simplex Viruses In Vivo. J Exp Med. 1999;189: 663–672.

86. Broz P, Dixit VM. Inflammasomes: mechanism of assembly, regulation and signalling. Nat Rev Immunol. 2016;16: 407–420. doi:10.1038/nri.2016.58

87. Hornung V, Ablasser A, Charrel-Dennis M, Bauernfeind F, Horvath G, Caffrey DR, et al. AIM2 recognizes cytosolic dsDNA and forms a caspase-1 activating inflammasome with ASC. Nature. 2009;458: 514–518. doi:10.1038/nature07725

88. Karaba AH, Figueroa A, Massaccesi G, Botto S, DeFilippis VR, Cox AL. Herpes simplex virus type 1 inflammasome activation in proinflammatory human macrophages is dependent on NLRP3, ASC, and caspase-1. PLoS ONE. 2020;15. doi:10.1371/journal.pone.0229570

89. Johnson KE, Chikoti L, Chandran B. Herpes Simplex Virus 1 Infection Induces Activation and Subsequent Inhibition of the IFI16 and NLRP3 Inflammasomes. J Virol. 2013;87: 5005–5018. doi:10.1128/JVI.00082-13

90. Sergerie Y, Rivest S, Boivin G. Tumor Necrosis Factor-α and Interleukin-1β Play a Critical Role in the Resistance against Lethal Herpes Simplex Virus Encephalitis. J Infect Dis. 2007;196: 853–860. doi:10.1086/520094

91. Barr DP, Belz GT, Reading PC, Wojtasiak M, Whitney PG, Heath WR, et al. A role for plasmacytoid dendritic cells in the rapid IL-18-dependent activation of NK cells following HSV-1 infection. Eur J Immunol. 2007;37: 1334–1342. doi:10.1002/eji.200636362

92. Reading PC, Whitney PG, Barr DP, Wojtasiak M, Mintern JD, Waithman J, et al. IL-18, but not IL-12, Regulates NK Cell Activity following Intranasal Herpes Simplex Virus Type 1 Infection. J Immunol. 2007;179: 3214–3221. doi:10.4049/jimmunol.179.5.3214

93. Harandi AM, Svennerholm B, Holmgren J, Eriksson K. Interleukin-12 (IL-12) and IL-18 Are Important in Innate Defense against Genital Herpes Simplex Virus Type 2 Infection in Mice but Are Not Required for the Development of Acquired Gamma Interferon-Mediated Protective Immunity. J Virol. 2001;75: 6705–6709. doi:10.1128/JVI.75.14.6705-6709.2001

94. Gimenez F, Bhela S, Dogra P, Harvey L, Varanasi SK, Jaggi U, et al. The inflammasome NLRP3 plays a protective role against a viral immunopathological lesion. J Leukoc Biol. 2016;99: 647–657. doi:10.1189/jlb.3HI0715-321R

95. Cuddy SR, Schinlever AR, Dochnal S, Seegren PV, Suzich J, Kundu P, et al. Neuronal hyperexcitability is a DLK-dependent trigger of herpes simplex virus reactivation that can be induced by IL-1. eLife. 2020;9. doi:10.7554/eLife.58037

96. Michael BD, Griffiths MJ, Granerod J, Brown D, Keir G, Wnęk G, et al. The Interleukin-1 Balance During Encephalitis Is Associated With Clinical Severity, Blood-Brain Barrier Permeability, Neuroimaging Changes, and Disease Outcome. J Infect Dis. 2016;213: 1651–1660. doi:10.1093/infdis/jiv771

97. Langenberg AGM, Corey L, Ashley RL, Leong WP, Straus SE. A Prospective Study of New Infections with Herpes Simplex Virus Type 1 and Type 2. N Engl J Med. 1999;341: 1432–1438. doi:10.1056/NEJM199911043411904

98. Brown ZA, Wald A, Morrow RA, Selke S, Zeh J, Corey L. Effect of Serologic Status and Cesarean Delivery on Transmission Rates of Herpes Simplex Virus From Mother to Infant. JAMA. 2003;289: 203–209. doi:10.1001/jama.289.2.203

99. Corey L, Wald A. Maternal and Neonatal Herpes Simplex Virus Infections. N Engl J Med. 2009;361: 1376–1385. doi:10.1056/NEJMra0807633

100. Audry M, Ciancanelli M, Yang K, Cobat A, Chang H-H, Sancho-Shimizu V, et al. NEMO is a key component of NF-κB- and IRF-3-dependent TLR3-mediated immunity to herpes simplex virus. J Allergy Clin Immunol. 2011;128: 610-617.e4. doi:10.1016/j.jaci.2011.04.059

101. Casrouge A, Zhang S-Y, Eidenschenk C, Jouanguy E, Puel A, Yang K, et al. Herpes Simplex Virus Encephalitis in Human UNC-93B Deficiency. Science. 2006;314: 308–312. doi:10.1126/science.1128346

102. Guo Y, Audry M, Ciancanelli M, Alsina L, Azevedo J, Herman M, et al. Herpes simplex virus encephalitis in a patient with complete TLR3 deficiency: TLR3 is otherwise redundant in protective immunity. J Exp Med. 2011;208: 2083–2098. doi:10.1084/jem.20101568

103. Herman M, Ciancanelli M, Ou Y-H, Lorenzo L, Klaudel-Dreszler M, Pauwels E, et al. Heterozygous TBK1 mutations impair TLR3 immunity and underlie herpes simplex encephalitis of childhood. J Exp Med. 2012;209: 1567–1582. doi:10.1084/jem.20111316

104. Sancho-Shimizu V, Pérez de Diego R, Lorenzo L, Halwani R, Alangari A, Israelsson E, et al. Herpes simplex encephalitis in children with autosomal recessive and dominant TRIF deficiency. J Clin Invest. 2011;121: 4889–4902. doi:10.1172/JCI59259

105. Zhang S-Y, Jouanguy E, Ugolini S, Smahi A, Elain G, Romero P, et al. TLR3 deficiency in patients with herpes simplex encephalitis. Science. 2007;317: 1522–1527. doi:10.1126/science.1139522

106. Maródi L. Innate cellular immune responses in newborns. Clin Immunol. 2006;118: 137–144. doi:10.1016/j.clim.2005.10.012

107. Angelone DF, Wessels MR, Coughlin M, Suter EE, Valentini P, Kalish LA, et al. Innate Immunity of the Human Newborn Is Polarized Toward a High Ratio of IL-6/TNF-α Production In Vitro and In Vivo. Pediatr Res. 2006;60: 205–209. doi:10.1203/01.pdr.0000228319.10481.ea

108. Zawatzky R, Hilfenhaus J, Marcucci F, Kirchner HY 1981. Experimental Infection of Inbred Mice with Herpes Simplex Virus Type 1. I. Investigation of Humoral and Cellular Immunity and of Interferon Induction. J Gen Virol. 53: 31–38. doi:10.1099/0022-1317-53-1-31

109. Zawatzky R, Engler H, Kirchner HY 1982. Experimental Infection of Inbred Mice with Herpes Simplex Virus. III. Comparison between Newborn and Adult C57BL/6 Mice. J Gen Virol. 60: 25–29. doi:10.1099/0022-1317-60-1-25

110. Wilcox DR, Folmsbee SS, Muller WJ, Longnecker R. The Type I Interferon Response Determines Differences in Choroid Plexus Susceptibility between Newborns and Adults in Herpes Simplex Virus Encephalitis. mBio. 2016;7. doi:10.1128/mBio.00437-16

111. Giraldo D, Wilcox DR, Longnecker R. The Innate Immune Response to Herpes Simplex Virus 1 Infection Is Dampened in the Newborn Brain and Can Be Modulated by Exogenous Interferon Beta To Improve Survival. mBio. 2020;11. doi:10.1128/mBio.00921-20

112. Edwards RG, Kopp SJ, Karaba AH, Wilcox DR, Longnecker R. Herpesvirus Entry Mediator on Radiation-Resistant Cell Lineages Promotes Ocular Herpes Simplex Virus 1 Pathogenesis in an Entry-Independent Manner. mBio. 2015;6: e01532-15. doi:10.1128/mBio.01532-15

113. Kimberlin DW, Lin CY, Jacobs RF, Powell DA, Frenkel LM, Gruber WC, et al. Natural history of neonatal herpes simplex virus infections in the acyclovir era. Pediatrics. 2001;108: 223–229. doi:10.1542/peds.108.2.223

114. Whitley R, Arvin A, Prober C, Corey L, Burchett S, Plotkin S, et al. Predictors of Morbidity and Mortality in Neonates with Herpes Simplex Virus Infections. N Engl J Med. 1991;324: 450–454. doi:10.1056/NEJM199102143240704

115. Akhtar LN, Bowen CD, Renner DW, Pandey U, Della Fera AN, Kimberlin DW, et al. Genotypic and Phenotypic Diversity of Herpes Simplex Virus 2 within the Infected Neonatal Population. mSphere. 4: e00590-18. doi:10.1128/mSphere.00590-18

116. Edwards TG, Bloom DC. Lund Human Mesencephalic (LUHMES) Neuronal Cell Line Supports Herpes Simplex Virus 1 Latency In Vitro. J Virol. 2019;93: e02210-18. doi:10.1128/JVI.02210-18

117. Scholz D, Pöltl D, Genewsky A, Weng M, Waldmann T, Schildknecht S, et al. Rapid, complete and large-scale generation of post-mitotic neurons from the human LUHMES cell line. J Neurochem. 2011;119: 957–971. doi:10.1111/j.1471-4159.2011.07255.x

118. Schildknecht S, Karreman C, Pöltl D, Efrémova L, Kullmann C, Gutbier S, et al. Generation of genetically-modified human differentiated cells for toxicological tests and the study of neurodegenerative diseases. ALTEX - Altern Anim Exp. 2013;30: 427–444. doi:10.14573/altex.2013.4.427

119. Zhou Y, Zhong Y, Wang Y, Zhang X, Batista DL, Gejman R, et al. Activation of p53 by MEG3 Non-coding RNA. J Biol Chem. 2007;282: 24731–24742. doi:10.1074/jbc.M702029200

120. Mariathasan S, Weiss DS, Newton K, McBride J, O'Rourke K, Roose-Girma M, et al. Cryopyrin activates the inflammasome in response to toxins and ATP. Nature. 2006;440: 228–232. doi:10.1038/nature04515

121. Mariathasan S, Newton K, Monack DM, Vucic D, French DM, Lee WP, et al. Differential activation of the inflammasome by caspase-1 adaptors ASC and Ipaf. Nature. 2004;430: 213–218. doi:10.1038/nature02664

122. Wilcox DR, Muller WJ, Longnecker R. HSV targeting of the host phosphatase PP1α is required for disseminated disease in the neonate and contributes to pathogenesis in the brain. Proc Natl Acad Sci U S A. 2015;112: e6937-6944. doi:10.1073/pnas.1513045112

123. Babicki S, Arndt D, Marcu A, Liang Y, Grant JR, Maciejewski A, et al. Heatmapper: web-enabled heat mapping for all. Nucleic Acids Res. 2016;44: W147–W153. doi:10.1093/nar/gkw419

124. Gaublomme JT, Li B, McCabe C, Knecht A, Yang Y, Drokhlyansky E, et al. Nuclei multiplexing with barcoded antibodies for single-nucleus genomics. Nat Commun. 2019;10: 2907. doi:10.1038/s41467-019-10756-2

125. Stuart T, Butler A, Hoffman P, Hafemeister C, Papalexi E, Mauck WM, et al. Comprehensive integration of single-cell data. Cell. 2019;177: 1888-1902.e21. doi:10.1016/j.cell.2019.05.031

126. Blighe K. EnhancedVolcano: publication-ready volcano plots with enhanced colouring and labeling. 2022. Available: https://github.com/kevinblighe/EnhancedVolcano

127. Gu Z, Eils R, Schlesner M. Complex heatmaps reveal patterns and correlations in multidimensional genomic data. Bioinformatics. 2016;32: 2847–2849. doi:10.1093/bioinformatics/btw313

128. Yu G, Wang L-G, Han Y, He Q-Y. clusterProfiler: an R Package for Comparing Biological Themes Among Gene Clusters. OMICS J Integr Biol. 2012;16: 284–287. doi:10.1089/omi.2011.0118

129. Cao J, Spielmann M, Qiu X, Huang X, Ibrahim DM, Hill AJ, et al. The single-cell transcriptional landscape of mammalian organogenesis. Nature. 2019;566: 496–502. doi:10.1038/s41586-019-0969-x

130. Jin S, Guerrero-Juarez CF, Zhang L, Chang I, Ramos R, Kuan C-H, et al. Inference and analysis of cell-cell communication using CellChat. Nat Commun. 2021;12: 1088. doi:10.1038/s41467-021-21246-9

131. Sili U, Kaya A, Mert A. Herpes simplex virus encephalitis: Clinical manifestations, diagnosis and outcome in 106 adult patients. J Clin Virol. 2014;60: 112–118. doi:10.1016/j.jcv.2014.03.010

132. Lundberg P, Ramakrishna C, Brown J, Tyszka JM, Hamamura M, Hinton DR, et al. The Immune Response to Herpes Simplex Virus Type 1 Infection in Susceptible Mice Is a Major Cause of Central Nervous System Pathology Resulting in Fatal Encephalitis. J Virol. 2008 [cited 14 Feb 2022]. doi:10.1128/JVI.00619-08

133. Marques CP, Cheeran MC-J, Palmquist JM, Hu S, Urban SL, Lokensgard JR. Prolonged Microglial Cell Activation and Lymphocyte Infiltration Following Experimental Herpes Encephalitis. J Immunol Baltim Md 1950. 2008;181: 6417–6426.

134. Aurelius E, Andersson B, Forsgren M, Sköldenberg B, Strannegård Φ. Cytokines And Other Markers Of Intrathecal Immune Response In Patients With Herpes Simplex Encephalitis. J Infect Dis. 1994;170: 678–681. doi:10.1093/infdis/170.3.678

135. Giraldo D, Wilcox DR, Longnecker R. The Type I Interferon Response and Age-Dependent Susceptibility to Herpes Simplex Virus Infection. DNA Cell Biol. 2017;36: 329–334. doi:10.1089/dna.2017.3668

136. Fann DY-W, Lee SY, Manzanero S, Tang SC, Gelderblom M, Chunduri P, et al. Intravenous immunoglobulin suppresses NLRP1 and NLRP3 inflammasome-mediated neuronal death in ischemic stroke. Cell Death Dis. 2013;4: e790. doi:10.1038/cddis.2013.326

137. Gris D, Ye Z, Iocca HA, Wen H, Craven RR, Gris P, et al. NLRP3 Plays a Critical Role in the Development of Experimental Autoimmune Encephalomyelitis by Mediating Th1 and Th17 Responses. J Immunol Baltim Md 1950. 2010;185: 974–981. doi:10.4049/jimmunol.0904145

138. Heneka MT, Kummer MP, Latz E. Innate immune activation in neurodegenerative disease. Nat Rev Immunol. 2014;14: 463–477. doi:10.1038/nri3705

139. Zhang H, Luo J, Alcorn JF, Chen K, Fan S, Pilewski J, et al. AIM2 Inflammasome Is Critical for Influenza-Induced Lung Injury and Mortality. J Immunol Author Choice. 2017;198: 4383–4393. doi:10.4049/jimmunol.1600714

140. Ichinohe T, Lee HK, Ogura Y, Flavell R, Iwasaki A. Inflammasome recognition of influenza virus is essential for adaptive immune responses. J Exp Med. 2009;206: 79–87. doi:10.1084/jem.20081667

141. He Z, Chen J, Zhu X, An S, Dong X, Yu J, et al. NLRP3 Inflammasome Activation Mediates Zika Virus–Associated Inflammation. J Infect Dis. 2018;217: 1942–1951. doi:10.1093/infdis/jiy129

142. Kaushik DK, Gupta M, Kumawat KL, Basu A. NLRP3 Inflammasome: Key Mediator of Neuroinflammation in Murine Japanese Encephalitis. PLoS ONE. 2012;7: e32270. doi:10.1371/journal.pone.0032270

143. Chen W, Foo S-S, Zaid A, Teng T-S, Herrero LJ, Wolf S, et al. Specific inhibition of NLRP3 in chikungunya disease reveals a role for inflammasomes in alphavirus-induced inflammation. Nat Microbiol. 2017;2: 1435–1445. doi:10.1038/s41564-017-0015-4

144. Ansari MA, Dutta S, Veettil MV, Dutta D, Iqbal J, Kumar B, et al. Herpesvirus Genome Recognition Induced Acetylation of Nuclear IFI16 Is Essential for Its Cytoplasmic Translocation, Inflammasome and IFN-β Responses. PLoS Pathog. 2015;11: e1005019. doi:10.1371/journal.ppat.1005019

145. Wang W, Hu D, Wu C, Feng Y, Li A, Liu W, et al. STING promotes NLRP3 localization in ER and facilitates NLRP3 deubiquitination to activate the inflammasome upon HSV-1 infection. PLOS Pathog. 2020;16: e1008335. doi:10.1371/journal.ppat.1008335

146. de Sousa JR, Azevedo R do S da S, Martins Filho AJ, de Araujo MTF, Cruz E do RM, Vasconcelos BCB, et al. In situ inflammasome activation results in severe damage to the central nervous system in fatal Zika virus microcephaly cases. Cytokine. 2018;111: 255–264. doi:10.1016/j.cyto.2018.08.008

147. Perry VH, Nicoll JAR, Holmes C. Microglia in neurodegenerative disease. Nat Rev Neurol. 2010;6: 193–201. doi:10.1038/nrneurol.2010.17

148. Lee SW, de Rivero Vaccari JP, Truettner JS, Dietrich WD, Keane RW. The role of microglial inflammasome activation in pyroptotic cell death following penetrating traumatic brain injury. J Neuroinflammation. 2019;16: 27. doi:10.1186/s12974-019-1423-6

149. Sheppard O, Coleman MP, Durrant CS. Lipopolysaccharide-induced neuroinflammation induces presynaptic disruption through a direct action on brain tissue involving microglia-

derived interleukin 1 beta. J Neuroinflammation. 2019;16: 106. doi:10.1186/s12974-019-1490-8

150. Reinert LS, Lopušná K, Winther H, Sun C, Thomsen MK, Nandakumar R, et al. Sensing of HSV-1 by the cGAS–STING pathway in microglia orchestrates antiviral defence in the CNS. Nat Commun. 2016;7: 13348. doi:10.1038/ncomms13348

151. LaFleur AM, Lukacs NW, Kunkel SL, Matsukawa A. Role of CC chemokine CCL6/C10 as a monocyte chemoattractant in a murine acute peritonitis. Mediators Inflamm. 2004;13: 349–355. doi:10.1155/S0962935104000511

152. Ma B, Zhu Z, Homer RJ, Gerard C, Strieter R, Elias JA. The C10/CCL6 Chemokine and CCR1 Play Critical Roles in the Pathogenesis of IL-13-Induced Inflammation and Remodeling. J Immunol. 2004;172: 1872–1881. doi:10.4049/jimmunol.172.3.1872

153. Garlanda C, Dinarello CA, Mantovani A. THE INTERLEUKIN-1 FAMILY: BACK TO THE FUTURE. Immunity. 2013;39: 1003–1018. doi:10.1016/j.immuni.2013.11.010

154. Wuest TR, Carr DJJ. Dysregulation of CXCR3 Signaling due to CXCL10 Deficiency Impairs the Antiviral Response to Herpes Simplex Virus 1 Infection. J Immunol. 2008;181: 7985–7993. doi:10.4049/jimmunol.181.11.7985

155. Zimmermann J, Hafezi W, Dockhorn A, Lorentzen EU, Krauthausen M, Getts DR, et al. Enhanced viral clearance and reduced leukocyte infiltration in experimental herpes encephalitis after intranasal infection of CXCR3-deficient mice. J Neurovirol. 2017;23: 394–403. doi:10.1007/s13365-016-0508-6

156. de Alba E. Structure, interactions and self-assembly of ASC-dependent inflammasomes. Arch Biochem Biophys. 2019;670: 15–31. doi:10.1016/j.abb.2019.05.023

157. Coulon P-G, Dhanushkodi N, Prakash S, Srivastava R, Roy S, Alomari NI, et al. NLRP3, NLRP12, and IFI16 Inflammasomes Induction and Caspase-1 Activation Triggered by Virulent HSV-1 Strains Are Associated With Severe Corneal Inflammatory Herpetic Disease. Front Immunol. 2019;10: 1631. doi:10.3389/fimmu.2019.01631

158. Wang Y, Jia J, Wang Y, Li F, Song X, Qin S, et al. Roles of HSV-1 infection-induced microglial immune responses in CNS diseases: friends or foes? Crit Rev Microbiol. 2019;45: 581–594. doi:10.1080/1040841X.2019.1660615

159. Kanno M, Suzuki S, Fujiwara T, Yokoyama A, Sakamoto A, Takahashi H, et al. Functional expression of CCL6 by rat microglia: A possible role of CCL6 in cell–cell communication. J Neuroimmunol. 2005;167: 72–80. doi:10.1016/j.jneuroim.2005.06.028

160. Gupta P, Sharma A, Han J, Yang A, Bhomia M, Knollmann-Ritschel B, et al. Differential host gene responses from infection with neurovirulent and partially-neurovirulent strains of

Venezuelan equine encephalitis virus. BMC Infect Dis. 2017;17: 309. doi:10.1186/s12879-017-2355-3

161. Wang W, Li G, De Wu, Luo Z, Pan P, Tian M, et al. Zika virus infection induces host inflammatory responses by facilitating NLRP3 inflammasome assembly and interleukin-1β secretion. Nat Commun. 2018;9: 106. doi:10.1038/s41467-017-02645-3

162. Walsh JG, Reinke SN, Mamik MK, McKenzie BA, Maingat F, Branton WG, et al. Rapid inflammasome activation in microglia contributes to brain disease in HIV/AIDS. Retrovirology. 2014;11: 35. doi:10.1186/1742-4690-11-35

163. Perkins D, Gyure KA, Pereira EFR, Aurelian L. Herpes simplex virus type 1-induced encephalitis has an apoptotic component associated with activation of c-Jun N-terminal kinase. J Neurovirol. 2003;9: 101–111. doi:10.1080/13550280390173427

164. Ramos-Estebanez C, Lizarraga KJ, Merenda A. A Systematic Review on the Role of Adjunctive Corticosteroids in Herpes Simplex Virus Encephalitis: Is Timing Critical for Safety and Efficacy? Antivir Ther. 2014;19: 133–139. doi:10.3851/IMP2683

165. Wolf S, Taylor A, Zaid A, Freitas J, Herrero LJ, Rao S, et al. Inhibition of Interleukin-1β Signaling by Anakinra Demonstrates a Critical Role of Bone Loss in Experimental Arthritogenic Alphavirus Infections. Arthritis Rheumatol. 2019;71: 1185–1190. doi:10.1002/art.40856

166. Lei J, Vermillion MS, Jia B, Xie H, Xie L, McLane MW, et al. IL-1 receptor antagonist therapy mitigates placental dysfunction and perinatal injury following Zika virus infection. JCI Insight. 4: e122678. doi:10.1172/jci.insight.122678

167. Cantarini L, Vitale A, Scalini P, Dinarello CA, Rigante D, Franceschini R, et al. Anakinra treatment in drug-resistant Behcet's disease: a case series. Clin Rheumatol. 2015;34: 1293–1301. doi:10.1007/s10067-013-2443-8

168. Goldbach-Mansky R, Dailey NJ, Canna SW, Gelabert A, Jones J, Rubin BI, et al. Neonatal-Onset Multisystem Inflammatory Disease Responsive to Interleukin-1β Inhibition. N Engl J Med. 2006;355: 581–592. doi:10.1056/NEJMoa055137

169. Bradshaw MJ, Venkatesan A. Herpes Simplex Virus-1 Encephalitis in Adults: Pathophysiology, Diagnosis, and Management. Neurotherapeutics. 2016;13: 493–508. doi:10.1007/s13311-016-0433-7

170. PrabhuDas M, Adkins B, Gans H, King C, Levy O, Ramilo O, et al. Challenges in infant immunity: implications for responses to infection and vaccines. Nat Immunol. 2011;12: 189–194. doi:10.1038/ni0311-189

171. Samies NL, James SH, Kimberlin DW. Neonatal Herpes Simplex Virus Disease: Updates and Continued Challenges. Clin Perinatol. 2021;48: 263–274. doi:10.1016/j.clp.2021.03.003

172. Casrouge A, Zhang S-Y, Eidenschenk C, Jouanguy E, Puel A, Yang K, et al. Herpes simplex virus encephalitis in human UNC-93B deficiency. 2006;314: 308–312.

173. Sancho-Shimizu V, de Diego RP, Jouanguy E, Zhang S-Y, Casanova J-L. Inborn errors of anti-viral interferon immunity in humans. Curr Opin Virol. 2011;1: 487–496. doi:10.1016/j.coviro.2011.10.016

174. Zhang S-Y, Jouanguy E, Ugolini S, Smahi A, Elain G, Romero P, et al. TLR3 Deficiency in Patients with Herpes Simplex Encephalitis. Science. 2007;317: 1522–1527. doi:10.1126/science.1139522

175. Bost P, Giladi A, Liu Y, Bendjelal Y, Xu G, David E, et al. Host-Viral Infection Maps Reveal Signatures of Severe COVID-19 Patients. Cell. 2020;181: 1475-1488.e12. doi:10.1016/j.cell.2020.05.006

176. Lebratti T, Lim YS, Cofie A, Andhey P, Jiang X, Scott J, et al. A sustained type I IFN-neutrophil-IL-18 axis drives pathology during mucosal viral infection. Schiffer JT, Taniguchi T, Lund JM, Rivera A, editors. eLife. 2021;10: e65762. doi:10.7554/eLife.65762

177. Melms JC, Biermann J, Huang H, Wang Y, Nair A, Tagore S, et al. A molecular single-cell lung atlas of lethal COVID-19. Nature. 2021; 1–6. doi:10.1038/s41586-021-03569-1

178. Steuerman Y, Cohen M, Peshes-Yaloz N, Valadarsky L, Cohn O, David E, et al. Dissection of Influenza Infection In Vivo by Single-Cell RNA Sequencing. Cell Syst. 2018;6: 679-691.e4. doi:10.1016/j.cels.2018.05.008

179. Zanini F, Robinson ML, Croote D, Sahoo MK, Sanz AM, Ortiz-Lasso E, et al. Virus-inclusive single-cell RNA sequencing reveals the molecular signature of progression to severe dengue. Proc Natl Acad Sci. 2018;115: E12363–E12369. doi:10.1073/pnas.1813819115

180. Hayes CK, Wilcox DR, Yang Y, Coleman GK, Brown MA, Longnecker R. ASC-dependent inflammasomes contribute to immunopathology and mortality in herpes simplex encephalitis. PLoS Pathog. 2021;17: e1009285. doi:10.1371/journal.ppat.1009285

181. Hayes CK, Giraldo D, Wilcox DR, Longnecker R. The Astrocyte Type I Interferon Response Is Essential for Protection against Herpes Simplex Encephalitis. J Virol. 2022;96: e0178321. doi:10.1128/JVI.01783-21

182. Wong FK, Marín O. Developmental Cell Death in the Cerebral Cortex. Annu Rev Cell Dev Biol. 2019;35: 523–542. doi:10.1146/annurev-cellbio-100818-125204

183. From R, Eilam R, Bar-Lev DD, Levin-Zaidman S, Tsoory M, LoPresti P, et al. Oligodendrogenesis and myelinogenesis during postnatal development effect of glatiramer acetate. Glia. 2014;62: 649–665. doi:10.1002/glia.22632

184. Wilcox DR, Wadhwani NR, Longnecker R, Muller WJ. Differential Reliance on Autophagy for Protection from HSV Encephalitis between Newborns and Adults. PLoS Pathog. 2015;11: e1004580. doi:10.1371/journal.ppat.1004580

185. Kang D, Gopalkrishnan RV, Wu Q, Jankowsky E, Pyle AM, Fisher PB. mda-5: An interferon-inducible putative RNA helicase with double-stranded RNA-dependent ATPase activity and melanoma growth-suppressive properties. Proc Natl Acad Sci U S A. 2002;99: 637–642. doi:10.1073/pnas.022637199

186. Melchjorsen J, Rintahaka J, Søby S, Horan KA, Poltajainen A, Østergaard L, et al. Early Innate Recognition of Herpes Simplex Virus in Human Primary Macrophages Is Mediated via the MDA5/MAVS-Dependent and MDA5/MAVS/RNA Polymerase III-Independent Pathways. J Virol. 2010;84: 11350–11358. doi:10.1128/JVI.01106-10

187. Thery F, Martina L, Asselman C, Zhang Y, Vessely M, Repo H, et al. Ring finger protein 213 assembles into a sensor for ISGylated proteins with antimicrobial activity. Nat Commun. 2021;12: 5772. doi:10.1038/s41467-021-26061-w

188. Hovanessian AG. The double stranded RNA-activated protein kinase induced by interferon: dsRNA-PK. J Interferon Res. 1989;9: 641–647. doi:10.1089/jir.1989.9.641

189. Sterpka A, Chen X. Neuronal and Astrocytic Primary Cilia in the Mature Brain. Pharmacol Res. 2018;137: 114–121. doi:10.1016/j.phrs.2018.10.002

190. Minten C, Alt C, Gentner M, Frei E, Deutsch U, Lyck R, et al. DARC shuttles inflammatory chemokines across the blood–brain barrier during autoimmune central nervous system inflammation. Brain. 2014;137: 1454–1469. doi:10.1093/brain/awu045

191. Veroni C, Gabriele L, Canini I, Castiello L, Coccia E, Remoli ME, et al. Activation of TNF receptor 2 in microglia promotes induction of anti-inflammatory pathways. Mol Cell Neurosci. 2010;45: 234–244. doi:10.1016/j.mcn.2010.06.014

192. Li R, Fang L, Pu Q, Bu H, Zhu P, Chen Z, et al. MEG3-4 is a miRNA decoy that regulates IL-1β abundance to initiate and then limit inflammation to prevent sepsis during lung infection. Sci Signal. 2018;11. doi:10.1126/scisignal.aao2387

193. Zhang H, Tao J, Zhang S, Lv X. LncRNA MEG3 Reduces Hippocampal Neuron Apoptosis via the PI3K/AKT/mTOR Pathway in a Rat Model of Temporal Lobe Epilepsy</p>. Neuropsychiatr Dis Treat. 2020;16: 2519–2528. doi:10.2147/NDT.S270614

194. Zhou Y, Cheunsuchon P, Nakayama Y, Lawlor MW, Zhong Y, Rice KA, et al. Activation of paternally expressed genes and perinatal death caused by deletion of the Gtl2 gene. Dev Camb Engl. 2010;137: 2643–2652. doi:10.1242/dev.045724

195. Jerome KR, Fox R, Chen Z, Sears AE, Lee H, Corey L. Herpes Simplex Virus Inhibits Apoptosis through the Action of Two Genes, Us5 and Us3. J Virol. 1999;73: 8950–8957.

196. Koyama AH, Miwa Y. Suppression of apoptotic DNA fragmentation in herpes simplex virus type 1-infected cells. J Virol. 1997;71: 2567–2571.

197. Munger J, Chee AV, Roizman B. The US3 Protein Kinase Blocks Apoptosis Induced by the d120 Mutant of Herpes Simplex Virus 1 at a Premitochondrial Stage. J Virol. 2001 [cited 7 Feb 2022]. doi:10.1128/JVI.75.12.5491-5497.2001

198. Kopp SJ, Banisadr G, Glajch K, Maurer UE, Grünewald K, Miller RJ, et al. Infection of neurons and encephalitis after intracranial inoculation of herpes simplex virus requires the entry receptor nectin-1. Proc Natl Acad Sci U S A. 2009;106: 17916–17920. doi:10.1073/pnas.0908892106

199. Lin S-P, Youngson N, Takada S, Seitz H, Reik W, Paulsen M, et al. Asymmetric regulation of imprinting on the maternal and paternal chromosomes at the Dlk1-Gtl2 imprinted cluster on mouse chromosome 12. Nat Genet. 2003;35: 97–102. doi:10.1038/ng1233

200. Takahashi N, Okamoto A, Kobayashi R, Shirai M, Obata Y, Ogawa H, et al. Deletion of Gtl2 , imprinted non-coding RNA, with its differentially methylated region induces lethal parent-origin-dependent defects in mice. Hum Mol Genet. 2009;18: 1879–1888. doi:10.1093/hmg/ddp108

201. Zhang L, Yang Z, Trottier J, Barbier O, Wang L. LncRNA MEG3 induces cholestatic liver injury by interaction with PTBP1 to facilitate Shp mRNA decay. Hepatol Baltim Md. 2017;65: 604–615. doi:10.1002/hep.28882

202. Xue Y, Ouyang K, Huang J, Zhou Y, Ouyang H, Li H, et al. Direct Conversion of Fibroblasts to Neurons by Reprogramming PTB-Regulated microRNA Circuits. Cell. 2013;152: 82–96. doi:10.1016/j.cell.2012.11.045

203. Ramos AD, Andersen RE, Liu SJ, Nowakowski TJ, Hong SJ, Gertz C, et al. The long noncoding RNA Pnky regulates neuronal differentiation of embryonic and postnatal neural stem cells. Cell Stem Cell. 2015;16: 439–447. doi:10.1016/j.stem.2015.02.007

204. Buss RR, Sun W, Oppenheim RW. Adaptive roles of programmed cell death during nervous system development. Annu Rev Neurosci. 2006;29: 1–35. doi:10.1146/annurev.neuro.29.051605.112800

205. You Y, Cheng A-C, Wang M-S, Jia R-Y, Sun K-F, Yang Q, et al. The suppression of apoptosis by α-herpesvirus. Cell Death Dis. 2017;8: e2749–e2749. doi:10.1038/cddis.2017.139

206. Looker KJ, Magaret AS, May MT, Turner KME, Vickerman P, Newman LM, et al. First estimates of the global and regional incidence of neonatal herpes infection. Lancet Glob Health. 2017;5: e300–e309. doi:10.1016/S2214-109X(16)30362-X

207. Pinninti SG, Kimberlin DW. Neonatal herpes simplex virus infections. Semin Perinatol. 2018;42: 168–175. doi:10.1053/j.semperi.2018.02.004

208. Whitley RJ, Corey L, Arvin A, Lakeman FD, Sumaya CV, Wright PF, et al. Changing presentation of herpes simplex virus infection in neonates. J Infect Dis. 1988;158: 109–116. doi:10.1093/infdis/158.1.109

209. Kimberlin DW, Lin C-Y, Jacobs RF, Powell DA, Corey L, Gruber WC, et al. Safety and efficacy of high-dose intravenous acyclovir in the management of neonatal herpes simplex virus infections. Pediatrics. 2001;108: 230–238. doi:10.1542/peds.108.2.230

210. Whitley R, Arvin A, Prober C, Corey L, Burchett S, Plotkin S, et al. Predictors of morbidity and mortality in neonates with herpes simplex virus infections. N Engl J Med. 1991;324: 450–454. doi:10.1056/NEJM199102143240704

211. Kimberlin DW, Lin C-Y, Jacobs RF, Powell DA, Frenkel LM, Gruber WC, et al. Natural history of neonatal herpes simplex virus infections in the acyclovir era. Pediatrics. 2001;108: 223–229. doi:10.1542/peds.108.2.223

212. Kimberlin DW, Powell DA, Palmer A, Bradley JS, Dennehy PH, Abughali N, et al. Oral acyclovir suppression and neurodevelopment after neonatal herpes. N Engl J Med. 2011;365: 1284–1292.

213. Lim HK, Seppanen M, Hautala T, Ciancanelli MJ, Itan Y, Lafaille FG, et al. TLR3 deficiency in herpes simplex encephalitis: High allelic heterogeneity and recurrence risk. Neurology. 2014;83: 1888–1897. doi:10.1212/WNL.0000000000000999

214. Tscherne DM, García-Sastre A. Virulence determinants of pandemic influenza viruses. J Clin Invest. 2011;121: 6–13. doi:10.1172/JCI44947

215. Müller V, Fraser C, Herbeck JT. A strong case for viral genetic factors in HIV virulence. Viruses. 2011;3: 204–216. doi:10.3390/v3030204

216. Akhtar LN, Bowen CD, Renner DW, Pandey U, Della Fera AN, Kimberlin DW, et al. Genotypic and phenotypic diversity of herpes simplex virus 2 within the infected neonatal population. mSphere. 2019;4: e00590-18.

217. Shipley MM, Renner DW, Pandey U, Ford B, Bloom DC, Grose C, et al. Personalized viral genomic investigation of herpes simplex virus 1 perinatal viremic transmission with dual fatality. Cold Spring Harb Mol Case Stud. 2018;5: a004382.

218. Shipley MM, Renner DW, Ott M, Bloom DC, Koelle DM, Johnston C, et al. Genome-wide surveillance of genital herpes simplex virus type 1 from multiple anatomic sites over time. J Infect Dis. 2018;218: 595–605. doi:10.1093/infdis/jiy216

219. Szpara ML, Gatherer D, Ochoa A, Greenbaum B, Dolan A, Bowden RJ, et al. Evolution and diversity in human herpes simplex virus genomes. J Virol. 2014;88: 1209–27. doi:10.1128/JVI.01987-13

220. Minaya MA, Jensen TL, Goll JB, Korom M, Datla SH, Belshe RB, et al. Molecular evolution of herpes simplex virus 2 complete genomes: comparison between primary and recurrent infections. J Virol. 2017;91: e00942-17.

221. Renzette N, Gibson L, Bhattacharjee B, Fisher D, Schleiss MR, Jensen JD, et al. Rapid intrahost evolution of human cytomegalovirus is shaped by demography and positive selection. PLoS Genet. 2013;9: e1003735. doi:10.1371/journal.pgen.1003735

222. Newman RM, Lamers SL, Weiner B, Ray SC, Colgrove RC, Diaz F, et al. Genome sequencing and analysis of geographically diverse clinical isolates of herpes simplex virus 2. J Virol. 2015;89: 8219–32. doi:10.1128/JVI.01303-15

223. Johnson RT. The pathogenesis of herpes virus encephalitis. J Exp Med. 1964;119: 343–356. doi:10.1084/jem.119.2.343

224. Tran RK, Lieu PT, Aguilar S, Wagner EK, Bloom DC. Altering the Expression Kinetics of VP5 Results in Altered Virulence and Pathogenesis of Herpes Simplex Virus Type 1 in Mice. J Virol. 2002;76: 2199–2205. doi:10.1128/jvi.76.5.2199-2205.2002

225. Gordon YJ, Gilden DM, Becker Y. HSV-1 thymidine kinase promotes virulence and latency in the mouse. Invest Ophthalmol Vis Sci. 1983;24: 599–602.

226. Boivin G, Coulombe Z, Rivest S. Intranasal herpes simplex virus type 2 inoculation causes a profound thymidine kinase dependent cerebral inflammatory response in the mouse hindbrain. Eur J Neurosci. 2002;16: 29–43. doi:10.1046/j.1460-9568.2002.02057.x

227. Price NB, Wood KE. Distinguishing Features Common to Dual Fatal Herpes Simplex Virus Infections That Occur in Both a Pregnant Woman and Her Newborn Infant. Viruses. 2021;13: 2542. doi:10.3390/v13122542

228. Akhtar LN, Szpara ML. Viral genetic diversity and its potential contributions to the development and progression of neonatal herpes simplex virus (HSV) disease. Curr Clin Microbiol Rep. 2019;6: 249–256. doi:10.1007/s40588-019-00131-6

229. Uyar O, Laflamme N, Piret J, Venable M-C, Carbonneau J, Zarrouk K, et al. An Early Microglial Response Is Needed To Efficiently Control Herpes Simplex Virus Encephalitis. J Virol. 2020;94: e01428-20. doi:10.1128/JVI.01428-20

230. Hu X, Zeng Q, Xiao J, Qin S, Wang Y, Shan T, et al. Herpes Simplex Virus 1 Induces Microglia Gasdermin D-Dependent Pyroptosis Through Activating the NLR Family Pyrin Domain Containing 3 Inflammasome. Front Microbiol. 2022;13: 838808. doi:10.3389/fmicb.2022.838808

231. Uyar O, Dominguez JM, Bordeleau M, Lapeyre L, Ibáñez FG, Vallières L, et al. Single-cell transcriptomics of the ventral posterolateral nucleus-enriched thalamic regions from HSV-1-infected mice reveal a novel microglia/microglia-like transcriptional response. J Neuroinflammation. 2022;19: 81. doi:10.1186/s12974-022-02437-7

232. Sethuraman S, Gay LA, Jain V, Haecker I, Renne R. microRNA dependent and independent deregulation of long non-coding RNAs by an oncogenic herpesvirus. PLoS Pathog. 2017;13: e1006508. doi:10.1371/journal.ppat.1006508

233. Wang Z, Fan P, Zhao Y, Zhang S, Lu J, Xie W, et al. NEAT1 modulates herpes simplex virus-1 replication by regulating viral gene transcription. Cell Mol Life Sci. 2017;74: 1117–1131. doi:10.1007/s00018-016-2398-4

234. Shirahama S, Onoguchi-Mizutani R, Kawata K, Taniue K, Miki A, Kato A, et al. Long noncoding RNA U90926 is crucial for herpes simplex virus type 1 proliferation in murine retinal photoreceptor cells. Sci Rep. 2020;10: 19406. doi:10.1038/s41598-020-76450-2